Supporting Information

Osmium(II) Tethered Half-Sandwich Complexes: pH-dependent Aqueous Speciation and Transfer Hydrogenation in Cells

Sonia Infante-Tadeo,[a] *Vanessa Rodríguez-Fanjul,*[a] *Abraha Habtemariam*[a,b] *and Ana M. Pizarro*[a,c]*

[a] IMDEA Nanociencia, Faraday 9, 28049 Madrid, Spain

[b] Department of Chemistry, University of Warwick, Gibbet Hill Road, Coventry, UK

[c] Unidad Asociada de Nanobiotecnología CNB-CSIC-IMDEA, 28049 Madrid, Spain

INDEX

General Experimental Details

Materials for synthesis and analysis

$OsCl_3 \cdot 3H_2O$ was acquired from Heralab Technologies, S.L. 3-Phenylpropanoic acid and 8-hydroxyquinoline were purchase from Alfa Aesar. Diethyl ether, acetone, $LiAlH_4$, 1,10-phenantroline and picolinic acid were purchased from Acros Organics; ethylenediamine from Fluka; 2,2'-bipyridine, lithium wires, L-lactic dehydrogenase from bovine heart, glycine buffer solution, β-nicotinamide adenine dinucleotide hydrate (NAD^+), sodium L-lactate, sodium phosphate dibasic and 1-(2-pyridinyl)methanamine from Sigma Aldrich; ethyl acetate, iodine and RIPA Lysis and Extraction Buffer from Fisher; and 6-methylpicolinic acid, 2-ethynyl-4-methylpyridine, hydrazine and 2,4-pyridinedicarboxylic acid from FluoroChem. Dry methanol and sodium methoxide were acquired from VWR International. Ethanol and sodium metal were purchased from Sharlau. For NMR spectroscopy, the solvents used were DMSO-d_6 from abcr GmbH, $CDCl_3$ and CD_3OD from VWR, and D_2O from Fisher.

Instrumentation

Nuclear Magnetic Resonance (NMR) spectroscopy. ^1H and proton-decoupled ^{13}C NMR spectra were acquired in 5 mm NMR tubes using a Bruker DPX 400 MHz spectrometer by dissolving the compounds at ca. 10 mM concentrations unless otherwise stated. Time zero (t_0) is defined as the time at which the first measurement is recorded, ranging between 5–15 min after sample preparation, except for T-dependent hydrolysis of complexes **9**–**12** where $t_0 \leq 5$ min, time that was considered in the data analysis. The chemical shifts in NMR were internally referenced to 1,4-dioxane for D_2O (3.75 and 67.19 ppm, for ^1H and $^{13}C\{^1H\}$ NMR, respectively) or via the residual ^1H and ^{13}C signals of the corresponding solvents: $CDCl_3$ (^1H: 7.26 ppm and ^{13}C: 77.16 ppm), DMSO-d_6 (^1H: 2.50 ppm and ^{13}C: 39.52 ppm) and CD_3OD (^1H: 3.31 ppm and ^{13}C: 49.00 ppm). 2D [^1H,^1H] COSY, ^1H-decoupled [^1H,^{13}C] HMQC and ^1H-decoupled [^1H,^{13}C] HMBC NMR spectra were recorded using standard pulse sequences. Data processing was carried out using MestreNova, version 6.0 (Mestrelab Research, S.L.).

Elemental analysis. Elemental analysis (C, H, N) of complexes **1**–**13**, **2C** and **3C** was carried out using a Leco analytical elemental analyser CHNS-932. The CHN analyses of complexes bearing highly acidic protons can give rise to large deviations from expected values than normally found for high purity compounds. Additionally, they often present high hygroscopicity. This was found for complexes **4C**, **8C**, **10C**, **11C**, and **13C**. However, their ^1H

and $^{13}C\{^{1}H\}$ NMR, and MS data (vide infra) are consistent with the expected compositions and high purity.

Mass spectrometry. Samples were prepared using reagent-grade methanol at ca. 20 μg/mL. 0.1% Formic acid in MeOH or MeOH/H_2O (4/1, v/v) was used as the mobile phase. The mass spectra were recorded with a scan range of m/z 300–900 for positive and negative ions using ion electrospray ionization mass spectra (ESI-MS) on an Advion expression Compact mass spectrometer.

pH* measurements. The pH* values of NMR samples in D_2O were measured at 298 K after every recording of the NMR spectra, using a pH-metre LAQUAtwin B-712 calibrated with HORIBA buffer solutions at pH 4 and 7. pH* values are defined as the pH-metre readings in D_2O solutions without correction for effects of deuterium on the glass electrode. pH* values can be converted to pH values by using the equation pH = 0.929 × pH* + 0.42, suggested by Krezel and Bal.[1]

Conductivity. The conductivity values (μS/cm) of samples (ca. 1 mM) in methanol solutions were measured at 298 K, using a FiveEasy pH-metre equipped with a Crison micro-electrode calibrated with Crison buffer solutions at pH 4 and 7. Molar conductivity, Λ_M ($S{\cdot}cm^2/mol$), depends on the concentration of the electrolyte. To calculate it, the specific conductance is divided by concentration ($S{\cdot}cm^2/mol$).

UV–vis absorption spectroscopy. UV–vis absorption data were collected using an Agilent Cary 5000 UV–vis–NIR or an Agilent Cary 60 both equipped with temperature controller, using 1 cm path length quartz cuvettes (800 μL). Spectra were recorded at 298 K from 600 to 300 nm unless otherwise stated. Data were processed using OriginPro version 9.0.0 (OriginLab, Northampton, MA).

Single crystal X-Ray diffraction. Single suitable crystals of closed tether compounds **3C·PF_6** and dichlorido [Os(η^6:κ^1-$C_6H_5(CH_2)_3OH)Cl_2$], and open tether compounds **5·PF_6**, **8·PF_6**, **9**, **10**, **11** and **13**, were coated with mineral oil, mounted on Mitegen MicroMounts and measured in a Bruker D8 KAPPA APEX II diffractometer with CCD area-detector at 150K, equipped with graphite-monochromated Mo-Kα radiation source (λ = 0.71073 Å). The substantial redundancy in data allowed empirical absorption corrections (SADABS)[2] to be applied using multiple measurements of symmetry-equivalent reflections. Raw intensity data frames were integrated with the SAINT program, which also applied corrections for Lorentz and polarization effects. The Bruker SHELXTL Software Package was used for space group determination, structure

solution, and refinement.[3] The space group determination was based on a check of the Laue symmetry, and systematic absences were confirmed using the structure solution. The structures were solved by direct methods (SHELXL-2014/7),[4, 5] completed with different Fourier syntheses, and refined with full-matrix least-squares using SHELXS minimizing $\omega(F_o^2-F_c^2)^2$. Weighted R factors (R_w) and goodness of fit (S) are based on F^2; conventional R factors (R) are based on F. All non-H atoms were refined with anisotropic displacement parameters. Hydrogen atom positions were geometrically calculated and allowed to ride on their parent carbon or nitrogen atoms with fixed isotropic U. All scattering factors and anomalous dispersion factors are contained in the SHELXTL 6.10 program library. Mercury 3.9 was used for visualization and analysis of the crystal structures. Open tether compounds **5·PF$_6$**, **8·PF$_6$**, **9**, **10**, **11** and **13** and closed tether compounds **3C·PF$_6$** and dichlorido [Os(η^6:κ^1-$C_6H_5(CH_2)_3OH$)Cl_2], correspond to the CCDC identifiers 2026997–2027004, respectively. These data are provided free of charge by The Cambridge Crystallographic Data Centre. A summary of the crystal data collection and refinement parameters for all compounds is given in Table S4.

Experimental details for chemical reactions

Room or ambient temperature (RT) refers to 20–25 °C. Reactions involving heating were performed using blocks and a contact thermocouple. Under reduced pressure refers to the use of a Büchi Rotavapor® R-200/210 with a Büchi V-491 heating bath and a Büchi V-800/850 vacuum controller. The rotary evaporator condenser is fitted to Huber Minichiller 280 recirculating cooler filled with ethylene glycol and set to -5 °C. Microwave-assisted reactions were carried out using a Biotage Initiator+ microwave reactor, using the programme as described for individual syntheses in the appropriated microwave vials of different capacity depending on the reaction volume. The vials are able to work beyond 30 bar yet our reactions usually reached 5–15 bars.

Aqueous Solution Studies

Hydrolysis of the Os–Cl bond. Initial hydrolysis studies were carried out on **1**–**13** by ^{1}H NMR with the Os(II) compounds at ca. 5 mM in D_2O. Spectra were recorded at t_0 and at 24 h upon incubation at 310 K. ^{1}H NMR experiments of all samples were recorded again after 1 week at 298 K to assess further speciation and stability of the species in aqueous solution. Speciation of each complex into chlorido, aqua, and closed-tether species was quantified by integrating the signals of H_m (proton in *meta* position to the alcohol-substituted arene) in the ^{1}H NMR spectra.

pH-Dependence of Os–Cl hydrolysis. Hydrolysis studies were also carried out on complexes **1**, **2**, **5**, **8**, **9**, **10**, **11**, and **13** by ^{1}H NMR (5 mM Os) in unbuffered D_2O solutions with pH previously adjusted to 1, 4, 7 and 10. Spectra were recorded at t_0 (< 15 min) and at 24 h upon incubation at 310 K. Speciation of each complex into chlorido, aqua, and closed-tether species was quantified as above.

Kinetics of Os–Cl hydrolysis. Complexes **9**–**12** were dissolved in unbuffered D_2O to a final concentration of 5 mM. The spectra were recorded at various time intervals (t_0 < 5 min) at 300 ± 2, 310.00 ± 0.01 and 320.00 ± 0.01 K. The rate of hydrolysis was determined by fitting plots of concentrations (determined from ^{1}H NMR peak integrals) versus time to a pseudo first-order equation using OriginPro 9.0.0 program (OriginLab, Northampton, MA). The activation enthalpies ($\Delta H^{\ddagger}$) and activation entropies ($\Delta S^{\ddagger}$) were determined using the Eyring equation and plotting ln *k*/T vs 1/T, where the calculated slope and intercept in the linear fit were used to obtain ΔH and ΔS, respectively.

Hydrolysis of the Os–O bond. Complexes **2C**, **8C, 10C** and **11C** were dissolved in unbuffered solutions of D_2O (5 mM) at pH 1, 7 and 12 and the ^{1}H NMR were recorded at t_0 (< 15 min) and at 24 h upon incubation at 310 K. Speciation of each complex into chlorido, aqua, and closed-tether species was quantified by integrating the signals of H_m (proton in *meta* position to the alcohol-substituted arene) in the ^{1}H NMR spectra.

Additionally, the water-mediated reactivity of the Os–O bond in isolated closed tether complexes **2C**, **3C**, **8C** and **10C** was investigated by dissolving the Os(II) tether complexes (ca. 5 mM) in (i) 0.1 M DCl, and (ii) 0.1 M $DClO_4$. ^{1}H NMR spectra were recorded at t_0 (< 5 min) and t = 24 h at 298 K.

Calculation of pK_a* values. We determined the pK_a* values (pK_a values determined in D_2O solutions) of the two species susceptible of acid/base equilibria in aqueous solution: the open tether aqua/hydroxido adduct for complexes **1A**, **2A**, **2ARu**, **3A**, **3ARu**, **8A**, **12A** and **13A** of general formula $[Os/Ru(\eta^6\text{-}C_6H_5(CH_2)_3OH)(XY)(\mathbf{OH_2/OH})]^{n+/(n-1)+}$, and the Ru/Os-$\kappa^1$-bond alcohol/alkoxy group in the tether arm of closed tether complexes **1C**, **2C**, **2CRu**, **3C**, **3CRu**, **8C** and **12C** with general formula $[Os/Ru(\eta^6\text{:}\kappa^1\text{-}C_6H_5(CH_2)_3\mathbf{OH/O})(XY)]^{n+/(n-1)+}$.

pH Titration curves were traced by plotting the variation of the ^{1}H NMR chemical shifts corresponding to coordinated arene protons in closed and aqua adducts **1C**–**3C**, **3CRu**, **1A**–**3A** and **3ARu**, or chelating ligand protons in **8A**, **8C**, **12A**, **12C** and **13A**, over the 0–12 pH range. The pH* titration curves were fitted to the Henderson−Hasselbalch equation using the

OriginPro 9.0.0 program (OriginLab, Northampton, MA) with the assumption that the observed chemical shifts are weighted averages according to the populations of the protonated and deprotonated species.

Catalysis. Solutions containing 1 mM of complexes **1**, **2**, **3**, **5**, **8**–**13**; 2 mM sodium pyruvate and 100 mM sodium formate (1:2:100 ratio for catalyst/substrate/H-source) were prepared in D_2O and the pH adjusted to 4. Lactate formation mediated by Os(II) complexes was followed by ^{1}H NMR spectra recorded at 298 K at different times until the reaction was complete, whereby the pyruvate has disappeared. The solutions were incubated at 310 K at all times. Further experiments under similar conditions using a different concentration of sodium formate (ratio 1:2:400), a different incubation temperature (300, 320 and 333 K) and pH* values (3, 5, 7) were also carried out. Appropriate control experiments were also carried out to unambiguously implicate the osmium complex in the hydrogenation reaction. Molar ratios of pyruvate to lactate conversion were determined by integrating the ^{1}H NMR peaks corresponding to pyruvate (3H, singlet, 2.36 ppm) and lactate (3H, doublet, 1.33 ppm).

$$\text{Conversion (\% of lactate formed)} = \frac{I_{1.33}}{I_{1.33} + I_{2.36}}\, x\, 100$$

The turnover number (TON) was calculated as a function of time taking into account the conversion to lactate at different specific times (t) as follows.

$$\text{TON}_t = \frac{[\text{conversion}]_t}{100} \cdot \frac{[\text{substrate}]_0}{[\text{catalyst}]_0}; \text{TOF} \frac{\delta[\text{TON}]_t}{\delta \text{t}}$$

TON was calculated as the product of conversion (%) and the $[substrate]_0$ / $[catalyst]_0$ ratio.[6] Where $[substrate]_0$ and $[catalyst]_0$ are the concentration of pyruvate and osmium complex at the start of the reaction, 2 and 1 mM, respectively.

Transfer hydrogenation of pyruvate to lactate mediated by Os, and validation of lactate as LDH substrate. We followed a variation of the manufacture's protocol for lactate determination using L-Lactic Dehydrogenase from bovine heart (Catalogue Number L3916, Sigma Aldrich). Solutions containing 1.5 mM of **11**, 3 mM of sodium pyruvate and 600 mM of sodium formate (1:2:400 ratio for Os-catalyst:substrate:H-source) were prepared in ultrapure water, heated at 333 K and lactate was measured at different time points. Aliquots (200 µL) of these solutions were added to two parts (400 µL) of freshly prepared phosphate buffer solution containing NAD^+ (ca. 2 mM), LDH and hydrazine (0.5 mM, to capture readily formed pyruvate) at t_0 (less than 5 min), and

after 1, 2 and 4 h upon incubation. The resulting mixture was incubated for 15 min at 310 K and the UV–vis spectra recorded in the range 600–300 nm. The resulting newly formed NADH (as determined by UV–vis; λ 340 nm; Figure S39A) was direct confirmation of Os-mediated lactate production. Appropriate controls were recorded to ensure that lactate production only occurred as prompted by the Os complex (Figure S39A, lines 1–3).

In vitro cell studies

Cell culture. The human MDA-MB-231 and MCF7 breast cancer cell lines were purchased from American Type Culture Collection (ATCC). MDA-MB-231 was maintained in Dulbecco's modified Eagle's medium (DMEM) High Glucose (LabClinics) supplemented with 10% foetal bovine serum (Gibco, Life Technologies), 1% of 2 mM GlutaMAX-I (Gibco, Life Technologies) and 1% penicillin/streptomycin (VWR), while MCF7 was maintained in Dulbecco's modified Eagle's medium (DMEM) Low Glucose (LabClinics) containing the same supplements. Human colorectal carcinoma cells HCT116 were obtained from ATCC and cultured in McCoy's 5A medium (LabClinics) also supplemented with 10% foetal bovine serum, 1% of 2 mM GlutaMAX-I and 1% penicillin/streptomycin.

All cell lines were grown as adherent monolayers at 37 °C in a 5% CO_2 humidified atmosphere, cultured for at least 10–14 days prior to use, and sub-cultured at approximately 70–80% confluency. Experiments were conducted on exponentially growing cells.

Exposure to Os(II) compounds. Stock solutions of the Os(II) complexes were weighed using an analytical balance XS105DU (Mettler Toledo AG) and then prepared by dissolving the compounds **1**–**13** and closed complexes **2C**, **3C**, **10C**, **11C**, and **13C**, in 100% sterile DMSO (Sigma-Aldrich) to assist dissolution to obtain a concentration of 40 mM, and stored at -20 ºC. All experiments were performed in parallel with DMSO as vehicle control. Os(II) complexes were then diluted into supplemented media to the desired working concentrations. The maximum final concentration of DMSO in the cell-seeded wells was 1.25%, which had no effect in cell viability as corroborated by appropriate controls. Cisplatin, a metal-based cytotoxic agent used to treat various types of cancer in the clinic, was used as a positive control in cell viability assays. Cisplatin also required DMSO to assist dissolution, followed by dilution into saline (0.9% NaCl).

Cell viability. For the evaluation of cellular cytotoxicity, 5,000 MDA-MB-231, 1,000 HCT116, and 5,000 MCF7 cells were seeded in 96-well plates (VWR) and grown for 48 h at 37 °C in complete medium. Solutions of osmium and ruthenium complexes were prepared by serial dilution in culture medium to obtain a final concentration ranging from 1 to 400 μM (the maximum concentration of DMSO to which cells were exposed never exceeded 1.25% v/v), and the cells were incubated for 24 h at 37ºC. Following 24 h of drug exposure, media containing Os(II) complexes were removed by suction and cells were washed with PBS (Fisher Scientific), supplied with fresh media, and allowed to grow for 72 h. The protein content (proportional to living cells in culture) was then measured using the Sulforhodamine B (SRB) assay[7, 8] using a UV–visible spectrophotometer (BioTek Sinergy H4 microplate reader) at 510 nm. The percentage of surviving cells was calculated from the ratio of absorbance of treated to non-treated cells (control cells). The IC_{50} value was calculated as the concentration reducing the proliferation of cell population by 50% compared to non-treated cells, and is presented as a mean ± SD of three to four independent experiments of four replicates each. Data were processed using Microsoft Excel and sigmoidal curves fitted using OriginPro 9.0.

Cellular accumulation in MDA-MB-231 and HCT116 cells. MDA-MB-231 and HCT116 cells were seeded at a density of 2.5×10^5 and 1.5×10^5 cells/60 mm Petri dish, respectively, in 4 mL of culture medium (four dishes were prepared per compound tested, and four untreated control dishes). After 72 h of incubation at 37 ºC, cells were exposed to the Os(II) complexes after the removal of the medium used for seeding of the cells. Solutions of the Os(II) compounds were prepared by diluting a freshly prepared stock solution (40 mM in DMSO) of the corresponding complex in medium to a final concentration of 50 μM. After 24 h of drug exposure at 37 ºC in a 5% CO_2 incubator, the drug-containing medium was removed, and the cells were washed with PBS. One dish from each Os(II) complex treatment and untreated cells was trypsinised, and counted using a hemocytometer. Digestion in acid was avoided to prevent osmium oxidation as advised by Klose et al. and RIPA buffer lysis was used instead.[9] For the rest of the dishes, the cells were lysed with 1 mL of RIPA lysis Buffer (ThermoFisher Scientific) per dish for 24 h at 4 °C. Lysed cells were then scrapped and centrifuged for 5 min at 1000 rpm. Supernatants (800 μL) were transferred to a 15 mL tube. Additional 700 μL of ultrapure water were added to the pellets, which were re-suspended and centrifuged for another 5 min at 1,000 rpm. Supernatants (500 μL) were transferred to the 800 μL in the 15 mL tube, and finally, additional 700 μL of ultrapure water completed a total volume of 2 mL. These 2 mL samples were then processed for ICP-MS analysis for ^{192}Os content. Osmium content was normalised

to 10^6 cells per sample. Each value represents the mean ± SD. All values were compared to the untreated controls.

ICP-MS Analysis. ICP-MS analyses were carried out on a Perkin Elmer NexION 300 ICP-MS instrument. The water used for ICP-MS analysis was purified using a Millipore Milli-Q® Element System. The osmium standard (SCP Science, 1000 ppm, 10% HCl solution) was diluted with ultrapure water to 10 ppm. The standards for calibration were freshly prepared by diluting this stock solution with 2% HNO_3 + 0.5% HCl (v/v) in ultrapure water. The concentrations used for the calibration of the instrument were 500, 50, 5, 0.5, 0.05 ppb. Samples were diluted 1:10 with 2% HNO_3 + 0.5% HCl (v/v) in ultrapure water. All calibrants and samples contained 30 ppb Re and 30 ppb Rh as internal standards.

Lactate Determination in MDA-MB-231 and MCF7 Cells. MDA-MB-231 and MCF7 cells were seeded at a density of 0.8 x 10^5 cells/60 mm Petri dish in 4 mL of culture medium (four dishes were prepared per compound tested, and four untreated control dishes). After 24 h of incubation at 37 ºC, cells were exposed to 300 μM **11**, 10 mM formate with 1 (MCF7) or 2 mM (MDA-MB-231) pyruvate upon removal of the medium used for seeding of the cells. Solution of **11** was prepared by diluting a freshly prepared stock solution (6 mM in ultrapure water) in medium to a final concentration of 300 μM. After 12 and 24 h of drug exposure at 37 ºC in a 5% CO_2 incubator, the drug-containing medium was removed, and the cells were washed with cold PBS. Then, the cells were lysed with cold RIPA Buffer (Thermo Scientific) by incubation for 5 min on ice and subsequent scraping, followed by centrifugation at 14,000 × g for 15 min at 4 °C. The supernatant was collected and 450 μL were transferred into a centrifuge tube containing 900 μL of 10% trichloroacetic acid (TCA) for deproteination. Samples were vortexed for 30 s, incubated for 5 min on ice and centrifuged at 1,500 × g for 10 min. Then, the clear TCA supernatant was subjected to lactate determination as follows. Supernatants were added two-parts of ca. 2 mM NAD^+ in hydrazine-containing glycine buffer (0.6 M glycine and 0.5 M hydrazine; Sigma-Aldrich). These solutions served as blanks. Upon addition of LDH and following 15 min incubation at 310 K, the UV–vis trace (600–300 nm) revealed the formation of NADH (λ 340 nm), which is directly proportional to the amount of L-lactate in the deproteinated supernatant cell lysate. Quantification of NADH was possible by the use of appropriate L-lactate calibrants at concentrations between 0.9–9 mM, treated in the exact same conditions as the samples.

Statistical Analysis. All statistical analysis was performed using R Statistical Software (version 3.3.2 (2016-10-31); R Foundation for Statistical Computing, Vienna, Austria) by *one*-way *analysis* of variance (***ANOVA***) (*$p<0.05$, **$p<0.01$, and ***$p<0.001$) unless otherwise stated.

Synthesis and Characterization

Synthesis of ligands

4-Methylpicolinic acid was synthesized and purified as previously reported by van Rijt et al.,[10] while picolinic acid, 6-methylpicolinic acid and 2,4-pyridinedicarboxylic acid were acquired from commercial sources and used without further purification. The four electron-rich N,N'-iminomethylpyridine ligands were synthesized by the condensation reaction between 2-pyridinecarboxaldhehyde and the corresponding substituted aniline (or phenethylamine) in DCM. The imine condensation affords Schiff-base ligands directly bound to a pyridine, which were used without further purification for the preparation of the Os(II) complexes.

3-(1,4-Cyclohexadien-1-yl)propanoic acid

Birch reduction of 3-phenylpropanoic acid was carried out to afford 3-(cyclohexa-1,4-dien-1-yl)propanoic acid following a reported procedure for a similar reduction product.[11] Briefly, 3-phenylpropanoic acid (9.9 g, 66 mmol) reacted with Li(s) in *t*-BuOH, to afford 9.03 g of the reduced cyclohexadiene, which was used in the synthesis of 3-(1,4-cyclohexadien-1-yl)-1-propanol without further purification.

^{1}H NMR (400 MHz, $CDCl_3$, δ): 5.75 – 5.66 (m, 2H, ArC*H*), 5.47 (d, J = 1.1 Hz, 1H, ArC*H*), 2.73 – 2.56 (m, 4H, ArCH_2), 2.50 (dd, J = 8.6, 6.9 Hz, 2H, CH_2COOH), 2.31 (q, J = 7.7 Hz, 2H, CH_2).

3-(1,4-Cyclohexadien-1-yl)-1-propanol

3-(1,4-Cyclohexadien-1-yl)propanoic acid (1.00 g) was reduced to the corresponding alcohol by the addition of $LiAlH_4$ (750 mg, ca. 3 mol equiv.) in anhydrous diethyl ether (45 mL) at 273 K for 2 h.[12] The reaction was then quenched with 5 mL of water and extracted with ethyl acetate (3 x 50 mL). The combined organic extracts were washed with brine, dried over $MgSO_4$, filtered through a cotton filter, and dried under vacuum. The crude product (yellow oil) was used in the next step, the synthesis of dimer $[Os(\eta^6\text{-}C_6H_5(CH_2)_3OH)(\mu\text{-}Cl)Cl]_2$, without further purification (1.25 g).

^{1}H NMR (400 MHz, $CDCl_3$, δ): 5.71 (s, 2H, ArC*H*), 5.47 (s, 1H, ArC*H*), 3.72 – 3.62 (m, 2H, CH_2OH), 2.75 – 2.56 (m, 4H, ArCH_2), 2.05 (t, J = 7.6 Hz, 2H, CH_2), 1.70 (dd, J = 8.2, 6.8 Hz, 2H, CH_2).

Cyclohexa-2,5-diene-1-carboxylic acid

Birch reduction of benzoic acid was carried out to afford cyclohexa-1,3-diene-1-carboxylic acid following a reported procedure for a similar reduction product.[11] Briefly, benzoic acid (5 g, 41 mmol) reacted with Na(s) in dry EtOH, to afford 4.75 g of the reduced cyclohexadiene, which was used in the synthesis of ethyl cyclohexa-1,3-diene-1-carboxylate without further purification.

^{1}H NMR (400 MHz, $CDCl_3$, δ): 5.93 (ddd, J = 10.4, 5.2, 3.2 Hz, 2H, ArC*H*), 5.84 (ddt, J = 10.4, 3.6, 1.9 Hz, 2H, ArC*H*), 3.87 – 3.74 (m, 1H, ArC*H*), 2.82 – 2.60 (m, 2H, ArCH_2).

Ethyl cyclohexa-1,3-diene-1-carboxylate

The esterification of cyclohexa-1,3-diene-1-carboxylic acid (4.5 g, 36.7 mmol) was carried out following a reported procedure.[11] The cyclohexadiene was heated under reflux in dry ethanol and sulfuric acid for 18 h under nitrogen atmosphere. After that, the pH is adjusted to ca. 8 by addition of a large excess of NaOH. The reaction was then extracted with dichloromethane (3 x 70 mL). The combined organic layers were combined washed with brine, dried over $MgSO_4$, filtered through a cotton filter, and dried under vacuum. The crude product (yellow oil) was distilled (3.63 g), and then used to synthesise the Ru(II) dimer necessary to follow Reaction Pathway 2 (vide infra) for the synthesis of **2Ru** and **3Ru**.

^{1}H NMR (400 MHz, $CDCl_3$-*d*, δ): 7.02 – 6.84 (m, 1H, ArC*H*), 6.37 (ddd, J = 9.9, 3.5, 1.9 Hz, 1H, ArC*H*), 5.90 (dtd, J = 9.8, 4.4, 0.9 Hz, 1H, ArC*H*), 4.22 (q, J = 7.1 Hz, 2H, CH_2), 2.43 – 2.27 (m, 2H, ArCH_2), 2.25 – 2.08 (m, 2H, ArCH_2), 1.30 (t, J = 7.1 Hz, 3H, CH_3).

***N*-phenyl-1-(pyridin-2-yl)methanimine (Ph-impy)**

2-Pyridinecarboxaldehyde (480 µL, 5 mmol) was dissolved in 3 mL of dry DCM and left to stir at RT overnight. Aniline (640 µL, 7 mmol) was then added and the reaction was stirred at RT under argon atmosphere using 4 Å molecular sieves for 2 days, in a similar procedure to the described previously.[13] The solution was filtered, the solvent removed by rotary evaporation to afford ca. 500 mg of a yellow oil that was no further purified.

^{1}H NMR (400 MHz, $CDCl_3$, δ): 8.72 (ddd, J = 4.8, 1.7, 0.9 Hz, 1H), 8.62 (d, J = 4.5 Hz, 1H), 8.21 (dt, J = 7.9, 1.0 Hz, 1H), 7.86 – 7.78 (m, 1H), 7.40 (dddd, J = 14.7, 7.5, 4.8, 1.5 Hz, 3H), 7.32 – 7.27 (m, 3H).

***N*-(4-(tert-butyl)phenyl)-1-(pyridin-2-yl)methanimine (tBuPh-impy)**

Synthesis as for *N*-phenyl-1-(pyridin-2-yl)methanimine using 2-pyridinecarboxaldehyde (210 µL, 2 mmol) and 4-tert-Butylaniline (319 µL, 2 mmol) overnight. An orange oil was obtained (417 mg) that was used for the synthesis of complex [Os(η^6-$C_6H_5(CH_2)_3OH$)(tBuPh-impy))Cl]Cl without further purification.

^{1}H NMR (400 MHz, $CDCl_3$, δ): 8.71 (dd, J = 4.1, 0.8 Hz, 1H), 8.64 (s, 1H), 8.21 (d, J = 7.9 Hz, 1H), 7.81 (td, J = 7.5, 1.3 Hz, 1H), 7.46 – 7.42 (m, 2H), 7.36 (ddd, J = 7.5, 4.8, 1.2 Hz, 1H), 7.27 (dd, J = 5.1, 3.0 Hz, 2H), 1.35 (s, 9H).

***N*-(2-bromophenyl)-1-(pyridin-2-yl)methanimine (BrPh-impy)**

Synthesis as for *N*-phenyl-1-(pyridin-2-yl)methanimine using 2-pyridinecarboxaldehyde (210 µL, 2 mmol) and 2-bromoaniline (226 µL, 2 mmol). 452 mg of yellow-orange oil were obtained that was used for the synthesis of [Os(η^6-$C_6H_5(CH_2)_3OH$)(BrPh-impy)Cl]Cl without further purification.

^{1}H NMR (400 MHz, $CDCl_3$, δ): 8.76 – 8.68 (m, 1H), 8.50 (s, 1H), 8.31 (t, J = 7.4 Hz, 1H), 7.84 (td, J = 7.5, 1.2 Hz, 1H), 7.65 (dd, J = 7.9, 1.2 Hz, 1H), 7.40 (ddd, J = 7.5, 4.8, 1.2 Hz, 1H), 7.35 (td, J = 7.7, 1.3 Hz, 1H), 7.14 – 7.07 (m, 2H).

***N*-phenethyl-1-(pyridin-2-yl)methanimine (PhEt-impy)**

Synthesis as for *N*-phenyl-1-(pyridin-2-yl)methanimine using 2-pyridinecarboxaldehyde (480 µL, 5 mmol), phenylethylamine (640 µL, 5 mmol) and the addition of approx. 300 mg of $MgSO_4$ in a similar procedure to the described previously.[13] The formation of the product was followed by TLC. The reaction was stirred at room temperature for 6 days. Approximately 1 g of green-yellow oil was obtained and used for the synthesis of complex [Os(η^6-$C_6H_5(CH_2)_3OH$)(PhEt-impy)Cl]Cl without further purification.

^{1}H NMR (400 MHz, $CDCl_3$, δ): 8.68 – 8.58 (m, 1H), 8.30 (s, 1H), 7.98 (d, J = 7.9 Hz, 1H), 7.75 (td, J = 7.6, 1.4 Hz, 1H), 7.34 – 7.31 (m, 1H), 7.30 – 7.27 (m, 2H), 7.24 (d, J = 6.8 Hz, 2H), 7.23 – 7.17 (m, 1H), 3.93 (td, J = 7.7, 1.3 Hz, 2H), 3.04 (t, J = 7.6 Hz, 2H).

Synthesis of metal complexes

DIMERS

$[Os(\eta^6\text{-}C_6H_5(CH_2)_3OH)(\mu\text{-}Cl)Cl]_2$

$OsCl_3 \cdot 3H_2O$ (170 mg, 0.49 mmol) and 3-(1,4-cyclohexadien-1-yl)-1-propanol (140 µL, ca. 2 mol equiv.) were suspended in 4 mL of acetone/water (3:1) in an 11 mL microwave vial. The reaction mixture was heated at 413 K for 40 min in the microwave reactor. The resulting dark suspension was centrifuged and the precipitate discarded. The decanted supernatant was reduced under vacuum to a fourth of its volume and addition of some drops of diethyl ether triggered the precipitation of a pale brown powder. The supernatant was then removed with a pipette and the solid washed with diethyl ether and dried on vacuum. Yield: 175 mg, 0.22 mmol, 91%.

^{1}H NMR (400 MHz, DMSO-d_6, δ): 6.19 (t, J = 5.5 Hz, 2H, Ar*H*), 6.02 (d, J = 5.2 Hz, 1H, Ar*H*), 5.95 (d, J = 5.7 Hz, 2H, Ar*H*), 4.55 (t, J = 5.1 Hz, 1H, O*H*), 3.45 (t, J = 6.3 Hz, 2H, CH_2OH), 2.44 – 2.38 (m, 2H, ArCH_2), 1.78 – 1.68 (m, 2H, CH_2). **^{13}C{^{1}H} NMR** (101 MHz, DMSO-d_6, δ): 100.33 (s, Ar*C*), 80.73 (s, Ar*C*H), 76.44 (s, Ar*C*H), 74.91 (s, Ar*C*H), 60.10 (s, *C*H_2OH), 32.47 (s, *C*H_2), 29.25 (s, Ar*C*H_2).

Two different reaction pathways, leading to the same Ru dimer, were used as follows.

<u>Reaction Pathway 1</u>

$[Ru(\eta^6\text{-}C_6H_5(CH_2)_3OH)(\mu\text{-}Cl)Cl]_2$

Synthesis as for $[Os(\eta^6\text{-}C_6H_5(CH_2)_3OH)(\mu\text{-}Cl)Cl]_2$ using $RuCl_3 \cdot 3H_2O$ (140 mg, 0.53 mmol) and 3-(1,4-cyclohexadien-1-yl)-1-propanol (230 µL, ca. 3equiv.) in 4 mL of acetone/water (3:1). The reaction mixture was heated at 413 K for 20 min in the microwave reactor. Yield: 140 mg, 0.23 mmol, 84%.

^{1}H NMR (400 MHz, DMSO-d_6, δ): 5.69 (t, J = 5.7 Hz, 2H, Ar*H*), 5.60 (t, J = 5.5 Hz, 1H, Ar*H*), 5.45 (d, J = 5.8 Hz, 2H, Ar*H*), 3.60 – 3.54 (m, 2H, CH_2OH), 2.62 – 2.58 (m, 2H, ArCH_2), 1.85 – 1.79 (m, 2H, CH_2).

Reaction Pathway 2

[Ru(η^6-etb)(μ-Cl)Cl]$_2$

$RuCl_3 \cdot 3H_2O$ (100 mg, 0.383 mmol) and ethyl cyclohexa-1,3-diene-1-carboxylate (166 µL, 1.2 mmol) were suspended in 3 mL of ethanol. The reaction mixture was heated at 393 K for 5 min in the microwave reactor. Yield: 111 mg, 0.172 mmol, 85%.

^{1}H NMR (400 MHz, $CDCl_3$, δ): 6.47 (d, J = 6.2 Hz, 2H, Ar*H*), 5.97 (t, J = 5.6 Hz, 1H, Ar*H*), 5.78 (t, J = 5.9 Hz, 2H, Ar*H*), 4.47 (q, J = 7.1 Hz, 2H, C*H*$_2$), 1.42 (t, J = 7.1 Hz, 3H, C*H*$_3$).

[Ru(η^6-C$_6$H$_5$(CH$_2$)$_3$OH)(μ-Cl)Cl]$_2$

[Ru(η^6-etb)(μ-Cl)Cl]$_2$ (47 mg, 0.07 mmol) and 3-phenyl-1-propanol (2 mL) were suspended in 1.5 mL of 1,2-dichloroethane. The reaction mixture was heated at 413 K for 30 min in the microwave reactor. A red powder was obtained. Yield: 34 mg, 0.55 mmol, 79%.

^{1}H NMR (400 MHz, CD_3CN-*d*$_3$, δ): 5.69 (t, J = 5.7 Hz, 2H, Ar*H*), 5.60 (d, J = 5.5 Hz, 1H, Ar*H*), 5.45 (d, J = 5.8 Hz, 2H, Ar*H*), 3.58 (dd, J = 11.6, 6.1 Hz, 2H, C*H*$_2$OH), 2.66 – 2.54 (m, 2H, ArC*H*$_2$), 1.83 (ddd, J = 13.8, 10.2, 6.2 Hz, 2H, C*H*$_2$).

MONOMERS

Complexes **1**–**13**, of general formula $[Os(\eta^6\text{-}C_6H_5(CH_2)_3OH(XY)Cl]^{+/0}$, were synthesized from the dimeric precursor $[Os(\eta^6\text{-}C_6H_5(CH_2)_3OH)(\mu\text{-}Cl)Cl]_2$, using procedures similar to those reported previously.[10, 11, 14-19] Closed tether complexes **2C**, **3C**, **4C**, **8C**, **10C**, **11C** and **13C** were successfully isolated. Complexes **1C**, **5C**, **6C**, **7C**, **9C** and **12C**, albeit not separated from their analogue chlorido and aqua species, were obtained in aqueous solution

$[Os(\eta^6\text{-}C_6H_5(CH_2)_3OH)(en)Cl]Cl$ (1)

$[Os(\eta^6\text{-}C_6H_5(CH_2)_3OH)(\mu\text{-}Cl)Cl]_2$ (35 mg, 0.044 mmol) and ethylenediamine (en; 6 µL, 0.09 mmol) were dissolved in 3 mL of dry EtOH and heated at 363 K overnight. The solution was filtered and the volume reduced to a fourth, then Et_2O was added to allow the precipitation of a brown powder which was filtered, washed with diethyl ether and dried in the vacuum line. Yield: 32 mg, 0.07 mmol, 79%.

^{1}H NMR (400 MHz, MeOD-d_4, δ): 6.86 (bs, 2H, NH_2), 5.90 (t, J = 5.3 Hz, 2H, Ar*H*), 5.77 (t, J = 5.1 Hz, 1H, Ar*H*), 5.74 (d, J = 5.5 Hz, 2H, Ar*H*), 4.60 (s, 2H, NH_2), 3.63 (t, J = 6.3 Hz, 2H, CH_2OH), 2.69 – 2.61 (m, 2H, enCH_2), 2.57 – 2.51 (m, 2H, ArCH_2), 2.40 – 2.31 (m, 2H, enCH_2), 1.90 – 1.82 (m, 2H, CH_2). **^{13}C{^{1}H} NMR** (101 MHz, MeOD-d_4, δ): 95.09 (s, Ar*C*), 75.29 (s, Ar*C*H), 73.06 (s, Ar*C*H), 70.35 (s, Ar*C*H), 61.97 (s, *C*H_2OH), 47.19 (s, en*C*H_2), 34.41 (s, *C*H_2), 30.88 (s, Ar*C*H_2). **MS (ESI)**: m/z calcd for $C_{11}H_{20}ClN_2OOs$ $[M]^+$ 423.1; found 423.1 and calcd for $C_{11}H_{21}N_2OOs$ $[M\text{-}Cl\text{-}H]^+$ 387.1; found 387.1. **Elemental analysis**: Calcd for $C_{11}H_{20}Cl_2N_2OOs$ (457.42) C, 28.88; H, 4.41; N 6.12%. Found C, 29.09; H, 4.43; N 6.22%.

$[Os(\eta^6\text{:}\kappa^1\text{-}C_6H_5(CH_2)_3O)(en)]^+$ (1C)

$[Os(\eta^6\text{-}C_6H_5(CH_2)_3OH)(en)Cl]Cl$ (20 mg, 0.044 mmol) and $AgNO_3$ (15.6 mg, 0.09 mmol) were suspended in 3 mL of dry methanol and stirred at 343 K for 48 h. The solution was then filtered over a pad of Celite, the solvent was reduced in the rotary evaporator to approximately a fourth of the initial volume, and a red powder precipitated by addition of some drops of diethyl ether. The supernatant was removed with a pipette and the red solid was washed with Et_2O and dried under vacuum. The red solid contained 48% of closed tether complex $[Os(\eta^6\text{:}\kappa^1\text{-}C_6H_5(CH_2)_3O)(en)]^+$, characterised by ^{1}H NMR below.

^{1}H NMR (400 MHz, MeOD-d_4, δ): 6.81 (bs, 2H, NH_2), 6.00 (t, J = 5.3 Hz, 2H, Ar*H*), 5.71 (d, J = 5.4 Hz, 2H, Ar*H*), 5.40 (t, J = 5.1 Hz, 1H, Ar*H*), 4.35 (bs, 2H, NH_2), 3.71 – 3.66 (m, 2H,

C*H*$_2$OH), 2.63 – 2.57 (m, 2H, enC*H*$_2$), 2.52 (dd, J = 18.1, 10.1 Hz, 2H, ArC*H*$_2$), 2.46 – 2.32 (m, 2H, enC*H*$_2$), 1.94 (dd, J = 12.2, 9.2 Hz, 2H, C*H*$_2$).

[Os(η^6-C$_6$H$_5$(CH$_2$)$_3$OH)(bipy)Cl]Cl (2)

[Os(η^6-C$_6$H$_5$(CH$_2$)$_3$OH)(μ-Cl)Cl]$_2$ (32 mg, 0.04 mmol) was dissolved in 3 mL of dry acetone. 2,2'-Bipyridine (bipy; 13 mg, 0.08 mmol) was added to the solution and stirred at RT overnight. The solution was centrifuged and the supernatant removed with a pipette; the solid was washed several times with diethyl ether and dried in vacuum. Yellow powder. Yield: 40 mg, 0.07 mmol, 90%.

^{1}H NMR (400 MHz, DMSO-*d*$_6$, δ): 9.51 (d, J = 5.4 Hz, 2H, bipy*H*), 8.74 (d, J = 8.1 Hz, 2H, bipy*H*), 8.28 (t, J = 7.3 Hz, 2H, bipy*H*), 7.75 (t, J = 6.3 Hz, 2H, bipy*H*), 6.44 (t, J = 5.6 Hz, 2H, Ar*H*), 6.20 (d, J = 5.9 Hz, 2H, Ar*H*), 6.02 (t, J = 5.4 Hz, 1H, Ar*H*), 4.58 (t, J = 5.0 Hz, 1H, O*H*), 3.44 (dd, J = 11.4, 6.1 Hz, 2H, C*H*$_2$OH), 2.57-2.45 (m, 2H, ArC*H*$_2$), 1.77 – 1.65 (m, 2H, C*H*$_2$). **^{13}C{^{1}H} NMR** (101 MHz, DMSO-*d*$_6$, δ): 155.73 (s, bipy*C*H), 155.29 (s, bipy*C*), 139.97 (s, bipy*C*H), 128.19 (s, bipy*C*H), 123.83 (s, bipy*C*H), 99.39 (s, Ar*C*), 80.70 (s, Ar*C*H), 73.96 (s, Ar*C*H), 72.55 (s, Ar*C*H), 60.00 (s, *C*H$_2$OH), 32.85 (s, *C*H$_2$), 29.46 (s, Ar*C*H$_2$). **MS (ESI)**: m/z calcd for C$_{19}$H$_{20}$ClN$_2$OOs [M]$^+$ 519.1; found 519.2. **Elemental analysis**: Calcd for C$_{19}$H$_{20}$Cl$_2$N$_2$OOs (553.51) C, 41.23; H, 3.64; N 5.06%. Found C, 40.93; H, 3.58; N 4.72%.

[Os(η^6:κ^1-C$_6$H$_5$(CH$_2$)$_3$O)(bipy)]NO$_3$ (2C)

Synthesis as for **1C** using [Os(η^6-C$_6$H$_5$(CH$_2$)$_3$OH)(bipy)Cl]Cl (30 mg, 0.05 mmol). A red powder was isolated that corresponded to closed tether complex [Os(η^6:κ^1-C$_6$H$_5$(CH$_2$)$_3$O)(bipy)]NO$_3$. Yield: 11 mg, 0.02 mmol, 56%.

^{1}H NMR (400 MHz, DMSO-*d*$_6$, δ): 9.41 (d, J = 5.6 Hz, 2H, bipy*H*), 8.71 (t, J = 10.4 Hz, 2H, bipy*H*), 8.28 (t, J = 7.3 Hz, 2H, bipy*H*), 7.69 (t, J = 6.1 Hz, 2H, bipy*H*), 6.28 (t, J = 5.5 Hz, 2H, Ar*H*), 5.79 (d, J = 5.5 Hz, 2H, Ar*H*), 5.59 (t, J = 5.4 Hz, 1H, Ar*H*), 3.26 (d, J = 8.5 Hz, 2H, C*H*$_2$OH), 2.67 – 2.61 (m, 2H, ArC*H*$_2$), 1.76 (s, 2H, C*H*$_2$). **^{13}C{^{1}H} NMR** (101 MHz, DMSO-*d*$_6$, δ): 155.40 (s, bipy*C*), 154.52 (s, bipy*C*H), 139.51 (s, bipy*C*H), 127.76 (s, bipy*C*H), 123.74 (s, bipy*C*H), 101.21 (s, Ar*C*), 80.76 (s, Ar*C*H), 69.52 (s, Ar*C*H), 69.03 (s, *C*H$_2$O), 64.98 (s, Ar*C*H), 34.31 (s, *C*H$_2$), 28.57 (s, Ar*C*H$_2$). **MS (ESI)**: m/z calcd for C$_{19}$H$_{19}$N$_2$OOs [M]$^+$ 483.1; found 483.2. **Elemental analysis**: Calcd for C$_{19}$H$_{19}$N$_3$O$_4$Os·0.5H$_2$O (552.59) C, 41.30; H, 3.65; N 7.60%. Found C, 41.12; H, 3.66; N 7.87.

[Os(η^6-C$_6$H$_5$(CH$_2$)$_3$OH)(phen)Cl]Cl (3)

Synthesis as for **2** using [Os(η^6-C$_6$H$_5$(CH$_2$)$_3$OH)(μ-Cl)Cl]$_2$ (30 mg, 0.04 mmol) and 1,10-phenanthroline (phen; 13 mg, 0.08 mmol). Yellow powder. Yield: 35 mg, 0.06 mmol, 76%.

^{1}H NMR (400 MHz, DMSO-*d*$_6$, δ): 9.89 (d, J = 4.5 Hz, 2H, phen*H*), 8.93 (d, J = 7.3 Hz, 2H, phen*H*), 8.34 (s, 2H, phen*H*), 8.15 (dd, J = 8.2, 5.3 Hz, 2H, phen*H*), 6.57 (t, J = 5.7 Hz, 2H, Ar*H*), 6.34 (d, J = 5.8 Hz, 2H, Ar*H*), 6.03 (t, J = 5.4 Hz, 1H, Ar*H*), 4.57 (t, J = 5.0 Hz, 1H, O*H*), 3.45 (dd, J = 11.4, 6.1 Hz, 2H, C*H*$_2$OH), 2.53-2.48 (m, 2H, ArC*H*$_2$ overlapped with DMSO), 1.75 (dd, J = 14.9, 6.9 Hz, 2H, C*H*$_2$). **^{13}C{^{1}H} NMR** (101 MHz, DMSO-*d*$_6$, δ): 155.80 (s, phen*C*H), 146.35 (s, phen*C*), 138.95 (s, phen*C*H), 130.25 (s, phen*C*), 127.69 (s, phen*C*H), 126.84 (s, phen*C*H), 98.82 (s, Ar*C*), 80.08 (s, Ar*C*H), 73.87 (s, Ar*C*H), 72.44 (s, Ar*C*H), 60.01 (s, *C*H$_2$OH), 32.90 (s, *C*H$_2$), 29.49 (s, Ar*C*H$_2$). **MS (ESI)**: m/z calcd for C$_{21}$H$_{20}$ClN$_2$OOs [M]$^+$ 543.1; found 543.2. **Elemental analysis**: Calcd for C$_{21}$H$_{20}$Cl$_2$N$_2$OOs (577.53) C, 43.68; H, 3.49; N 4.85%. Found C, 44.11; H, 3.52; N 4.79%.

[Os(η^6:κ^1-C$_6$H$_5$(CH$_2$)$_3$O)(phen)]NO$_3$ (3C)

Synthesis as for **1C** using [Os(η^6-C$_6$H$_5$(CH$_2$)$_3$OH)(phen)Cl]Cl (30 mg, 0.05 mmol). Red powder. Complex **3C** was redissolved in methanol containing an excess of NH$_4$PF$_6$ and clear light brown crystals suitable for X-ray diffraction of complex [Os(η^6:κ^1-C$_6$H$_5$(CH$_2$)$_3$O)(phen)]PF$_6$ (**3C·PF$_6$**) were obtained at 298 K. Yield: 26 mg, 0.045 mmol, 88%.

^{1}H NMR (400 MHz, DMSO-*d*$_6$, δ): 9.78 (d, J = 4.4 Hz, 2H, phen*H*), 8.91 (d, J = 8.1 Hz, 2H, phen*H*), 8.30 (s, 2H, phen*H*), 8.08 (dd, J = 8.2, 5.3 Hz, 2H, phen*H*), 6.43 (t, J = 5.5 Hz, 2H, Ar*H*), 5.95 (d, J = 5.4 Hz, 2H, Ar*H*), 5.50 (t, J = 5.3 Hz, 1H, Ar*H*), 3.18 (t, J = 7.3 Hz, 2H, C*H*$_2$OH), 2.66 (d, J = 6.3 Hz, 2H, ArC*H*$_2$), 1.77 (s, 2H, C*H*$_2$). **^{13}C{^{1}H} NMR** (101 MHz, MeOD-*d*$_4$, δ): 155.86 (s, phen*C*H), 148.69 (s, phen*C*), 140.13 (s, phen*C*H), 132.41 (s, phen*C*), 128.89 (s, phen*C*H), 127.84 (s, phen*C*H), 102.50 (s, Ar*C*), 82.56 (s, Ar*C*H), 69.71 (s, *C*H$_2$O), 68.98 (s, Ar*C*H), 67.64 (s, Ar*C*H), 34.40 (s, *C*H$_2$), 30.26 (s, Ar*C*H$_2$). **MS (ESI)**: m/z calcd for C$_{21}$H$_{19}$N$_2$OOs [M]$^+$ 507.1; found 507.2. **Elemental analysis**: Calcd for C$_{21}$H$_{19}$N$_3$O$_4$Os·2H$_2$O (603.66) C, 41.79; H, 3.84; N 6.96%. Found C, 41.94; H, 3.75; N 6.83%. **Λ$_M$** (Os 10^{-3} M in methanol, 298 K) = 106 S·cm^2/·mol, electrolyte 1:1 in solution.

[Os(η^6-C$_6$H$_5$(CH$_2$)$_3$OH)(ampy)Cl]Cl (4)

Synthesis as for **1** using [Os(η^6-C$_6$H$_5$(CH$_2$)$_3$OH)(μ-Cl)Cl]$_2$ (30 mg, 0.038 mmol) and 1-(2-pyridinyl)methanamine (ampy; 8.7 μL, 0.084 mmol). Yield: 29 mg of dark-red powder, 0.06 mmol, 75%.

^{1}H NMR (400 MHz, MeOD-*d*$_4$, δ): 9.06 (d, J = 5.3 Hz, 1H, ampy*H*), 7.94 (td, J = 7.8, 1.4 Hz, 1H, ampy*H*), 7.61 (d, J = 7.5 Hz, 1H, ampy*H*), 7.44 (t, J = 6.7 Hz, 1H, ampy*H*), 6.13 (t, J = 5.3 Hz, 1H, Ar*H*), 6.06 (t, J = 5.3 Hz, 1H, Ar*H*), 5.95 (d, J = 5.3 Hz, 1H, Ar*H*), 5.91 (t, J = 5.2 Hz, 1H, Ar*H*), 5.86 (d, J = 5.4 Hz, 1H, Ar*H*), 4.60 (d, J = 16.4 Hz, 1H, ampyC*H*$_2$), 4.20 (d, J = 15.9 Hz, 1H, ampyC*H*$_2$), 3.61 (dt, J = 13.6, 6.6 Hz, 2H, C*H*$_2$OH), 2.64 – 2.42 (m, 2H, ArC*H*$_2$), 1.95 – 1.78 (m, 2H, C*H*$_2$). **^{13}C{^{1}H} NMR** (101 MHz, DMSO-*d*$_6$, δ): 161.80 (s, ampy*C*), 154.49 (s, ampy*C*H), 139.44 (s, ampy*C*H), 125.20 (s, ampy*C*H), 120.92 (s, ampy*C*H), 95.06 (s, Ar*C*), 77.55 (s, Ar*C*H), 77.08 (s, Ar*C*H), 72.52 (s, Ar*C*H), 71.80 (s, Ar*C*H), 70.35 (s, Ar*C*H), 59.96 (s, *C*H$_2$OH), 53.22 (s, ampy*C*H$_2$), 33.23 (s, *C*H$_2$), 29.30 (s, Ar*C*H$_2$). **MS (ESI)**: m/z calcd for C$_{15}$H$_{20}$N$_2$OClOs [M]$^+$ 471.1; found 471.1 and m/z calcd for C$_{15}$H$_{20}$N$_2$OOs [M-Cl-H]$^+$ 435.1; found 435.1. **Elemental analysis**: Calcd for C$_{15}$H$_{21}$N$_2$OCl$_2$Os (505.47) C, 35.64; H, 3.99; N 5.54%. Found C, 35.54; H, 4.29; N 5.86%.

[Os(η^6:κ^1-C$_6$H$_5$(CH$_2$)$_3$O)(ampy)]NO$_3$ (4C)

Synthesis as for **1C** using [Os(η^6-C$_6$H$_5$(CH$_2$)$_3$OH)(ampy)Cl]Cl (30 mg, 0.05 mmol) at RT in methanol for 1 week. Brown powder. Yield: 26 mg, 0.045 mmol, 88%.

^{1}H NMR (400 MHz, MeOD-*d*$_4$, δ): 9.23 (d, J = 5.6 Hz, 1H, ampy*H*), 8.01 (t, J = 7.7 Hz, 1H, ampy*H*), 7.67 (d, J = 7.9 Hz, 1H, ampy*H*), 7.48 (t, J = 6.6 Hz, 1H, ampy*H*), 6.17 (q, J = 5.8 Hz, 2H, Ar*H*), 5.97 (dd, J = 12.9, 5.6 Hz, 2H, Ar*H*), 5.86 (t, J = 5.5 Hz, 1H, Ar*H*), 4.75 (d, J = 16.6 Hz, 1H, ampyC*H*$_2$), 4.28 (d, J = 16.5 Hz, 1H, ampyC*H*$_2$), 3.60 (t, J = 6.2 Hz, 2H, C*H*$_2$OH), 2.54 – 2.39 (m, 2H, ArC*H*$_2$), 1.90 – 1.73 (m, 2H, C*H*$_2$). **^{13}C{^{1}H} NMR** (101 MHz, MeOD-*d*$_4$, δ): 163.61 (s, ampy*C*), 155.81 (s, ampy*C*H), 141.51 (s, ampy*C*H), 126.81 (s), 122.56 (s, ampy*C*H), 100.95 (s, Ar*C*), 82.95 (s, Ar*C*H), 82.72 (s, Ar*C*H), 77.32 (s, Ar*C*H), 76.37 (s, Ar*C*H), 75.20 (s, Ar*C*H), 61.71 (s, *C*H$_2$OH), 56.03 (s, ampy*C*H$_2$), 34.43 (s, *C*H$_2$), 30.71 (s, Ar*C*H$_2$). **MS (ESI)**: m/z calcd for C$_{15}$H$_{19}$N$_2$OOs [M]$^+$ 435.1; found 434.8.

[Os(η^6-C$_6$H$_5$(CH$_2$)$_3$OH)(Ph-impy)Cl]Cl (5)

[Os(η^6-C$_6$H$_5$(CH$_2$)$_3$OH)(μ-Cl)Cl]$_2$ (34 mg, 0.043 mmol) and (*E*)-N-phenyl-1-(pyridin-2-yl)methanimine (Ph-impy; 23 mg, 0.126 mmol) were stirred at RT overnight in 3 mL of MeOH. The orange solution was filtered over a pad of Celite, the solvent reduced in the rotary evaporator to a fourth of the initial volume and a yellow powder precipitated upon addition of Et$_2$O. The supernatant was removed with a pipette and the powder washed with diethyl ether and dried under vacuum. Red crystals suitable for X-ray diffraction of [Os(η^6-C$_6$H$_5$(CH$_2$)$_3$OH)(Ph-impy)Cl]PF$_6$ (**5·PF$_6$**) were obtained from a mixture of NH$_4$PF$_6$ in MeOH/H$_2$O at room temperature. Yield: 43 mg of red powder, 0.07 mmol, 86%.

^{1}H NMR (400 MHz, DMSO-*d*$_6$, δ): 9.56 (d, J = 5.5 Hz, 1H, Ph-impy*H*), 9.31 (s, 1H, Ph-impy*H*), 8.39 (d, J = 7.1 Hz, 1H, Ph-impy*H*), 8.28 (td, J = 7.7, 1.1 Hz, 1H, Ph-impy*H*), 7.88 – 7.80 (m, 1H, Ph-impy*H*), 7.71 (d, J = 7.7 Hz, 2H, Ph-impy*H*), 7.59 (dt, J = 23.3, 7.2 Hz, 3H, Ph-impy*H*), 6.25 (t, J = 5.5 Hz, 1H, Ar*H*), 6.04 (d, J = 5.7 Hz, 1H, Ar*H*), 5.95 (t, J = 5.3 Hz, 1H, Ar*H*), 5.88 – 5.81 (m, 2H, Ar*H*), 4.56 (s, 1H, O*H*), 3.40 (dd, J = 7.8, 4.7 Hz, 2H, C*H*$_2$OH), 2.44 – 2.34 (m, 2H, ArC*H*$_2$), 1.71 – 1.59 (m, 2H, C*H*$_2$). **^{13}C{^{1}H} NMR** (101 MHz, MeOD-*d*$_4$, δ): 169.59 (s, Ph-impy*C*H), 157.82 (s, Ph-impy*C*), 156.73 (s, Ph-impy*C*H), 153.72 (s, Ph-impy*C*), 141.24 (s, Ph-impy*C*H), 131.26 (s, Ph-impy*C*H), 131.13 – 130.41 (m, Ph-impy*C*H), 123.84 (s, Ph-impy*C*H), 101.47 (s, Ar*C*), 82.56 (d, J = 16.8 Hz, Ar*C*H), 77.38 (d, J = 17.9 Hz, Ar*C*H), 75.66 (s, Ar*C*H), 61.84 (s, *C*H$_2$OH), 33.88 (s, *C*H$_2$), 31.01 (s, Ar*C*H$_2$). **MS (ESI)**: m/z calcd for C$_{21}$H$_{22}$ClN$_2$OOs [M]$^+$ 545.1; found 545.0. **Elemental analysis**: Calcd for C$_{21}$H$_{22}$Cl$_2$N$_2$OOs·H$_2$O (597.54) C, 42.21; H, 4.05; N 4.69%. Found C, 42.60; H, 4.04; N 4.66%.

[Os(η^6:κ^1-C$_6$H$_5$(CH$_2$)$_3$O)(Ph-impy)]$^+$ (5C)

Synthesis as for **1C** using [Os(η^6-C$_6$H$_5$(CH$_2$)$_3$OH)(Ph-impy)Cl]Cl (30 mg, 0.05 mmol). The solid contained 70% of closed tether complex [Os(η^6:κ^1-C$_6$H$_5$(CH$_2$)$_3$O)(Ph-impy)]$^+$, characterised by ^{1}H NMR below.

^{1}H NMR (400 MHz, MeOD-*d*$_4$, δ): 9.60 (d, J = 5.6 Hz, 1H, Ph-impy*H*), 9.27 (s, 1H, Ph-impy*H*), 8.40 (d, J = 6.9 Hz, 1H, Ph-impy*H*), 8.32 (td, J = 7.7, 1.3 Hz, 1H, Ph-impy*H*), 7.86 (ddd, J = 7.5, 5.6, 1.6 Hz, 1H, Ph-impy*H*), 7.76 (dd, J = 8.3, 1.2 Hz, 2H, Ph-impy*H*), 7.70 – 7.58 (m, 3H, Ph-impy*H*), 6.22 (t, J = 5.6 Hz, 1H, Ar*H*), 6.05 (t, J = 5.7 Hz, 1H, Ar*H*), 6.03 – 5.95 (m, 3H, Ar*H*), 3.54 (t, J = 6.1 Hz, 2H, C*H*$_2$OH), 2.50 – 2.41 (m, 1H, ArC*H*$_2$), 2.40 – 2.29 (m, 1H, ArC*H*$_2$), 1.74 (qd, J = 12.3, 6.2 Hz, 2H, C*H*$_2$).

[Os(η^6-C$_6$H$_5$(CH$_2$)$_3$OH)(tBuPh-impy)Cl]Cl (6)

Synthesis as for **5** using [Os(η^6-C$_6$H$_5$(CH$_2$)$_3$OH)(μ-Cl)Cl]$_2$ (37 mg, 0.047 mmol), and (*E*)-N-(4-(tert-butyl)phenyl)-1-(pyridin-2-yl)methanimine (tBuPh-impy; 23 mg, 0.152 mmol). Yield: 35 mg of red powder, 0.06 mmol, 87%.

^{1}H NMR (400 MHz, DMSO-d_6, δ): 9.55 (d, J = 5.6 Hz, 1H, tBuPh-impy*H*), 9.30 (s, 1H, tBuPh-impy*H*), 8.36 (d, J = 7.2 Hz, 1H, tBuPh-impy*H*), 8.27 (t, J = 7.7 Hz, 1H, tBuPh-impy*H*), 7.83 (t, J = 6.0 Hz, 1H, tBuPh-impy*H*), 7.64 (q, J = 8.8 Hz, 4H, tBuPh-impy*H*), 6.25 (t, J = 5.5 Hz, 1H, Ar*H*), 6.05 (d, J = 5.7 Hz, 1H, Ar*H*), 5.95 (dt, J = 5.5, 2.9 Hz, 1H, Ar*H*), 5.87 (d, J = 2.9 Hz, 2H, Ar*H*), 4.59 (s, 1H, O*H*), 3.42 – 3.39 (m, 2H, C*H*$_2$OH), 2.46 – 2.32 (m, 3H, ArC*H*$_2$), 1.66 (tt, J = 13.0, 6.4 Hz, 2H, C*H*$_2$), 1.36 (s, 9H, tBu). **^{13}C{^{1}H} NMR** (100 MHz, DMSO-d_6, δ): 168.22 (s, tBuPh-impy*C*H overlapped with tBuPh-impy*C*), 155.82 (d, J = 37.0 Hz, tBuPh-impy*C*H overlapped with tBuPh-impy*C*), 152.70 (s tBuPh-impy*C*), 149.18 (s, tBuPh-impy*C*H), 140.08 (s, tBuPh-impy*C*H), 129.57 (s, tBuPh-impy*C*H), 126.11 (s, tBuPh-impy*C*H), 122.56 (s, tBuPh-impy*C*H), 99.66 (s, Ar*C*), 81.51 (s, Ar*C*H), 81.15 (s, Ar*C*H), 75.31 (d, J = 14.4 Hz, Ar*C*H), 73.85 (s, Ar*C*H), 59.91 (s, *C*H$_2$OH), 34.64 (s, *C*H$_2$), 32.69 (s, Ar*C*H$_2$), 31.03 (s, tBuPh-impy*C*H$_3$), 29.30 (s tBuPh-impy*C*). **MS (ESI)**: m/z calcd for C$_{25}$H$_{30}$ClN$_2$OOs [M]$^+$ 601.2; found 600.7. **Elemental analysis**: Calcd for C$_{25}$H$_{30}$Cl$_2$N$_2$OOs (635.66) C, 47.28; H, 4.76; N 4.41%. Found C, 47.12; H, 4.94; N 4.34%.

[Os(η^6:κ^1-C$_6$H$_5$(CH$_2$)$_3$O)(tBuPh-impy)]$^+$ (6C)

Synthesis as for **1C** using [Os(η^6-C$_6$H$_5$(CH$_2$)$_3$OH)(tBuPh-impy)Cl]Cl (22 mg, 0.035 mmol). The solid contained the closed tether complex [Os(η^6:κ^1-C$_6$H$_5$(CH$_2$)$_3$O)(tBuPh-impy)]$^+$, characterised by ^{1}H NMR below.

^{1}H NMR (400 MHz, DMSO-d_6, δ): 9.42 (d, J = 5.9 Hz, 1H, tBuPh-impy*H*), 9.31 (s, 1H, tBuPh-impy*H*), 8.38 – 8.33 (m, 1H, tBuPh-impy*H*), 8.28 – 8.22 (m, 1H, tBuPh-impy*H*), 7.76 (t, J = 5.5 Hz, 1H, tBuPh-impy*H*), 7.61 (d, J = 8.6 Hz, 2H, tBuPh-impy*H*), 7.50 (d, J = 8.6 Hz, 2H, tBuPh-impy*H*), 6.32 (t, J = 5.2 Hz, 1H, Ar*H*), 5.93 (d, J = 5.3 Hz, 1H, Ar*H*), 5.48 (t, J = 5.8 Hz, 2H, Ar*H*), 5.21 (t, J = 5.3 Hz, 1H, Ar*H*), 3.52 – 3.43 (m, 1H), 2.60 (d, J = 14.0 Hz, 1H), 2.21 (d, J = 56.8 Hz, 1H), 1.94 (s, 1H), 1.76 (s, 1H), 1.56 (s, 1H), 1.36 (s, 9H, tBu).

[Os(η^6-C$_6$H$_5$(CH$_2$)$_3$OH)(BrPh-impy)Cl]Cl (7)

Synthesis as for **5** using [Os(η^6-C$_6$H$_5$(CH$_2$)$_3$OH)(μ-Cl)Cl]$_2$ (38 mg, 0.048 mmol), and (*E*)-N-(2-bromophenyl)-1-(pyridin-2-yl)methanimine (BrPh-impy; 27 mg, 0.103 mmol). Yield: 54 mg of red powder, 0.08 mmol, 85%.

^{1}H NMR (400 MHz, DMSO-d_6, δ): 9.63 (d, J = 5.5 Hz, 1H, BrPh-impy*H*), 9.50 (s, 1H, BrPh-impy*H*), 8.48 (d, J = 7.3 Hz, 1H, BrPh-impy*H*), 8.32 (t, J = 7.3 Hz, 1H, BrPh-impy*H*), 7.98 – 7.89 (m, 2H, BrPh-impy*H*), 7.70 – 7.60 (m, 2H, BrPh-impy*H*), 7.50 – 7.44 (m, 1H, BrPh-impy*H*), 6.34 (t, J = 5.5 Hz, 1H, Ar*H*), 6.16 (d, J = 5.6 Hz, 1H, Ar*H*), 6.08 (t, J = 5.4 Hz, 1H, Ar*H*), 5.78 (t, J = 5.5 Hz, 1H, Ar*H*), 5.69 (d, J = 5.7 Hz, 1H, Ar*H*), 4.58 (t, J = 5.1 Hz, 1H, O*H*), 3.41 – 3.37 (m, 2H, C*H*$_2$OH), 2.34 (d, J = 8.0 Hz, 2H, ArC*H*$_2$), 1.64 (dd, J = 14.3, 7.8 Hz, 2H, C*H*$_2$). **^{13}C{^{1}H} NMR** (101 MHz, MeOD-d_4, δ): 174.50 (s, BrPh-impy*C*H), 157.14 (s, BrPh-impy*C*H), 152.19 (s, BrPh-impy*C*), 141.45 (s, BrPh-impy*C*H), 134.87 (s, BrPh-impy*C*H), 131.92 (s, BrPh-impy*C*H), 131.66 (s, BrPh-impy*C*H), 130.06 (s, BrPh-impy*C*), 125.89 (s, Br-PhImpy*C*H), 115.26 (s, Br-PhImpy*C*), 101.72 (s, Ar*C*), 82.23 (s, Ar*C*H), 81.92 (s, Ar*C*H), 78.16 (s, Ar*C*H), 77.83 (s, Ar*C*H), 76.39 (s, Ar*C*H), 61.83 (s, *C*H$_2$OH), 33.82 (s, *C*H$_2$), 31.04 (s, Ar*C*H$_2$). **MS (ESI)**: m/z calcd for C$_{21}$H$_{21}$ClBrN$_2$OOs [M]$^+$ 623.1; found 622.5. **Elemental analysis**: Calcd for C$_{21}$H$_{21}$BrCl$_2$N$_2$OOs (658.45) C, 38.31; H, 3.21; N 4.25%. Found C, 38.64; H, 3.56; N 4.20%

[Os(η^6:κ^1-C$_6$H$_5$(CH$_2$)$_3$O)(BrPh-impy)]$^+$ (7C)

Synthesis as for **1C** using [Os(η^6-C$_6$H$_5$(CH$_2$)$_3$OH)(tBuPh-impy)Cl]Cl (33 mg, 0.05 mmol). The solid contained the closed tether complex [Os(η^6:κ^1-C$_6$H$_5$(CH$_2$)$_3$O)(BrPh-impy)]$^+$, characterised below by both ^{1}H NMR and MS.

^{1}H NMR (400 MHz, DMSO-d_6, δ): 9.48 (d, J = 5.6 Hz, 1H, BrPh-impy*H*), 9.28 (s, 1H, BrPh-impy*H*), 8.38 (d, J = 7.9 Hz, 1H, BrPh-impy*H*), 8.33 – 8.26 (m, 1H, BrPh-impy*H*), 7.92 – 7.89 (m, 1H, BrPh-impy*H*), 7.83 (ddd, J = 7.4, 5.7, 1.5 Hz, 1H, BrPh-impy*H*), 7.60 (dd, J = 12.0, 4.6 Hz, 1H, BrPh-impy*H*), 7.50 – 7.45 (m, 1H, BrPh-impy*H*), 7.45 – 7.38 (m, 1H, BrPh-impy*H*), 6.38 (t, J = 5.4 Hz, Ar*H*), 5.97 – 5.90 (m, Ar*H*), 5.61 (t, J = 5.4 Hz, Ar*H*), 5.36 (t, J = 5.5 Hz, Ar*H*), 5.15 (d, J = 5.4 Hz, Ar*H*), 3.54 (dd, J = 11.7, 5.6 Hz, 2H, C*H*$_2$OH), 2.71 (t, J = 6.3 Hz, 2H, ArC*H*$_2$), 2.06 – 1.95 (m, 1H, C*H*$_2$), 1.75 (td, J = 14.0, 7.0 Hz, 1H, C*H*$_2$). **MS (ESI)**: m/z calcd for C$_{21}$H$_{20}$BrN$_2$OOs [M]$^+$ 587.04; found 587.1.

[Os(η^6-C$_6$H$_5$(CH$_2$)$_3$OH)(PhEt-impy)Cl]Cl (8)

Synthesis as for **5** using [Os(η^6-C$_6$H$_5$(CH$_2$)$_3$OH)(μ-Cl)Cl]$_2$ (26 mg, 0.033 mmol), and (*E*)-N-phenethyl-1-(pyridin-2-yl)methanimine (PhEt-impy; 32 mg, 0.097 mmol). Orange crystals suitable for X-ray diffraction of **8·PF$_6$** were obtained by slow evaporation of a mixture of **8** and NH_4PF_6 in MeOH. Yield: 57 mg of red powder, 0.08 mmol, 85%.

^{1}H NMR (400 MHz, DMSO-*d*$_6$, δ): 9.51 (d, J = 5.5 Hz, 1H, PhEt-impy*H*), 9.18 (s, 1H, PhEt-impy*H*), 8.28 (d, J = 7.4 Hz, 1H, PhEt-impy*H*), 8.21 (t, J = 7.6 Hz, 1H, PhEt-impy*H*), 7.76 (dd, J = 9.5, 3.7 Hz, 1H, PhEt-impy*H*), 7.43 – 7.32 (m, 4H, PhEt-impy*H*), 7.28 (t, J = 7.3 Hz, 1H, PhEt-impy*H*), 6.43 (dt, J = 10.8, 5.6 Hz, 2H, Ar*H*), 6.24 (dd, J = 16.0, 5.7 Hz, 2H, Ar*H*), 6.02 (t, J = 5.3 Hz, 1H, Ar*H*), 4.74 – 4.64 (m, 2H, PhEt-impyC*H*$_2$), 4.61 (t, J = 5.1 Hz, 1H, O*H*), 3.45 (dd, J = 11.4, 6.2 Hz, 2H, C*H*$_2$OH), 3.30 – 3.23 (m, 1H, PhEt-impyC*H*$_2$), 3.10 – 2.96 (m, 1H, PhEt-impyC*H*$_2$), 2.5 (m, 2H, ArC*H*$_2$ overlapped with DMSO), 1.85 – 1.59 (m, 5H). 1.74 (td, J = 15.2, 7.6 Hz, 2H, C*H*$_2$). **^{13}C{^{1}H} NMR** (101 MHz, DMSO-*d*$_6$, δ): 168.83 (s, PhEt-impy*C*H), 155.69 (d, J = 13.6 Hz, PhEt-impy*C*, PhEt-impy*C*H), 139.95 (s, PhEt-impy*C*H), 137.79 (s, PhEt-impy*C*), 129.13 (d, J = 7.2 Hz, PhEt-impy*C*H), 128.52 (s, PhEt-impy*C*H), 126.65 (s, PhEt-impy*C*H), 98.47 (s, Ar*C*), 80.17 (s, Ar*C*H), 79.64 (s, Ar*C*H), 76.69 (s, Ar*C*H), 76.15 (s, Ar*C*H), 73.85 (s, Ar*C*H), 67.86 (s, PhEt-impy*C*H$_2$), 59.96 (s, *C*H$_2$OH), 35.62 (s, PhEt-impy*C*H$_2$), 32.88 (s, *C*H$_2$), 29.52 (s, Ar*C*H$_2$). **MS (ESI)**: m/z calcd for $C_{23}H_{26}ClN_2OOs$ $[M]^+$ 573.1; found 572.6. **Elemental analysis**: Calcd for $C_{23}H_{26}Cl_2N_2OOs$ (607.60) C, 45.47; H, 4.31; N 4.61%. Found C, 45.24; H, 4.85; N 4.63%

[Os(η^6:κ^1-C$_6$H$_5$(CH$_2$)$_3$O)(PhEt-impy)]NO$_3$ (8C)

Synthesis as for **1C** using [Os(η^6-C$_6$H$_5$(CH$_2$)$_3$OH)(PhEt-impy)Cl]Cl (35 mg, 0.058 mmol). Yield: 23 mg of brown powder, 0.038 mmol, 65%.

^{1}H NMR (400 MHz, MeOD-*d*$_4$, δ): 9.38 (d, J = 5.4 Hz, 1H, PhEt-impy*H*), 8.93 (s, 1H, PhEt-impy*H*), 8.19 (t, J = 7.2 Hz, 1H, PhEt-impy*H*), 8.13 (d, J = 7.6 Hz, 1H, PhEt-impy*H*), 7.69 (t, J = 5.9 Hz, 1H, PhEt-impy*H*), 7.35 (d, J = 4.5 Hz, 5H, PhEt-impy*H*), 6.35 (t, J = 5.5 Hz, 1H, Ar*H*), 6.28 (t, J = 5.4 Hz, 1H, Ar*H*), 5.89 (d, J = 5.6 Hz, 1H, Ar*H*), 5.80 (d, J = 5.3 Hz, 1H, Ar*H*), 5.44 (t, J = 5.4 Hz, 1H, Ar*H*), 4.64 (dd, J = 17.5, 8.6 Hz, 2H, PhEt-impyC*H*$_2$), 3.47 (dd, J = 6.9, 3.3 Hz, 2H, C*H*$_2$O), 3.30 – 3.24 (m, 1H, PhEt-impyC*H*$_2$), 3.13 – 2.99 (m, 1H, PhEt-impyC*H*$_2$), 2.83 – 2.69 (m, 2H, ArC*H*$_2$), 2.09 – 1.79 (m, 2H, C*H*$_2$). **MS (ESI)**: m/z calcd for $C_{23}H_{25}N_2OOs$ $[M]^+$ 537.16; found 537.1.

[Os(η^6-C$_6$H$_5$(CH$_2$)$_3$OH)(pico)Cl] (9)

[Os(η^6-C$_6$H$_5$(CH$_2$)$_3$OH)(μ-Cl)Cl]$_2$ (38 mg, 0.05 mmol) was stirred for 1 h in 4 mL of dry MeOH at RT. After that, sodium methoxide (NaOMe; 7.7 mg, 0.14 mmol) and picolinic acid (18.3 mg, 0.15 mmol) were added to the solution and the mixture was stirred at RT overnight. The orange solution was filtered over a pad of Celite, the solvent reduced in the rotary evaporator to a fourth of the initial volume and a yellow powder precipitated upon addition of Et$_2$O. The supernatant was removed with a pipette and the powder washed with diethyl ether and dried under vacuum. Yellow crystals suitable for X-ray diffraction were obtained by slow evaporation of a mixture of MeOH/DCM/hexane. Yield: 44 mg, 0.09 mmol, 94%.

^{1}H NMR (400 MHz, MeOD-*d*$_4$,δ): 9.18 (d, J = 5.5 Hz, 1H, pico*H*), 8.11 (dd, J = 7.7, 6.4 Hz, 1H, pico*H*), 8.01 (d, J = 7.0 Hz, 1H, pico*H*), 7.75 – 7.66 (m, 1H, pico*H*), 6.25 – 6.18 (m, 2H, Ar*H*), 6.02 (t, J = 5.2 Hz, 1H, Ar*H*), 5.97 (d, J = 7.0 Hz, 2H, Ar*H*), 3.64 (t, J = 6.3 Hz, 2H, C*H*$_2$OH), 2.64 – 2.54 (m, 2H, ArC*H*$_2$), 1.95 – 1.82 (m, 2H, C*H*$_2$). **^{13}C{^{1}H} NMR** (101 MHz, MeOD-*d*$_4$, δ): 176.80 (s, pico*C*), 155.41 (s, pico*C*H), 150.32 (s, pico*C*), 141.25 (s, pico*C*H), 130.42 (s, pico*C*H), 127.61 (s, pico*C*H), 95.95 (s, Ar*C*), 79.69 (s, Ar*C*H), 77.60 (s, Ar*C*H), 72.48 (s, Ar*C*H), 71.56 (s, Ar*C*H), 70.88 (s, Ar*C*H), 62.14 (s, *C*H$_2$OH), 33.87 (s, *C*H$_2$), 31.08 (s, Ar*C*H$_2$). **MS (ESI)**: m/z calcd for C$_{15}$H$_{16}$NO$_3$Os [M-Cl]$^+$ 450.1; found 449.7. **Elemental analysis**: Calcd for C$_{15}$H$_{16}$ClNO$_3$Os·H$_2$O (501.97) C, 35.89; H, 3.61; N 2.79%. Found C, 35.91; H, 3.27; N 2.85%

[Os(η^6:κ^1-C$_6$H$_5$(CH$_2$)$_3$OH)(pico)]$^+$ (9C)

Synthesis as for **1C** using [Os(η^6-C$_6$H$_5$(CH$_2$)$_3$OH)(pico)Cl] (37 mg, 0.076 mmol) and AgNO$_3$ (13 mg, 0.077 mmol) stirred at RT for 48 h. The solid contained the closed tether complex [Os(η^6:κ^1-C$_6$H$_5$(CH$_2$)$_3$OH)(pico)]$^+$, characterised by ^{1}H NMR below.

^{1}H NMR (400 MHz, MeOD-*d*$_4$, δ): 9.38 (d, J = 5.4 Hz, 1H, pico*H*), 8.26 (t, J = 7.0 Hz, 1H, pico*H*), 8.09 (d, J = 7.9 Hz, 1H, pico*H*), 7.86 – 7.81 (m, 1H, pico*H*), 6.54 – 6.45 (m, 2H, Ar*H*), 6.26 – 6.21 (m, 2H, Ar*H*), 5.83 (t, J = 5.2 Hz, 1H, Ar*H*), 3.64 (dd, J = 13.8, 7.5 Hz, 2H, C*H*$_2$OH), 2.98 – 2.89 (m, 1H, ArC*H*$_2$), 2.81 – 2.71 (m, 1H, ArC*H*$_2$), 2.15 (d, J = 8.0 Hz, 2H, C*H*$_2$).

[Os(η^6-C$_6$H$_5$(CH$_2$)$_3$OH)(6-Me-pico)Cl] (10)

Synthesis as for **9** using [Os(η^6-C$_6$H$_5$(CH$_2$)$_3$OH)(μ-Cl)Cl]$_2$ (50 mg, 0.063 mmol), NaOMe (7.4 mg, 0.137 mmol) and 6-methylpicolinic acid (19 mg, 0.138 mmol). Intense yellow crystals suitable for X-ray diffraction were obtained by slow diffusion of hexane in a DCM solution of **10**. Yield: 41 mg, 0.08 mmol, 94%.

^{1}H NMR (400 MHz, DMSO-*d*$_6$, δ): 7.94 (t, J = 7.6 Hz, 1H, 6-Me-pico*H*), 7.79 – 7.71 (m, 2H, 6-Me-pico*H*), 6.40 (t, J = 5.5 Hz, 2H, Ar*H*), 6.07 (t, J = 5.2 Hz, 1H, Ar*H*), 5.98 (dd, J = 10.7, 5.4 Hz, 2H, Ar*H*), 4.61 (t, J = 5.1 Hz, 1H, O*H*), 3.48 – 3.45 (m, 2H, C*H*$_2$OH), 2.93 (s, 3H, C*H*$_3$), 2.45 – 2.35 (m, 2H, ArC*H*$_2$), 1.80 – 1.71 (m, 2H, C*H*$_2$). **^{13}C{^{1}H} NMR** (101 MHz, DMSO-*d*$_6$, δ): 173.11 (s, 6-Me-pico*C*), 161.93 (s, 6-Me-pico*C*), 149.66 (s, 6-Me-pico*C*), 139.62 (s, 6-Me-pico*C*H), 129.18 (s, 6-Me-pico*C*H), 123.36 (s, 6-Me-pico*C*H), 96.82 (s, Ar*C*), 78.60 (s, Ar*C*H), 77.11 (s, Ar*C*H), 69.04 (s, Ar*C*H), 68.77 (s, Ar*C*H), 68.56 (s, Ar*C*H), 60.29 (s, *C*H$_2$OH), 32.69 (s, *C*H$_2$), 29.81 (s, Ar*C*H$_2$), 27.53 (s, 6-Me-pico*C*H$_3$). **MS (ESI)**: m/z calcd for C$_{16}$H$_{18}$NO$_3$Os [M-Cl]$^+$ 464.09; found 464.1. **Elemental analysis**: Calcd for C$_{16}$H$_{18}$ClNO$_3$Os·1.5H$_2$O (525.00) C, 36.61; H, 4.03; N 2.67%. Found C, 36.79; H, 3.61; N 2.53%.

[Os(η^6:κ^1-C$_6$H$_5$(CH$_2$)$_3$OH)(6-Me-pico)]NO$_3$ (10C)

Synthesis as for **1C** using [Os(η^6-C$_6$H$_5$(CH$_2$)$_3$OH)(6-Me-pico)Cl] (20 mg, 0.04 mmol). A dark brownish powder highly hygroscopic was obtained. Yield: 22 mg, 0.04 mmol, 99%.

^{1}H NMR (400 MHz, DMSO-*d*$_6$, δ): 8.14 – 8.06 (m, 1H, 6-Me-pico*H*), 7.88 (dd, J = 7.9, 1.5 Hz, 1H, 6-Me-pico*H*), 7.82 (t, J = 6.3 Hz, 1H, 6-Me-pico*H*), 6.79 (t, J = 5.6 Hz, 1H, Ar*H*), 6.70 (t, J = 5.6 Hz, 1H, Ar*H*), 6.36 (t, J = 5.5 Hz, 1H, Ar*H*), 6.24 (d, J = 5.7 Hz, 1H, Ar*H*), 6.17 (d, J = 5.8 Hz, 1H, Ar*H*), 4.64 (t, J = 5.0 Hz, 1H, O*H*), 3.46 (dd, J = 11.3, 6.2 Hz, 2H, C*H*$_2$OH), 2.89 (s, 3H, C*H*$_3$), 2.44 – 2.35 (m, 1H, ArC*H*$_2$), 2.31 – 2.23 (m, 1H, ArC*H*$_2$), 1.80 – 1.67 (m, 2H, C*H*$_2$). **^{13}C{^{1}H} NMR** (101 MHz, DMSO-*d*$_6$, δ): 173.25 (s, 6-Me-pico*C*), 163.29 (s, 6-Me-pico*C*), 149.49 (s, 6-Me-pico*C*), 140.70 (s, 6-Me-pico*C*H), 130.05 (s, 6-Me-pico*C*H), 124.79 (s, 6-Me-pico*C*H), 109.61 (s, Ar*C*), 85.63 (s, Ar*C*H), 84.28 (s, Ar*C*H), 77.69 (s, Ar*C*H), 74.14 (d, J = 19.6 Hz, Ar*C*H), 59.94 (s, *C*H$_2$OH), 31.55 (s, *C*H$_2$), 29.00 (s, Ar*C*H$_2$), 28.46 (s, 6-Me-pico*C*H$_3$). **MS (ESI)**: m/z calcd for C$_{16}$H$_{18}$NO$_3$Os [M]$^+$ 464.09; found 465.17. The high hygroscopicity of the solid hampered CHN analysis.

[Os(η^6-C$_6$H$_5$(CH$_2$)$_3$OH)(4-Me-pico)Cl] (11)

[Os(η^6-C$_6$H$_5$(CH$_2$)$_3$OH)(μ-Cl)Cl]$_2$ (35 mg, 0.044 mmol), NaOMe (5.0 mg, 0.093 mmol) and 4-methylpicolinic acid (12.6 mg, 0.092 mmol) were dissolved in 5 mL of dry methanol and heated at reflux for 4 h. After that, the mixture was filtered and the volume reduced to a fourth. Et$_2$O was added to allow the precipitation of a yellow powder which was dissolved in DCM and filtered. Finally, the yellow powder was precipitated again by the addition of Et$_2$O, the solvent was removed with a pipette and the solid washed with Et$_2$O and dried in the vacuum line. A mixture of two different shape yellow crystals (needles and polyhedrons) suitable for X-ray diffraction were obtained from a methanol solution at room temperature. The needles were resolved as compound **11** while the polyhedrons were resolved as a new complex: the dichlorido closed tether compound [Os(η^6:κ^1-C$_6$H$_5$(CH$_2$)$_3$OH)Cl$_2$], without any chelating ligand in the XY position. Yield: 41 mg, 0.08 mmol, 94%.

^{1}H NMR (400 MHz, DMSO-*d*$_6$, δ): 9.05 (d, J = 5.7 Hz, 1H, 4-Me-pico*H*), 7.72 (s, 1H, 4-Me-pico*H*), 7.55 (d, J = 5.8 Hz, 1H, 4-Me-pico*H*), 6.21 (dt, J = 13.2, 5.3 Hz, 2H, Ar*H*), 6.02 (t, J = 5.1 Hz, 1H, Ar*H*), 5.95 (d, J = 5.6 Hz, 2H, Ar*H*), 4.58 (s, 1H, O*H*), 3.45 (t, J = 6.3 Hz, 2H, C*H*$_2$OH), ca. 2.5 (s, 3H, C*H*$_3$ overlapped with DMSO), 2.41 (dd, J = 9.3, 6.3 Hz, 2H, ArC*H*$_2$), 1.72 (dq, J = 12.8, 6.6 Hz, 2H, C*H*$_2$). **^{13}C{^{1}H} NMR** (101 MHz, DMSO-*d*$_6$, δ): 173.54 (s, 4-Me-pico*C*), 153.53 (s, 4-Me-pico*C*H), 152.08 (s, 4-Me-pico*C*), 148.63 (s, 4-Me-pico*C*), 129.26 (s, 4-Me-pico*C*H), 126.37 (s, 4-Me-pico*C*H), 93.82 (s, Ar*C*), 77.93 (s, Ar*C*H), 75.95 (s, Ar*C*H), 70.21 (s, Ar*C*H), 69.27 (s, Ar*C*H), 68.84 (s, Ar*C*H), 60.22 (s, *C*H$_2$OH), 32.96 (s, *C*H$_2$), 29.64 (s, Ar*C*H$_2$), 20.49 (s, 4-Me-pico*C*H$_3$). **MS (ESI)**: m/z calcd for C$_{16}$H$_{18}$NO$_3$Os [M-Cl]$^+$ 464.1; found 464.1. **Elemental analysis**: Calcd for C$_{16}$H$_{18}$ClNO$_3$Os·0.5H$_2$O (506.99) C, 37.91; H, 3.78; N 2.76%. Found C, 37.94; H, 3.65; N 2.75%.

[Os(η^6:κ^1-C$_6$H$_5$(CH$_2$)$_3$OH)(4-Me-pico)]NO$_3$ (11C)

Synthesis as for **1C** using [Os(η^6-C$_6$H$_5$(CH$_2$)$_3$OH)(4-Me-pico)Cl] (20 mg, 0.04 mmol) and stirred for 3 days at 363 K. Brown powder. Yield: 14 mg, 0.027 mmol, 68%.

^{1}H NMR (400 MHz, DMSO-*d*$_6$, δ): 9.19 (d, J = 5.4 Hz, 1H, 4-Me-pico*H*), 8.97 (d, J = 5.7 Hz, 1H, 4-Me-pico*H*), 8.79 (s, 1H, 4-Me-pico*H*), 6.24 (dt, J = 20.7, 5.1 Hz, 2H, Ar*H*), 5.92 (t, J = 5.1 Hz, 1H, Ar*H*), 5.83 (dd, J = 8.8, 5.1 Hz, 2H, Ar*H*), 4.39 (s, 1H, O*H*), 4.18 (s, 3H, C*H*$_3$), 4.16 – 4.07 (m, 1H, ArC*H*$_2$), 3.96 (d, J = 8.0 Hz, 1H, C*H*$_2$OH), 3.38 (dd, J = 11.6, 4.6 Hz, 2H, ArC*H*$_2$), 2.63 (s, 1H, C*H*$_2$), 2.40 – 2.34 (m, 1H, C*H*$_2$). **^{13}C{^{1}H} NMR** (101 MHz, D$_2$O, δ): 168.50 (s, 4-Me-pico*C*), 154.27 (s, 4-Me-pico*C*), 153.66 (s, 4-Me-pico*C*), 153.12 (s, 4-Me-

pico*C*H), 130.51 (s, 4-Me-pico*C*H), 127.70 (s, 4-Me-pico*C*H), 95.07 (s, Ar*C*), 79.79 (s, Ar*C*H), 77.56 (s, Ar*C*H), 68.51 (s, Ar*C*H), 66.87 (s, Ar*C*H), 64.96 (s, Ar*C*H), 61.99 (s, *C*H_2OH), 33.08 (s, *C*H_2), 28.72 (s, Ar*C*H_2). **MS (ESI)**: m/z calcd for $C_{16}H_{18}NO_3Os$ $[M]^+$ 464.09; found 464.2. The high hygroscopicity of the solid hampered CHN analysis.

[Os(η^6-$C_6H_5(CH_2)_3OH$)(4-COOH-pico)Cl] (12)

Synthesis as for **11** using $[Os(\eta^6\text{-}C_6H_5(CH_2)_3OH)(\mu\text{-}Cl)Cl]_2$ (35 mg, 0.044 mmol), NaOMe (5.0 mg, 0.093 mmol) and 2,4-pyridinedicarboxylic acid (13.5 mg, 0.08 mmol). Yield: 43 mg of yellow powder, 0.08 mmol, 92%.

^{1}H NMR (400 MHz, DMSO-d_6, δ): 9.40 (d, J = 5.6 Hz, 1H, 4-COOH-pico*H*), 8.13 (d, J = 1.4 Hz, 1H, 4-COOH-pico*H*), 8.03 (dd, J = 5.7, 1.8 Hz, 1H, 4-COOH-pico*H*), 6.26 (dt, J = 16.7, 5.3 Hz, 2H, Ar*H*), 6.07 (t, J = 5.1 Hz, 1H, Ar*H*), 6.00 (t, J = 4.9 Hz, 2H, Ar*H*), 4.56 (s, 1H, O*H*), 3.46 (d, J = 4.1 Hz, 2H, CH_2OH), 2.46 – 2.40 (m, 2H, ArCH_2), 1.80 – 1.67 (m, 2H, CH_2). **^{13}C{^{1}H} NMR** (101 MHz, DMSO-d_6, δ): 172.93 (s, 4-COOH-pico*C*), 164.55 (s, 4-COOH-pico*C*), 155.13 (s, 4-COOH-pico*C*H), 150.00 (s, 4-COOH-pico*C*), 127.54 (s, 4-COOH-pico*C*H), 124.37 (s, 4-COOH-pico*C*H), 94.53 (s, Ar*C*), 78.35 (s, Ar*C*H), 76.42 (s, Ar*C*H), 70.71 (s, Ar*C*H), 69.64 (s, Ar*C*H), 69.32 (s, Ar*C*H), 60.15 (s, *C*H_2OH), 32.83 (s, *C*H_2), 29.56 (s, Ar*C*H_2).**MS (ESI)**: m/z calcd for $C_{16}H_{17}ClNO_5Os$ $[M\text{-}H]^-$ 528.0; found 528.5. **Elemental analysis**: Calcd for $C_{16}H_{16}ClNO_5Os\cdot 1.5H_2O$ (554.99) C, 34.63; H, 3.45; N 2.52. Found C, 34.77; H, 3.73; N 2.01

[Os(η^6:κ^1-$C_6H_5(CH_2)_3OH$)(4-COOH-pico)]$^+$ (12C)

Upon reaction of complex **12** with 1 mol equiv. of Ag^+, the tittle compound **12C** was identified during a titration of $[Os(\eta^6\text{-}C_6H_5(CH_2)_3OH)(4\text{-}COOH\text{-}pico)OH_2/OH]^{+/0}$ using NaOD at basic pH.

^{1}H NMR (400 MHz, D_2O, δ): 9.25 (d, J = 5.8 Hz, 1H, 4-COOH-pico*H*), 8.25 (s, 1H, 4-COOH-pico*H*), 8.05 – 7.94 (m, 1H, 4-COOH-pico*H*), 6.17 (q, J = 5.4 Hz, 2H, Ar*H*), 5.82 (m, 2H, Ar*H*), 5.59 (t, J = 5.1 Hz, 1H, Ar*H*), 3.51 (d, J = 3.8 Hz, 2H, CH_2OH), 2.65 (d, J = 4.8 Hz, 7H, ArCH_2), 1.94 – 1.79 (m, 2H, CH_2).

[Os(η^6-C$_6$H$_5$(CH$_2$)$_3$OH)(quinol)Cl] (13)

[Os(η^6-C$_6$H$_5$(CH$_2$)$_3$OH)(μ-Cl)Cl]$_2$ (30 mg, 0.04 mmol) were stirred at 323 K in 3 ml of dry MeOH for 1 h. After that, 8-hydroxyquinoline (11.5 mg, 0.08 mmol) and sodium methoxide (NaOMe; 4.6 mg, 0.08 mmol) were added and stirred at 323 K overnight. The mixture was then filtered, the volume of the solution reduced to a fourth and the title compound precipitated after the addition of some drops of Et$_2$O. The powder was washed with diethyl ether and dried in the vacuum line. Intense yellow-orange crystals suitable for X-ray diffraction were obtained by slow diffusion of hexane in DCM at 277 K. Yield: 32 mg, 0.07 mmol, 79%.

^{1}H NMR (400 MHz, MeOD-*d*$_4$, δ): 9.11 (d, J = 5.1 Hz, 1H, quinol*H*), 8.22 (d, J = 8.5 Hz, 1H, quinol*H*), 7.45 (dd, J = 8.4, 5.0 Hz, 1H, quinol*H*), 7.37 (t, J = 8.0 Hz, 1H, quinol*H*), 6.98 (d, J = 7.6 Hz, 1H, quinol*H*), 6.91 (d, J = 8.5 Hz, 1H, quinol*H*), 6.13 (dd, J = 12.5, 5.4 Hz, 2H, Ar*H*), 5.93 (d, J = 5.2 Hz, 1H, Ar*H*), 5.89 (dd, J = 11.2, 5.6 Hz, 2H, Ar*H*), 3.62 (t, J = 6.2 Hz, 2H, C*H*$_2$OH), 2.61 – 2.54 (m, 2H, ArC*H*$_2$), 1.88 (dd, J = 14.6, 6.5 Hz, 2H, C*H*$_2$). **^{13}C{^{1}H} NMR** (101 MHz, MeOD-*d*$_4$, δ): 151.53 (s, quinol*C*H), 139.20 (s, quinol*C*H), 131.54 (s, quinol*C*), 130.77 (d, J = 12.5 Hz, quinol*C*), 123.90 (s, quinol*C*H), 115.37 (s, quinol*C*H), 113.72 (s, quinol*C*H), 94.83 (s, Ar*C*), 78.40 (s, Ar*C*H), 76.45 (s, Ar*C*H), 71.80 (d, J = 16.1 Hz, Ar*C*H), 71.05 (s, Ar*C*H), 62.17 (s, *C*H$_2$OH), 34.14 (s, *C*H$_2$), 30.98 (s, Ar*C*H$_2$). **MS (ESI)**: m/z calcd for C$_{18}$H$_{18}$NO$_2$Os [M-Cl]$^+$ 472.1; found 472.2. **Elemental analysis**: Calcd for C$_{18}$H$_{18}$ClNO$_2$Os·1.2H$_2$O (527.62) C, 40.98; H, 3.9; N 2.65%. Found C, 40.80; H, 3.66; N 2.72% **Λ$_M$** (Os 10^{-3} M in methanol, 298 K) = 32 S·cm^2/·mol.

[Os(η^6:κ^1-C$_6$H$_5$(CH$_2$)$_3$OH)(quinol)]NO$_3$ (13C)

[Os(η^6-C$_6$H$_5$(CH$_2$)$_3$OH)(quinol)Cl] (10 mg, 0.02 mmol) and AgNO$_3$ (3.7 mg, 0.022 mmol) were suspended in 1.5 mL of water and stirred at 323 K overnight. The green suspension was then filtered over a pad of Celite, the solvent was reduced in the rotary evaporator to approximately a fourth of the initial volume, and the powder precipitated by addition of some drops of diethyl ether. The supernatant was removed with a pipette and the solid was washed with Et$_2$O and dried under vacuum. Yield: 9.7 mg, 0.018 mmol, 90%.

^{1}H NMR (400 MHz, MeOD-*d*$_4$, δ): 9.08 (dd, J = 5.0, 1.2 Hz, 1H, quinol*H*), 8.25 (dd, J = 8.4, 1.2 Hz, 1H, quinol*H*), 7.44 (dd, J = 8.4, 5.0 Hz, 1H, quinol*H*), 7.37 (t, J = 8.0 Hz, 1H, quinol*H*), 6.99 (d, J = 8.0 Hz, 1H, quinol*H*), 6.93 (d, J = 7.9 Hz, 1H, quinol*H*), 6.06 – 5.99 (m, 2H, Ar*H*), 5.69 (dd, J = 10.3, 5.2 Hz, 2H, Ar*H*), 5.30 (t, J = 5.2 Hz, 1H, Ar*H*), 3.55 (ddd, J = 10.0, 9.2, 5.8 Hz, 2H, C*H*$_2$OH), 2.67 (t, J = 6.3 Hz, 2H, ArC*H*$_2$), 2.00 (dd, J = 13.4, 6.6 Hz, 1H, C*H*$_2$), 1.90

(dd, J = 14.6, 7.5 Hz, 1H, C*H*$_2$). **^{13}C{^{1}H} NMR** (101 MHz, MeOD-*d*$_4$, δ): 149.91 (s), 138.10 (s), 130.41 (s), 129.61 (s), 122.47 (s), 114.00 (s), 112.43 (s), 94.67 (s, Ar*C*), 80.30 (s, Ar*C*H), 75.44 (s, Ar*C*H), 67.92 (s, Ar*C*H), 64.35 (s, Ar*C*H), 62.82 (s, *C*H$_2$OH), 32.59 (s, *C*H$_2$), 29.02 (s, Ar*C*H$_2$). **MS (ESI)**: m/z calcd for $C_{18}H_{18}NO_2Os$ $[M\text{-}NO_3]^+$ 472.1; found 472.2.

Both open and closed tether-Ru analogues of complexes **2** and **3**, here complexes **2Ru**, **2CRu**, **3Ru** and **3CRu**, were synthesised for comparison purposes using a slight variation of the synthetic procedure previously reported,[19, 20] and are detailed below.

[Ru(η^6-C$_6$H$_5$(CH$_2$)$_3$OH)(bipy)Cl]Cl (2Ru)

Synthesis as for **2** using [Ru(η^6-C$_6$H$_5$(CH$_2$)$_3$OH)(μ-Cl)Cl]$_2$ (20 mg, 0.034 mmol) and 2,2'-bipyridine (bipy; 11 mg, 0.07 mmol) in 3 mL of acetone to afford a yellow powder. Yield: 28 mg, 0.06 mmol, 89%.

^{1}H NMR (400 MHz, MeOD-*d*$_4$, δ): 9.49 (d, J = 5.5 Hz, 2H, bipy*H*), 8.50 (d, J = 8.2 Hz, 2H, bipy*H*), 8.23 (t, J = 7.5 Hz, 2H, bipy*H*), 7.75 (t, J = 6.5 Hz, 2H, bipy*H*), 6.21 (t, J = 6.0 Hz, 2H, Ar*H*), 5.95 (d, J = 6.2 Hz, 2H, Ar*H*), 5.83 (t, J = 5.8 Hz, 1H, Ar*H*), 3.63 (t, J = 6.1 Hz, 2H, C*H*$_2$OH), 2.80 – 2.59 (m, 2H, ArC*H*$_2$), 1.95 – 1.79 (m, 2H, C*H*$_2$). **MS (ESI)**: m/z calcd for $C_{19}H_{20}ClN_2ORu$ $[M\text{-}Cl]^+$ 429.03; found 428.9.

[Ru(η^6:κ^1-C$_6$H$_5$(CH$_2$)$_3$O)(bipy)]BF$_4$ (2CRu)

[Ru(η^6-C$_6$H$_5$(CH$_2$)$_3$OH)(bipy)Cl]Cl (20 mg, 0.043 mmol) and $AgBF_4$ (17.6 mg, 0.09 mmol) were suspended in 3 mL of dry methanol and stirred at room temperature overnight. The suspension was then filtered over a pad of Celite, the solvent was reduced in the rotary evaporator to approximately a fourth of the initial volume, and an orange powder precipitated by addition of some drops of diethyl ether. The supernatant was removed with a pipette and the solid was washed with Et_2O and dried in the vacuum line. Ochre powder. Yield: 16 mg, 0.028 mmol, 66%.

^{1}H NMR (400 MHz, MeOD-*d*$_4$, δ): 9.59 (d, J = 5.7 Hz, 2H, bipy*H*), 8.55 (d, J = 8.2 Hz, 2H, bipy*H*), 8.32 (t, J = 7.9 Hz, 2H, bipy*H*), 7.83 (t, J = 6.6 Hz, 2H, bipy*H*), 6.39 (t, J = 6.0 Hz, 2H, Ar*H*), 6.05 (d, J = 6.1 Hz, 2H, Ar*H*), 5.40 (t, J = 5.7 Hz, 1H, Ar*H*), 3.64 – 3.60 (m, 2H, C*H*$_2$OH), 2.90 – 2.81 (m, 2H, ArC*H*$_2$), 2.29 – 2.20 (m, 2H, C*H*$_2$). **MS (ESI)**: m/z calcd for $C_{19}H_{19}N_2ORu$ $[M]^+$ 393.05; found 393.1.

[Ru(η^6-C$_6$H$_5$(CH$_2$)$_3$OH)(phen)Cl]Cl (3Ru)

Synthesis as for **2** using [Ru(η^6-C$_6$H$_5$(CH$_2$)$_3$OH)(μ-Cl)Cl]$_2$ (22 mg, 0.034 mmol) and 1,10-phenanthroline (phen; 13 mg, 0.07 mmol) in 3 mL of acetone. Yellow powder. Yield: 32 mg, 0.066 mmol, 96%.

^{1}H NMR (400 MHz, MeOD-*d*$_4$, δ): 9.84 (d, J = 4.4 Hz, 2H, phen*H*), 8.83 (d, J = 7.4 Hz, 2H, phen*H*), 8.20 (s, 2H, phen*H*), 8.14 – 8.03 (m, 2H, phen*H*), 6.32 (t, J = 6.0 Hz, 2H, Ar*H*), 6.08 (d, J = 6.1 Hz, 2H, Ar*H*), 5.85 (t, J = 5.8 Hz, 1H, Ar*H*), 3.64 (t, J = 6.2 Hz, 2H, C*H*$_2$OH), 2.76 – 2.65 (m, 2H, ArC*H*$_2$), 1.97 – 1.82 (m, 2H, C*H*$_2$).

[Ru(η^6:κ^1-C$_6$H$_5$(CH$_2$)$_3$O)(phen)]BF$_4$ (3CRu)

Synthesis as for **2CRu** using [Ru(η^6-C$_6$H$_5$(CH$_2$)$_3$OH)(phen)Cl]Cl (19 mg, 0.039 mmol). Yellow powder. Yield: 9 mg, 0.015 mmol, 39%.

^{1}H NMR (400 MHz, MeOD-*d*$_4$, δ): 9.89 (d, J = 5.3 Hz, 2H, phen*H*), 8.89 (d, J = 8.0 Hz, 2H, phen*H*), 8.23 (s, 2H, phen*H*), 8.13 (dd, J = 8.2, 5.2 Hz, 2H, phen*H*), 6.45 (t, J = 6.1 Hz, 2H, Ar*H*), 6.08 (d, J = 4.6 Hz, 2H, Ar*H*), 5.35 (t, J = 5.9 Hz, 1H, Ar*H*), 3.58 – 3.45 (m, 2H, C*H*$_2$OH), 2.86 (t, J = 6.2 Hz, 2H, ArC*H*$_2$), 2.23 (dt, J = 9.2, 4.9 Hz, 2H, C*H*$_2$). **MS (ESI)**: m/z calcd for C$_{21}$H$_{19}$N$_2$ORu [M]$^+$ 417.05; found 417.0.

Crystallographic Analysis

The X-ray crystal structures of chlorido complexes **5·PF$_6$**, **8·PF$_6$**, **9**, **10**, **11**, **13**, closed tether complex **3C·PF$_6$**, and **dichlorido** complex [Os(η^6:κ^1-$C_6H_5(CH_2)_3OH)Cl_2$], have been determined. Selected bonds and angles are listed in Table S2, and crystallographic data are shown in Table S4.

Compounds containing an N,N-ligand present two different crystal systems. Compound **5·PF$_6$** crystallises in orthorhombic with space group *P* 2_1 2_1 2_1 while **8·PF$_6$** and **3C·PF$_6$** crystallise in the monoclinic unit cell, with space group *P* 1 2_1 1 and *P* 1 2_1/n 1, respectively. Compounds with N,O$^-$-ligands such as **10**, **11**, **13** and the neutral dichlorido compound [Os(η^6:κ^1-$C_6H_5(CH_2)_3OH)Cl_2$], crystallize in orthorhombic, trigonal, monoclinic and monoclinic systems, respectively, with *P* 3_1 2 1, *P* 1 2_1/c 1, *Pbca*, and *C* 1 2/c 1 as the space group.

Due to the chirality of compounds with a picolinate or quinolinate ligand, a mixture of 50% of both enantiomers, *R* and *S*, following the criteria used previously for this kind of organometallic compounds,[21] was obtained in the unit cell of complexes **9**, **11** and **13**. Compounds bearing an impy derivative as the chelating ligands, **5·PF$_6$** and **8·PF$_6$**, show an absolute *R* configuration. Compound **10**, with a picolinate derivative, shows an absolute *S* configuration at Os.

The Os–C(arene) bond lengths are in the range 2.133(14)–2.238(11) Å, which are similar to previously reported values of Os-arene structures.[14] Likewise, the Os–centroid distance for all tethered compounds, spanning 1.636–1.688 Å, is in the range to others already reported.[16, 21] The Os–N1 bond distances are in the range 2.082(8)–2.141(13) Å, being the shortest and the longest distances that of **5·PF$_6$** and of **10**, respectively. Os–Cl bond lengths for the open compounds **5·PF$_6$**, **8·PF$_6$**, **9**, **10**, **11** and **13** are in the range of 2.388(2)–2.4107(14) Å, in agreement with values in the literature for similar complexes.[21, 22]

For compounds **5·PF$_6$** and **8·PF$_6$**, with N,N-chelating ligands, the Os–N1/N2 bond distances are comparable to previously reported values in the range 2.074(5)–2.090(4).[16, 21] The N1–Os–N2 bite angle ranges between 76.1(4)–77.39(12)°, also in agreement with those reported for analogous Os(II)-impy complexes.[23]

Likewise, the N1–Os–N2 bite angle for **9**, **10**, **11** and **13** is similar to the previous values described for picolinate compounds (ca. 77.4°).[10] For these compounds, the Os–O2 bond lengths range from 2.057(10) Å to 2.100(10) Å, corresponding to **10** and **9**, respectively. Complex **10** presents the longest Os–N1 bond distance perhaps due to the presence of a methyl

group close to N1 (in the *ortho*-position), in agreement to a previous report.[10] Interestingly, the Os–Cl bond length is significantly longer for **11** (2.4107(14) Å) when compared to the other two picolinates **9** and **10** (2.398(3) and 2.395(3) Å, respectively), consistent with the higher bond reactivity observed for **11** (see main text).[24] Longer M–Cl bonds imply bond weakness and hydrolysis readiness. A similar relation between the bond length and hydrolysis rate was observed for Os(II) half-sandwich complexes such as [Os(η^6-arene)(N,O)Cl].[10, 24, 25]

The Os–O1 distances for **3C·PF$_6$** and **dichlorido** are 2.054(3) Å and 2.142(4) Å, respectively. A strong offset of C7 toward the osmium atom with regard to the plane that contains the η^6-bond arene was observed in the closed-tether compounds, with calculated values of 0.138 and 0.193 Å, respectively for both complexes. All the open tether complexes present C6-offsets close to nil ranging between 0.093 (toward the metal) to 0.036 (away from the metal). Similar results were reported for open versus closed Ru(II) tether complexes by Miyaki et al. (Table S2 and S7).[19] In particular, the ruthenium(II) analogue [Ru(η^6:κ^1-$C_6H_5(CH_2)_3O$)(phen)]$^+$ presents a C7-offset of 0.119 Å, slightly smaller than that of the Os congener **3C·PF$_6$** (0.138 Å) reported here. The size of the chelate ring formed by the tether arm appears to be the most impactful feature in such an offset; cation [Ru(η^6:κ^1-$C_6H_5CH_2COO$)($Me_2NCH_2CH_2Me_2$)]$^+$,[26] closed tether complex with a five-member tether ring, presented a 0.548 Å C7-offset toward the Ru centre. We can also compare the structure of dichlorido complex reported here [Os(η^6:κ^1-$C_6H_5(CH_2)_3OH$)Cl_2] with its ruthenium(II) analogue [Ru(η^6:κ^1-$C_6H_5(CH_2)_3OH$)Cl_2], reported by Čubrilo et al.[27] The Ru–O1 distance is 2.154(3) Å, while in the case of Os the analogous Os–O1 distance is 2.142(4) Å, not being significantly different to one another. The ruthenium dichlorido compound also shows a C7 offset toward the metal centre of 0.203 Å, which is also similar to that of our osmium dichlorido complex discussed above (0.193 Å).

There are no closed tether Os complexes reported in literature we can compare complex **3C·PF$_6$** with. However, while most of Ru versus Os analogues often present quasi-identical structures with negligible differences in angles and bond distances, in the case of complex **3C·PF$_6$** and its Ru(II) counterpart, the Os–O1 distance is significantly shorter for the osmium complex **3C·PF$_6$** with 2.054(3) Å, than for [Ru(η^6:κ^1-$C_6H_5(CH_2)_3OH$)(phen)]$^+$ (**3CRu** here) with 2.145(3) Å (Table S7).[19] Rather than justifying this difference based on the nature of the metal (atomic radius is 205 pm for Ru and 200 pm for Os), such a difference is better understood on the basis of the actual κ^1-*O* ligand bound to the metal. While **3C·PF$_6$** presents Os bound to a (deprotonated) alkoxy group closing the tether ring, the Ru counterpart is isolated with an alcohol group bound to the metal. In fact, the closed tether complex [Ru(η^6:κ^1-

$C_6H_5(CH_2)_3O)(bipy)]^+$, bearing a bipy chelating ligand instead of a phen, purposely synthesized in its deprotonated form by addition of NaOH by Miyaki et al.,[19] was reported to have a Ru–O1 distance of 2.050(5) Å, in agreement with that of an alkoxy (and not an alcohol) oxygen bound to the metal. This is also in agreement with the similarities found in Os–O1 and Ru–O1 distances in dichlorido neutral complexes discussed above.

In aromatic systems, π-π interactions are typically associated with interplanar separations of 3.3–3.8 Å.[28, 29] The crystal structure of complex **3C·PF$_6$** shows evidences for intermolecular π-π interactions between the phenyl ring of the phenanthroline of adjacent molecules, with a distance between centroids of 3.730 Å and a dihedral angle of 0° (Fig. S24). For complex **8·PF$_6$**, the intermolecular π-π interaction was found between the pyridine rings from the impy ligand and the phenyl ring of an adjacent molecule with a distance between centroids of 3.843 and a dihedral angle of 5.71°. Longer distances for π-π stacking have also been described (up to 4.7 Å).[28, 29] In the case of complex **9**, π-π interactions between the η^6-arene rings of adjacent molecules with a distance between centroids of 4.083 Å and a dihedral angle of 9.36° are found.

Hydrogen bonds with a strong electrostatic character based on the D···A and H···A distances, and a covalent component based on a strong directionality (Table S3) as classified by Jeffrey,[30, 31] are observed between the OH (alcohol) of tether arm and the O of the chelating ligand (picolinate or quinolinate) of adjacent molecules in the crystal structures of **9**, **11** and **13**, giving rise to dimers in the last two (Figure S24, Table S3).[14, 32] While disorder in the tethered alcohol of complex **10** hampered H-bonding analysis, complexes **9** and **11** show H-bonding between the OH (alcohol) of the tether arm and the picolinate CO (carboxylate) not involved in metal-binding of an adjacent molecule (O(1)H···O(6)) 2.80(1) Å (∠DHA 171.23) and (O(1)H···O(3)) 2.820(6) Å (∠DHA 164.05), respectively. For complex **13** the hydrogen bonding is observed between the OH (alcohol) of the tether arm and the metal-bound oxygen of the quinolinate of an adjacent molecule (O(1)H···O(2)) 2.723(4) Å (∠DHA 178.32). Importantly, for the closed tether complex **3C·PF$_6$**, hydrogen bonding is observed between the Os-coordinated alkoxy oxygen and a methanol molecule from crystallization (O(1)H···O(3W)) 2.592(4) Å (∠DHA 175.21), being the strongest of them all.

CCDC 2026997–2027004 contain the crystallographic data for this paper. These data are provided free of charge by The Cambridge Crystallographic Data Centre.

Supplementary Charts

Chart S1.

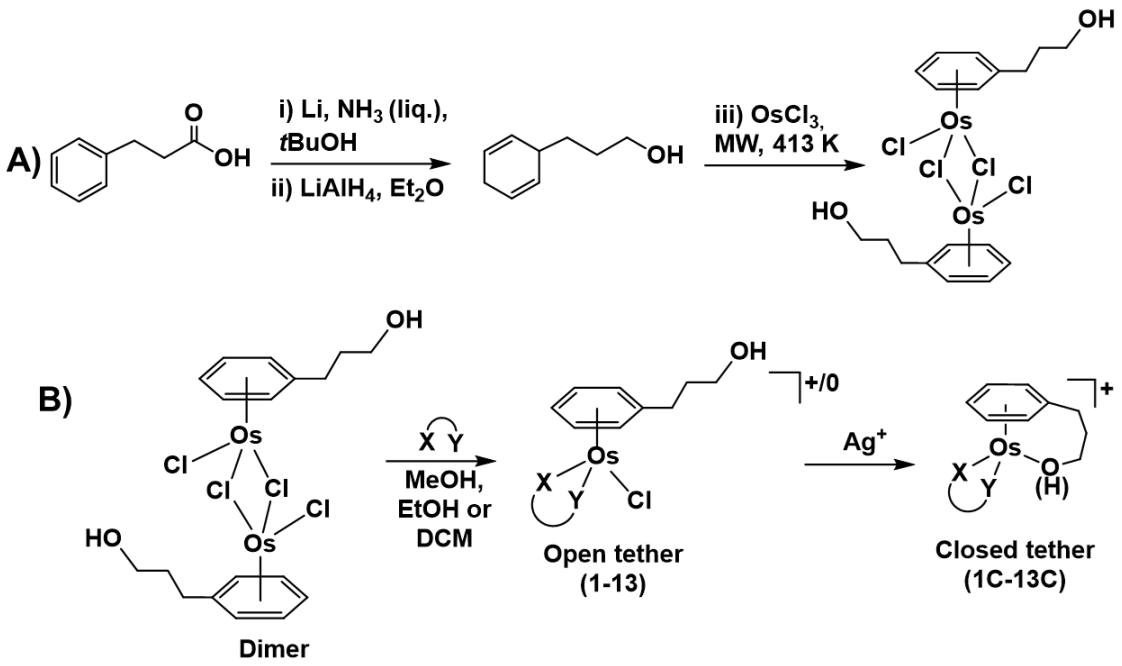

Chart S1. Synthetic scheme for Os(II) half-sandwich complexes described in this work. Synthetic scheme for (A) hemilabile ligand 3-(1,4-cyclohexadien-1-yl)-1-propanol and dimer $[Os(\eta^6\text{-}C_6H_5(CH_2)_3OH)(\mu\text{-}Cl)Cl]_2$, and (B) open tether complexes **1–13** and closed tether complexes **1C**–**13C**.

Supplementary Figures

Figure S1.

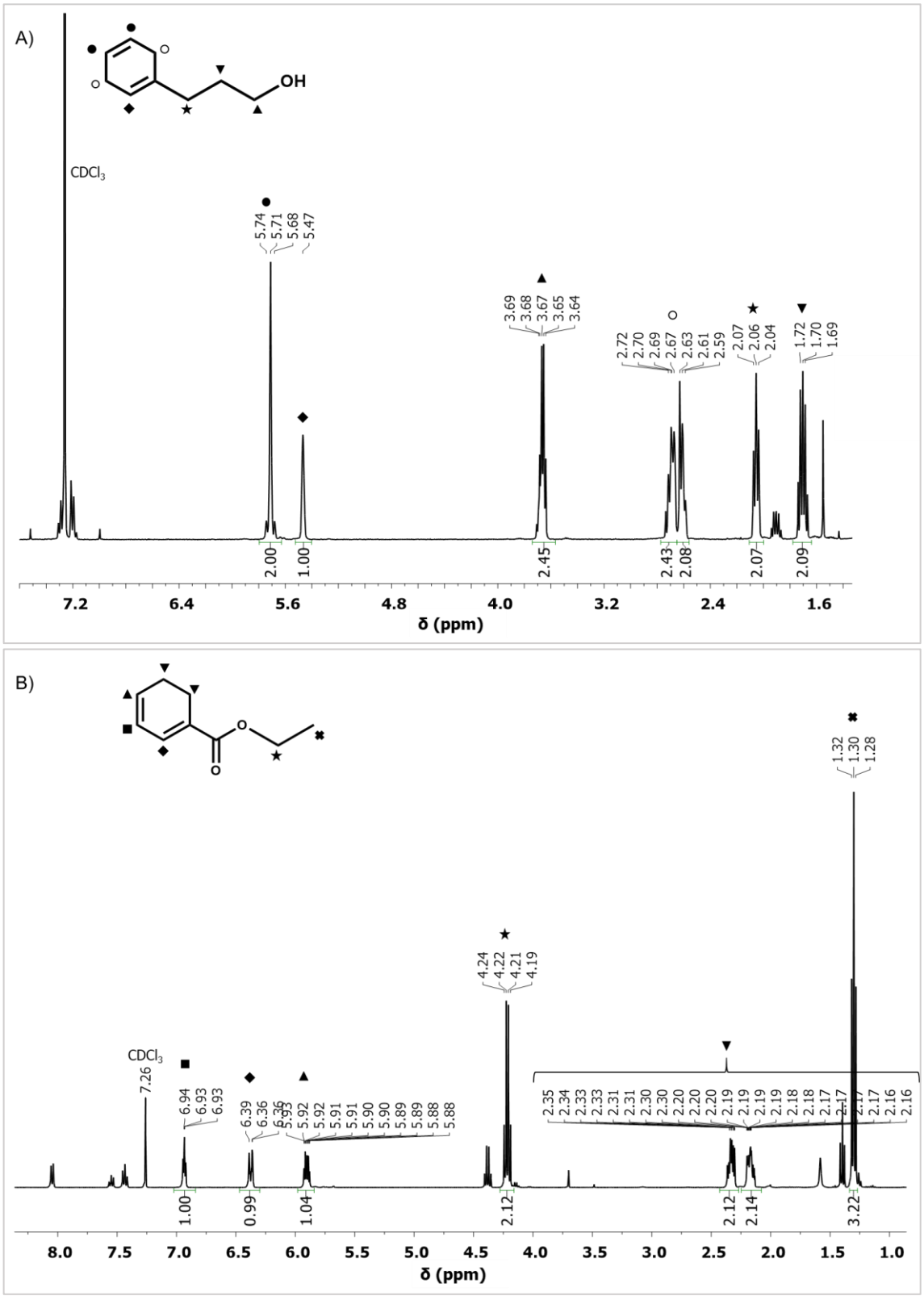

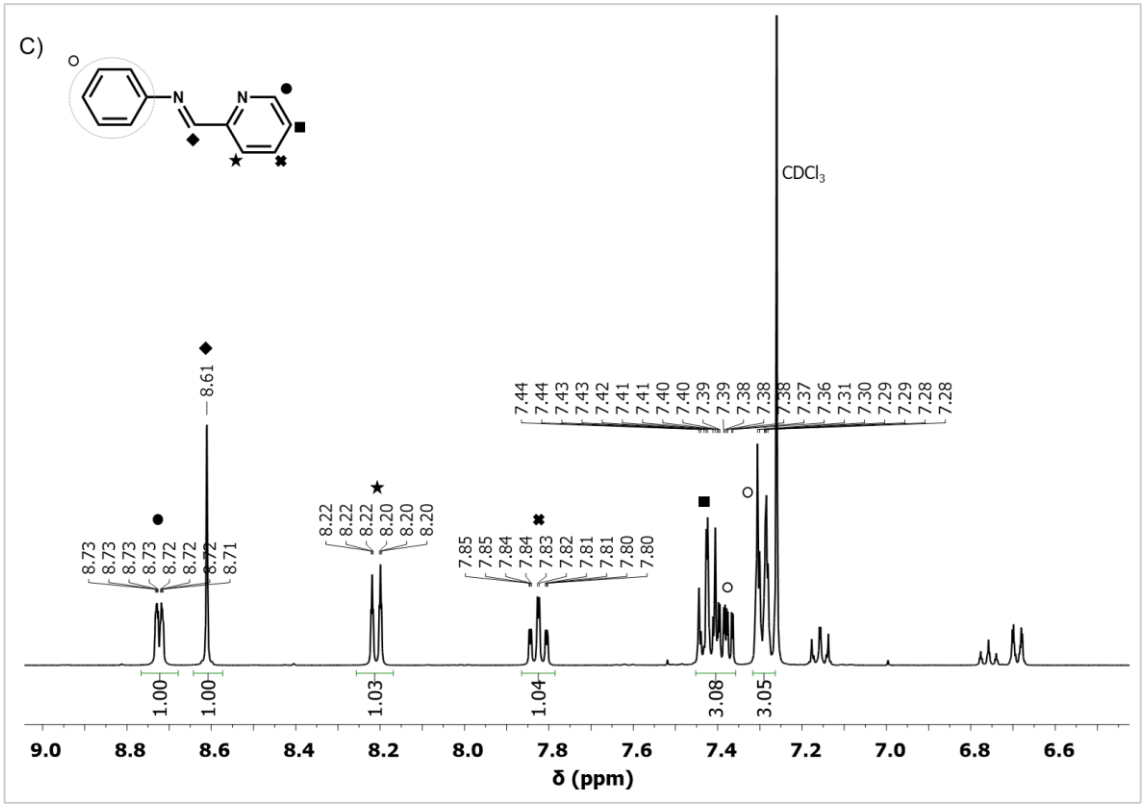
C)
CDCl3
8.73
8.73
8.73
8.72
8.72
8.72
8.71
8.61
8.22
8.22
8.22
8.20
8.20
8.20
7.85
7.85
7.84
7.84
7.83
7.82
7.81
7.81
7.80
7.80
7.44
7.44
7.43
7.43
7.42
7.41
7.41
7.40
7.40
7.39
7.39
7.38
7.38
7.38
7.37
7.36
7.31
7.30
7.29
7.29
7.28
7.28
1.00
1.00
1.03
1.04
3.08
3.05
9.0
8.8
8.6
8.4
8.2
8.0
7.8
7.6
7.4
7.2
7.0
6.8
6.6
δ (ppm)

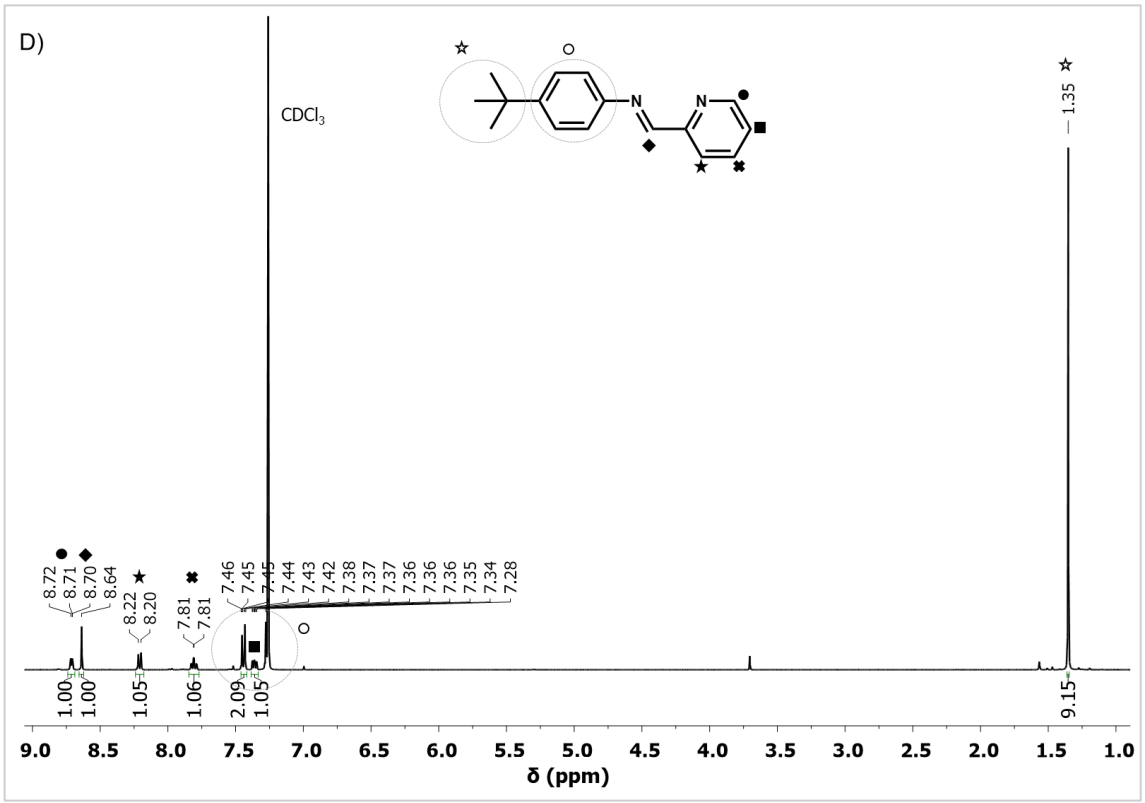
D)
CDCl3
1.35
8.72
8.71
8.70
8.64
8.22
8.20
7.81
7.81
7.46
7.45
7.45
7.44
7.43
7.42
7.38
7.37
7.37
7.36
7.36
7.36
7.35
7.34
7.28
1.00
1.00
1.05
1.06
2.09
1.05
9.15
9.0
8.5
8.0
7.5
7.0
6.5
6.0
5.5
5.0
4.5
4.0
3.5
3.0
2.5
2.0
1.5
1.0
δ (ppm)

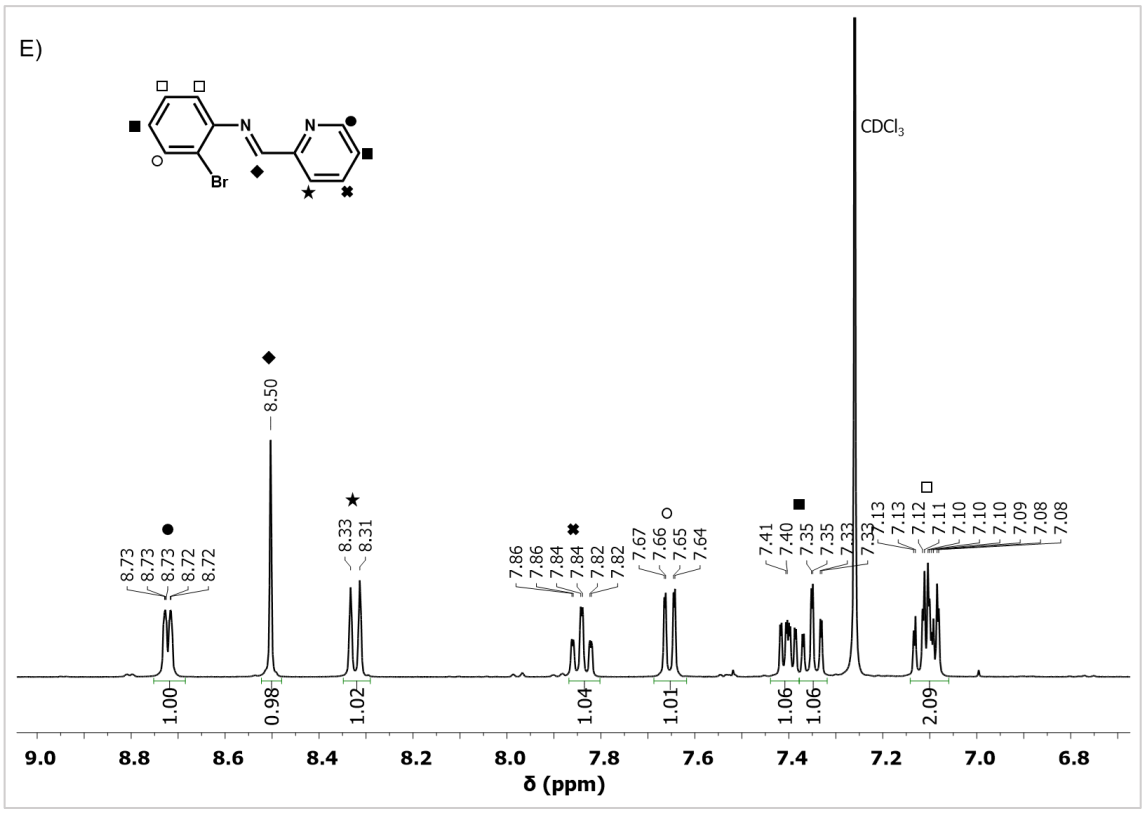
E)
CDCl3
Br
8.73
8.73
8.73
8.72
8.72
8.50
8.33
8.31
7.86
7.86
7.84
7.84
7.82
7.82
7.67
7.66
7.65
7.64
7.41
7.40
7.35
7.35
7.33
7.33
7.13
7.12
7.11
7.10
7.10
7.10
7.09
7.08
7.08
1.00
0.98
1.02
1.04
1.01
1.06
1.06
2.09
9.0
8.8
8.6
8.4
8.2
8.0
7.8
7.6
7.4
7.2
7.0
6.8
δ (ppm)

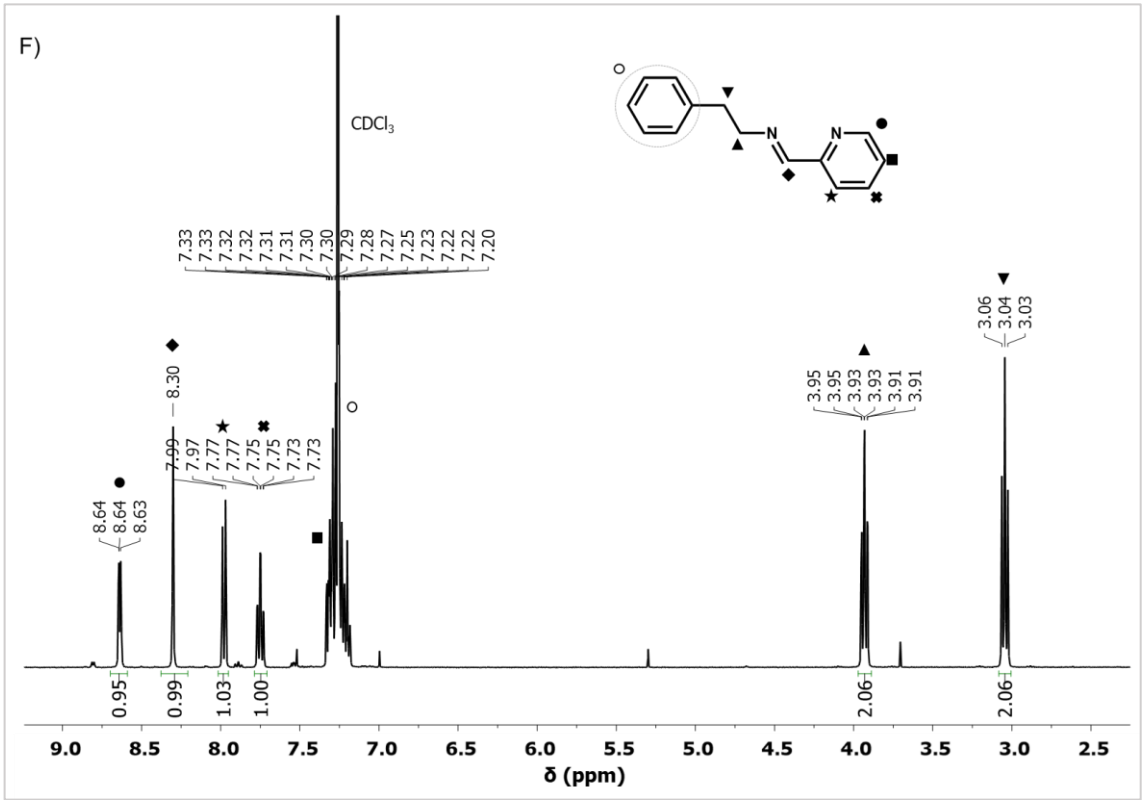
F)
CDCl3
N
N
7.33
7.33
7.32
7.32
7.31
7.31
7.30
7.30
7.29
7.28
7.27
7.25
7.23
7.22
7.22
7.20
8.64
8.64
8.63
8.30
7.99
7.97
7.77
7.77
7.75
7.75
7.73
7.73
3.95
3.95
3.93
3.93
3.91
3.91
3.06
3.04
3.03
0.95
0.99
1.03
1.00
2.06
2.06
9.0
8.5
8.0
7.5
7.0
6.5
6.0
5.5
5.0
4.5
4.0
3.5
3.0
2.5
δ (ppm)

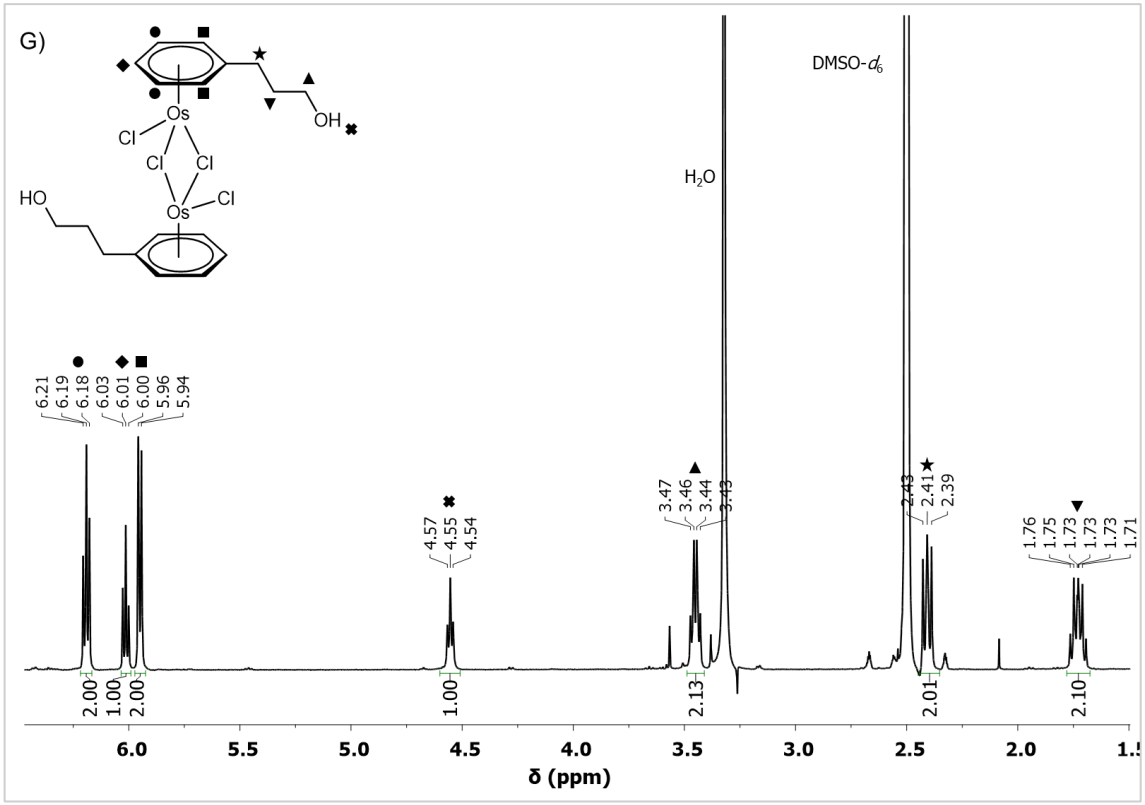
G)
Os
Cl
Cl
Cl
Cl
Os
Cl
HO
OH
DMSO-d_6
H_2O
6.21
6.19
6.18
6.03
6.01
6.00
5.96
5.94
4.57
4.55
4.54
3.47
3.46
3.44
3.43
2.43
2.41
2.39
1.76
1.75
1.73
1.73
1.73
1.71
2.00
1.00
2.00
1.00
2.13
2.01
2.10
6.0
5.5
5.0
4.5
4.0
3.5
3.0
2.5
2.0
δ (ppm)

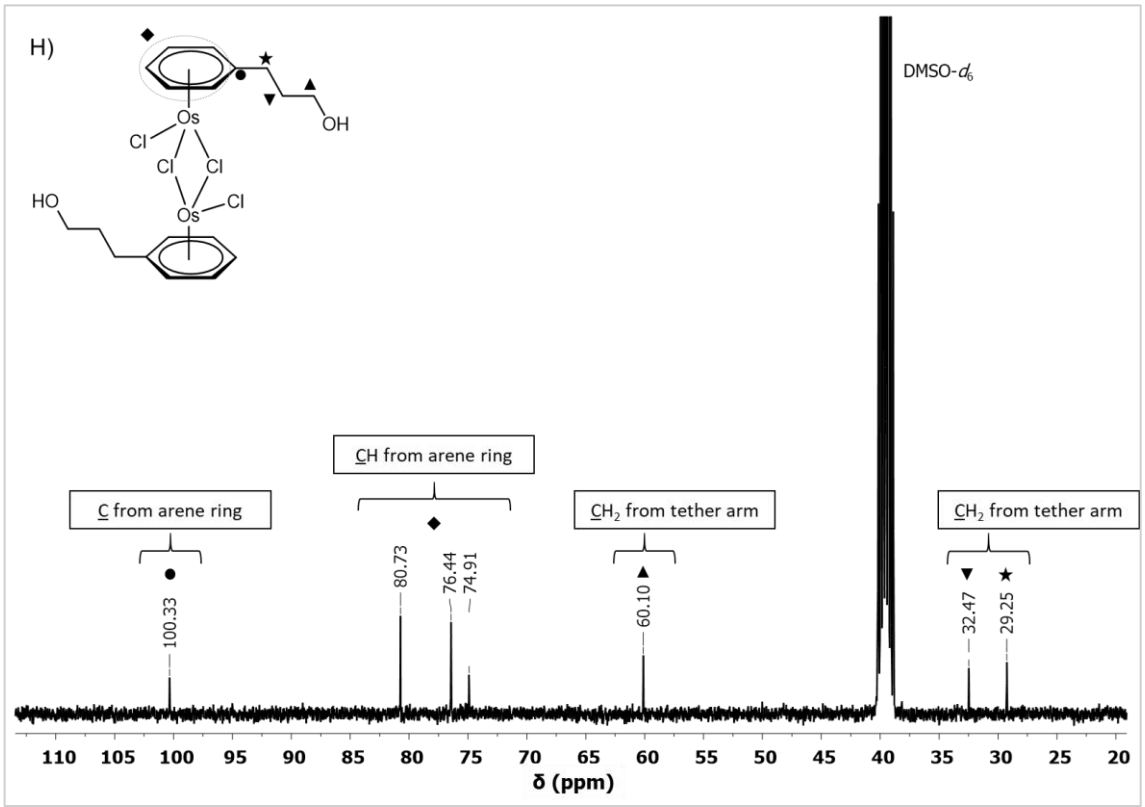
H)
Os
Cl
Cl
Cl
Cl
Os
Cl
HO
OH
DMSO-d_6
C from arene ring
CH from arene ring
CH_2 from tether arm
CH_2 from tether arm
100.33
80.73
76.44
74.91
60.10
32.47
29.25
110
105
100
95
90
85
80
75
70
65
60
55
50
45
40
35
30
25
20
δ (ppm)

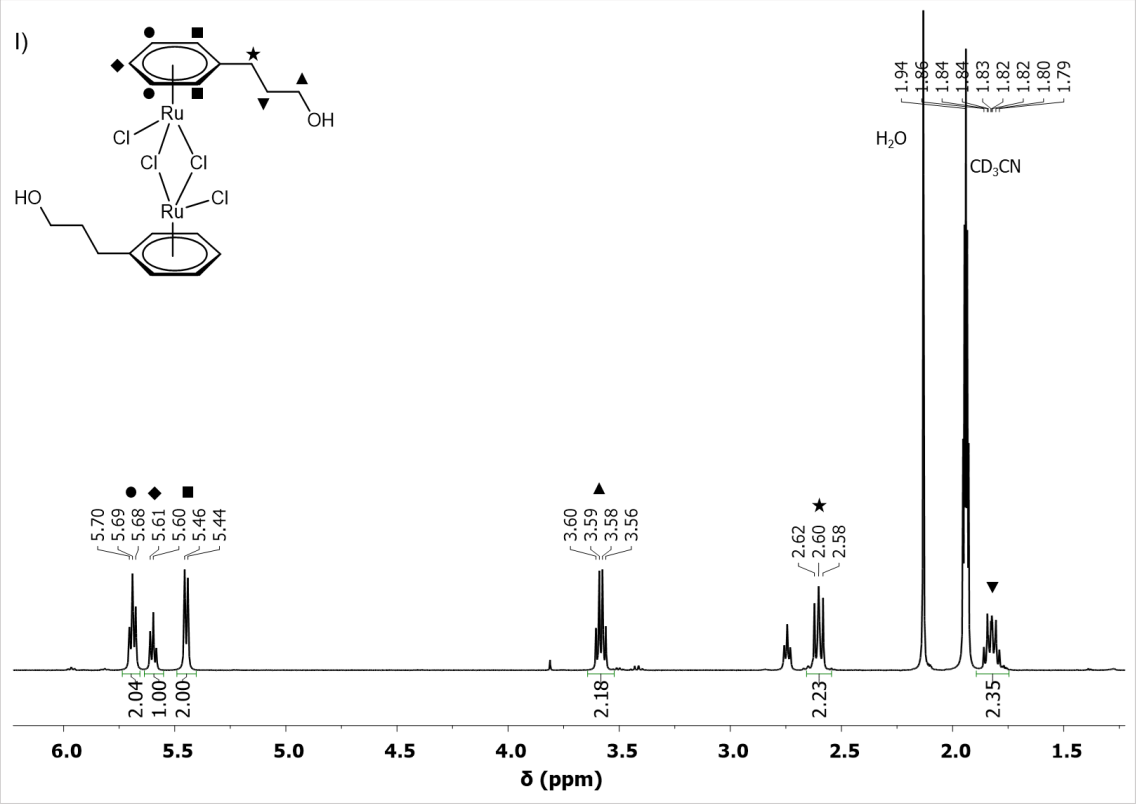

Figure S1. NMR spectra of organic ligand precursors. ^{1}H NMR spectra (400 MHz, $CDCl_3$) of (A) 3-(cyclohexa-1,4-dien-1-yl)propan-1-ol, (B) Ethyl cyclohexa-1,3-diene-1-carboxylate (C) (E)-N-phenyl-1-(pyridin-2-yl)methanimine, (D) (E)-N-(4-(tert-butyl)phenyl)-1-(pyridin-2-yl)methanimine, (E) (E)-N-(2-bromophenyl)-1-(pyridin-2-yl)methanimine, (F) (E)-N-phenethyl-1-(pyridin-2-yl)methanimine. (G) ^{1}H NMR spectrum (400 MHz, DMSO-d_6) of dimer precursor $[Os(\eta^6\text{-}C_6H_5(CH_2)_3OH)(\mu\text{-}Cl)Cl]_2$, (H) $^{13}C\{^{1}H\}$ NMR spectrum (101 MHz, DMSO-d_6) of dimer precursor $[Os(\eta^6\text{-}C_6H_5(CH_2)_3OH)(\mu\text{-}Cl)Cl]_2$ and (I) ^{1}H NMR spectrum (400 MHz, CD_3CN) of dimer precursor $[Ru(\eta^6\text{-}C_6H_5(CH_2)_3OH)(\mu\text{-}Cl)Cl]_2$.

Figure S2.

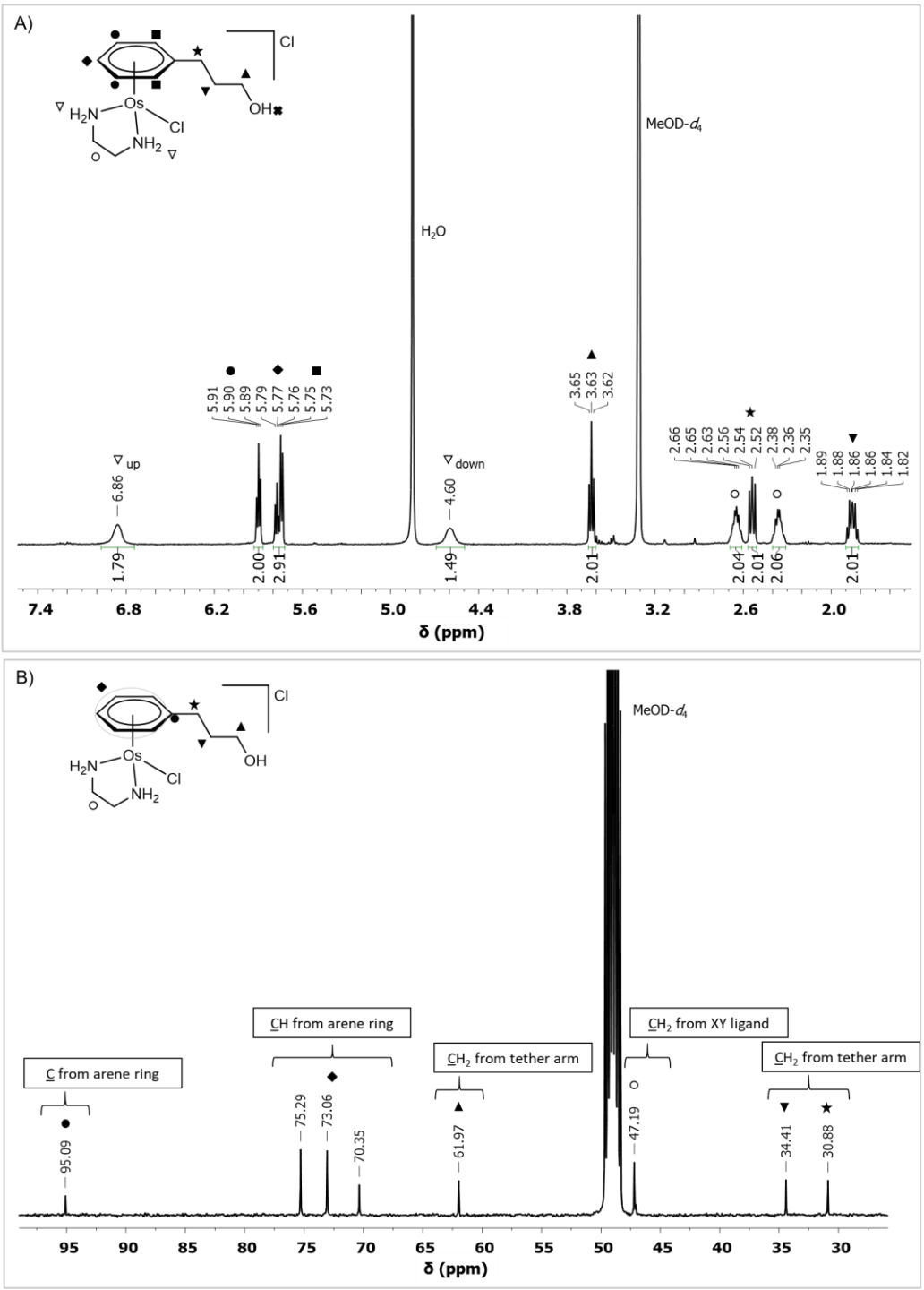

Figure S2. ^{1}H and $^{13}C\{^{1}H\}$ NMR spectra of complex **1**. (A) ^{1}H NMR (400 MHz, CD_3OD) and (B) $^{13}C\{^{1}H\}$ NMR spectra (101 MHz, CD_3OD) of $[Os(\eta^6\text{-}C_6H_5(CH_2)_3OH)(en)Cl]Cl$. In the case of the compounds with primary amines as chelating ligand such as ethylenediamine, two different signals for the NH_2 protons appear. The H (up, pointing towards the arene) are at downfield than the H(down), which are affected by a lower electron density environment as described by Chen et al.[28, 33]

Figure S3.

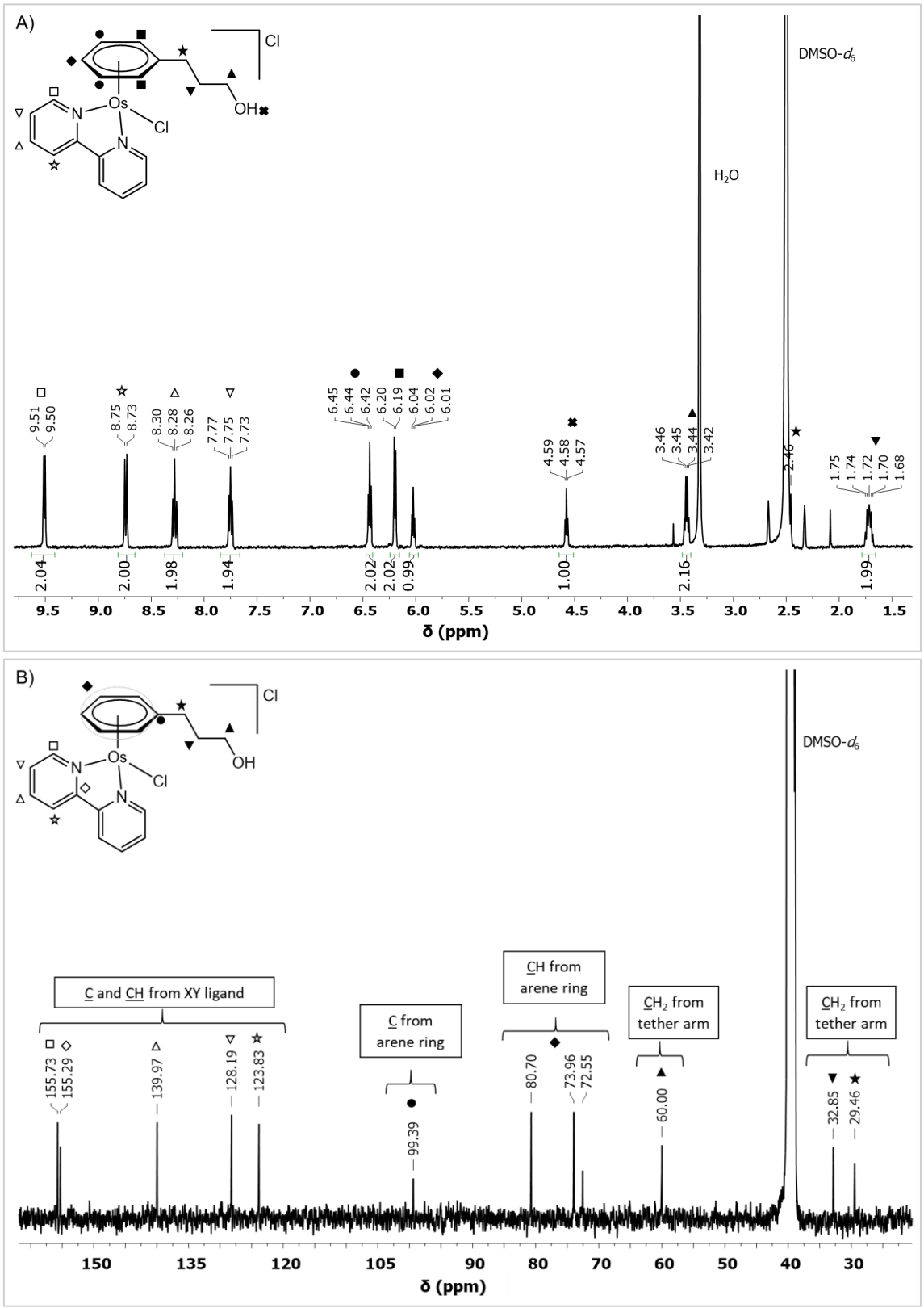

Figure S3. ^{1}H and $^{13}C\{^{1}H\}$ NMR spectra of complex **2**. (A) ^{1}H NMR (400 MHz, DMSO-d_6) and (B) $^{13}C\{^{1}H\}$ NMR spectra (101 MHz, DMSO-d_6) of [Os(η^6-$C_6H_5CH_2CH_2CH_2OH$)(bipy)Cl]Cl.

Figure S4.

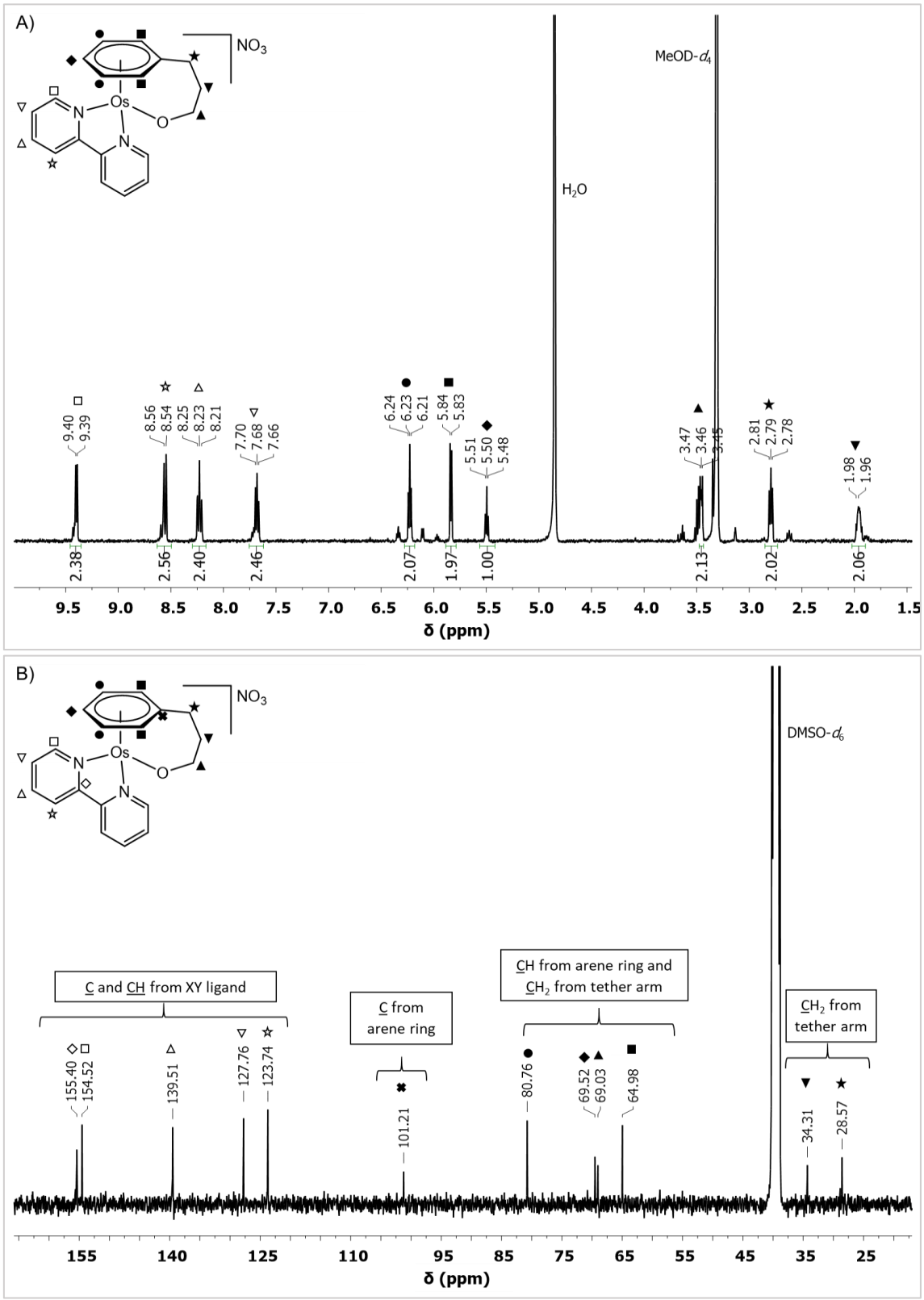

Figure S4. ^{1}H and $^{13}C\{^{1}H\}$ NMR spectra of complex **2C**. It includes assignment of signals using 2D NMR spectra. (A) ^{1}H NMR (400 MHz, CD_3OD) and (B) $^{13}C\{^{1}H\}$ NMR spectra (101 MHz, DMSO-d_6) of $[Os(\eta^6{:}\kappa^1\text{-}C_6H_5(CH_2)_3O)(bipy)]NO_3$.

Figure S5.

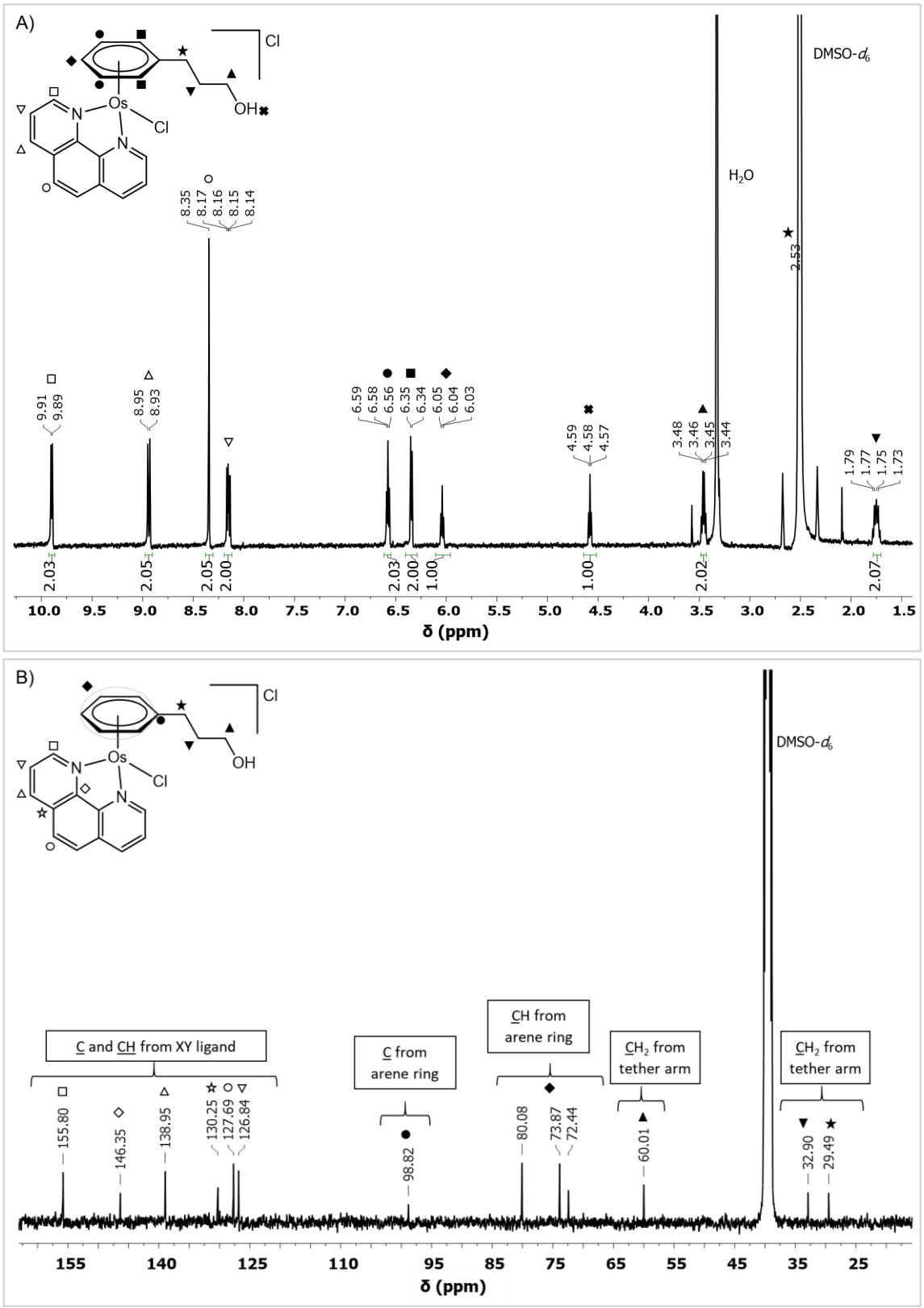

Figure S5. ^{1}H and ^{13}C{^{1}H} NMR spectra of complex **3**. (A) ^{1}H NMR (400 MHz, DMSO-d_6) and (B) ^{13}C{^{1}H} NMR spectra (101 MHz, DMSO-d_6) of [Os(η^6-$C_6H_5CH_2CH_2CH_2OH$)(phen)Cl]Cl.

Figure S6.

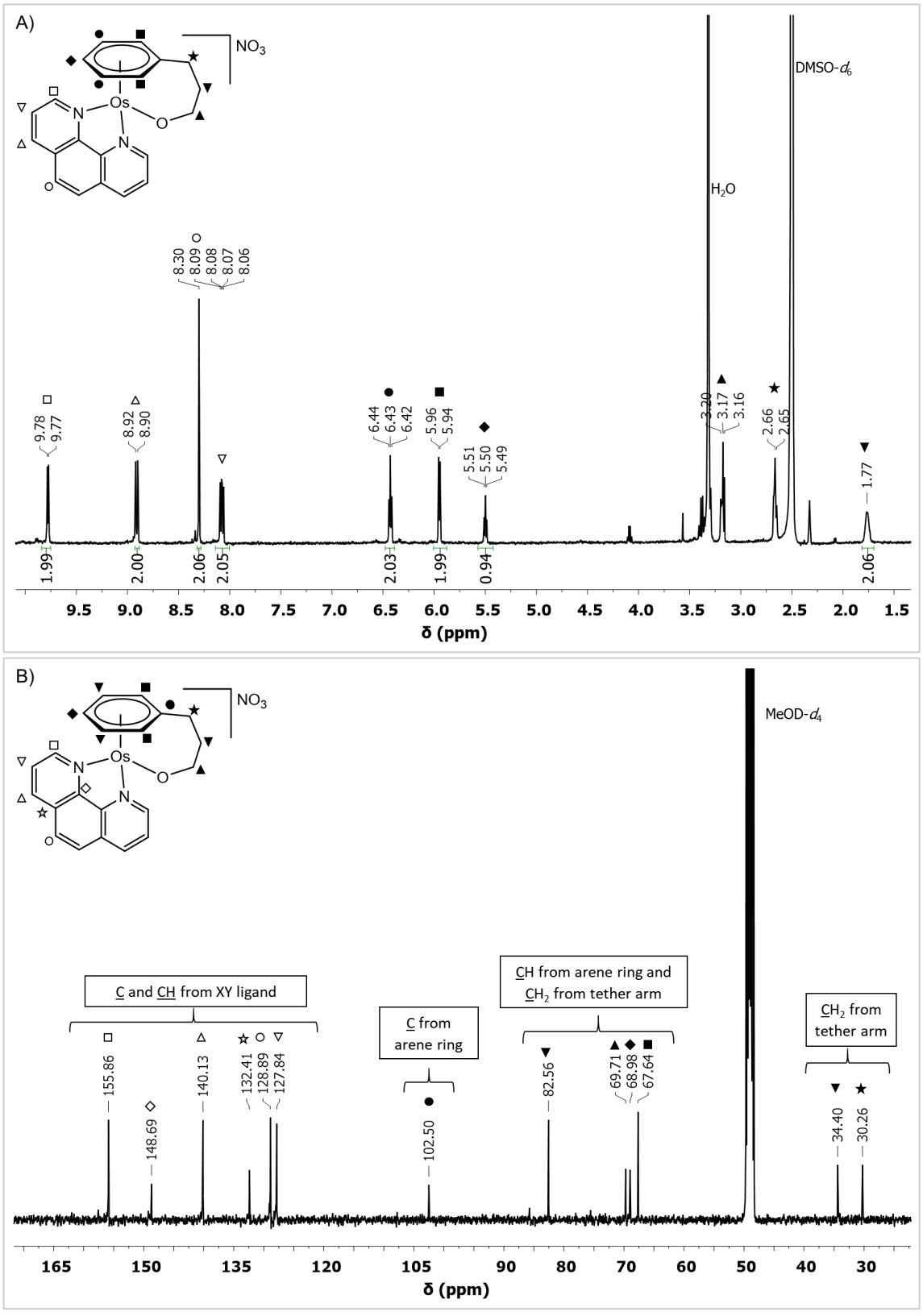

Figure S6. ^{1}H and $^{13}C\{^{1}H\}$ NMR spectra of complex **3C**. Include assignment of signals by means of 2D spectra. (A) ^{1}H NMR (400 MHz, DMSO-d_6) and (B) $^{13}C\{^{1}H\}$ NMR spectra (101 MHz, CD_3OD) of $[Os(\eta^6{:}\kappa^1\text{-}C_6H_5(CH_2)_3O)(phen)]NO_3$.

Figure S7.

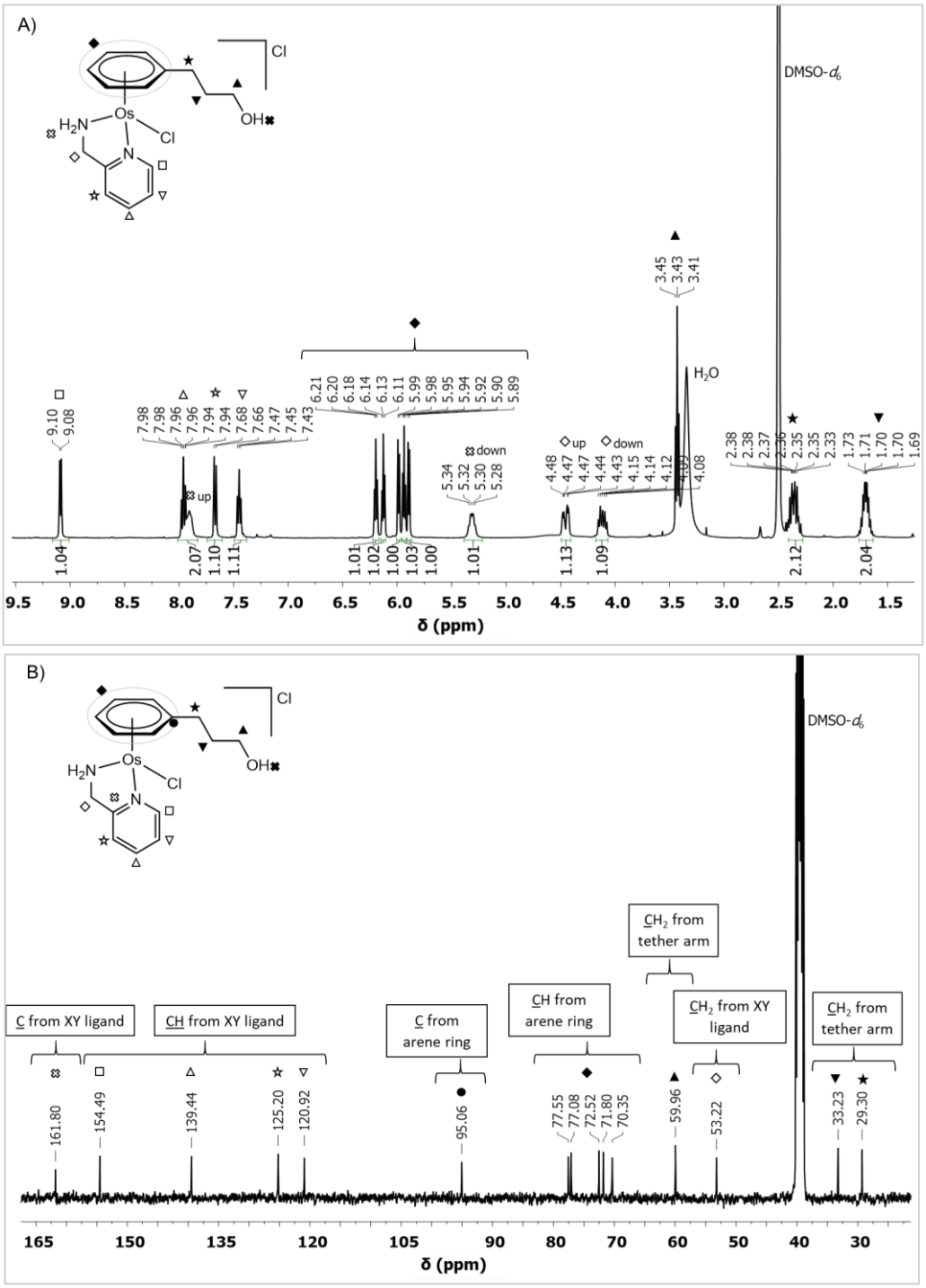

Figure S7. ^{1}H and $^{13}C\{^{1}H\}$ NMR spectra of complex **4**. (A) ^{1}H NMR (400 MHz, DMSO-d_6) and (B) $^{13}C\{^{1}H\}$ NMR spectra (101 MHz, DMSO-d_6) of [Os(η^6-$C_6H_5(CH_2)_3OH$)(ampy)Cl]Cl. In compounds with primary amines such as 2-picolylamine (ampy) as chelating ligand, two different signals for the NH_2 protons appear. The H(up, pointing towards the arene) are at downfield than the H(down), and they are affected by a lower electron density environment as described by Chen et al.[28, 33]

Figure S8.

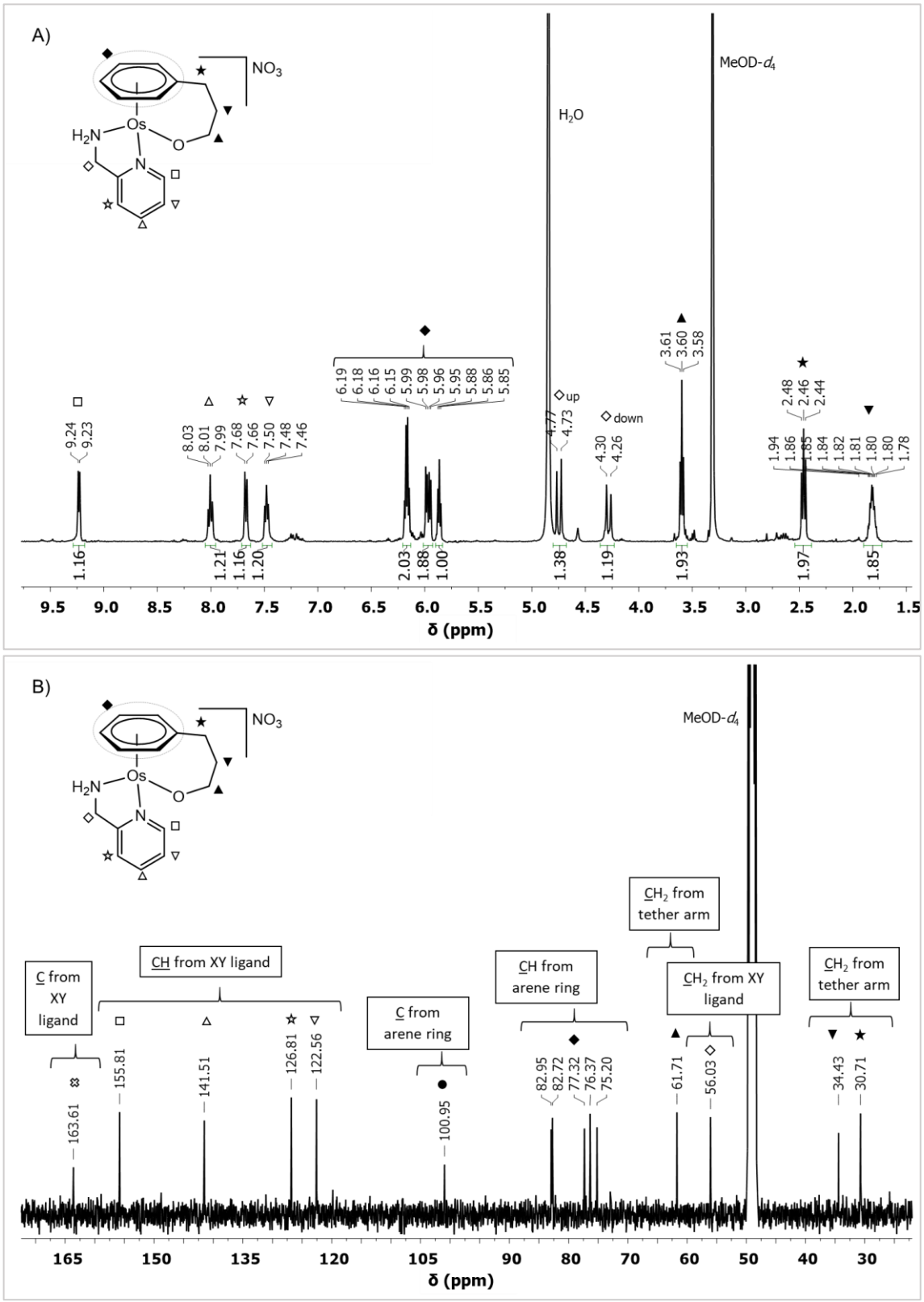

Figure S8. ^{1}H and $^{13}C\{^{1}H\}$ NMR spectra of complex **4C**. (A) ^{1}H NMR (400 MHz, CD_3OD) and (B) $^{13}C\{^{1}H\}$ NMR spectra (101 MHz, CD_3OD) of $[Os(\eta^6{:}\kappa^1\text{-}C_6H_5(CH_2)_3O)(ampy)]NO_3$.

Figure S9.

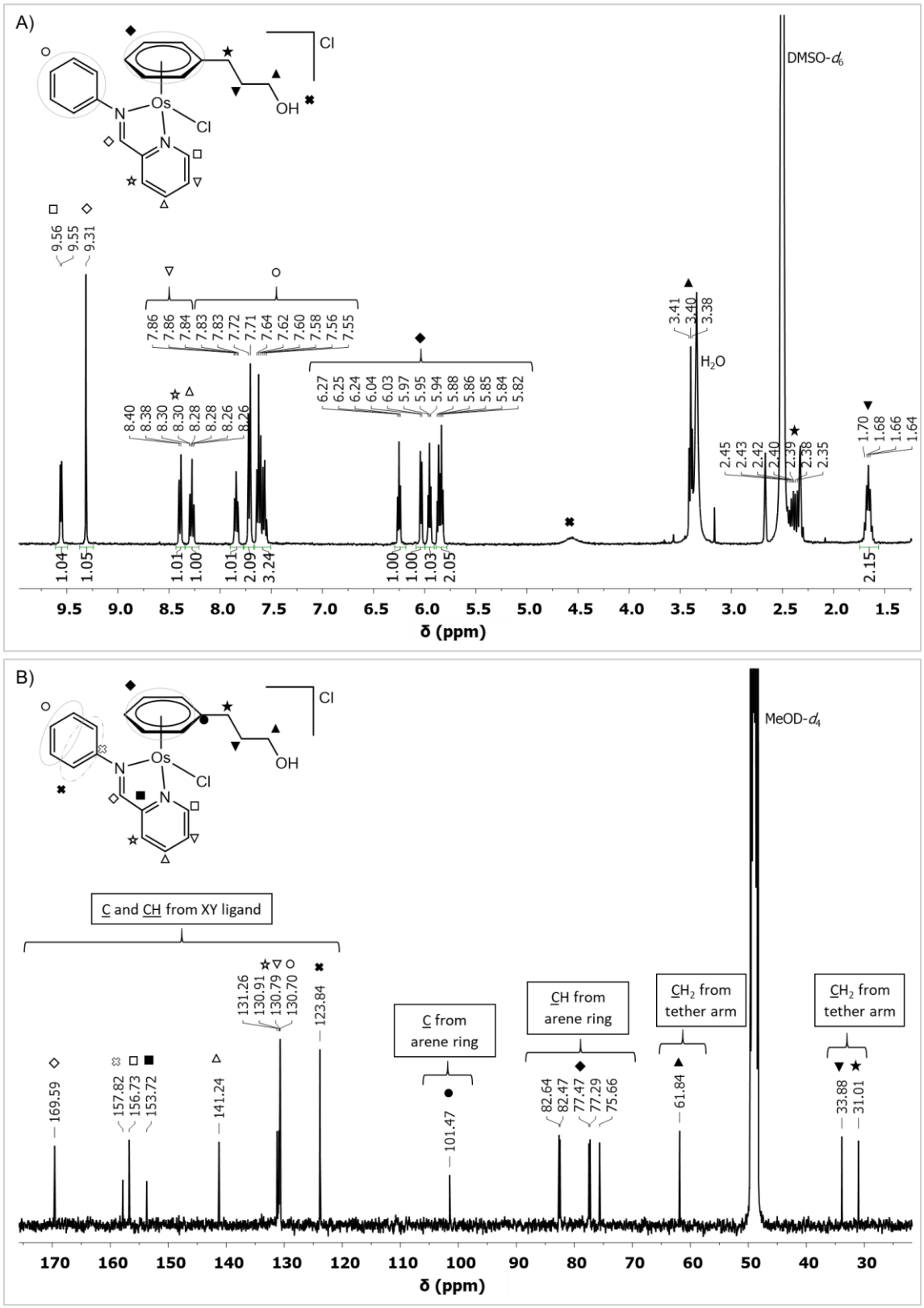

Figure S9. ^{1}H and ^{13}C{^{1}H} NMR spectra of complex **5**. (A) ^{1}H NMR (400 MHz, DMSO-d_6) and (B) ^{13}C{^{1}H} NMR spectra (101 MHz, CD_3OD) of [Os(η^6-$C_6H_5(CH_2)_3OH$)(Ph-impy)Cl]Cl.

Figure S10.

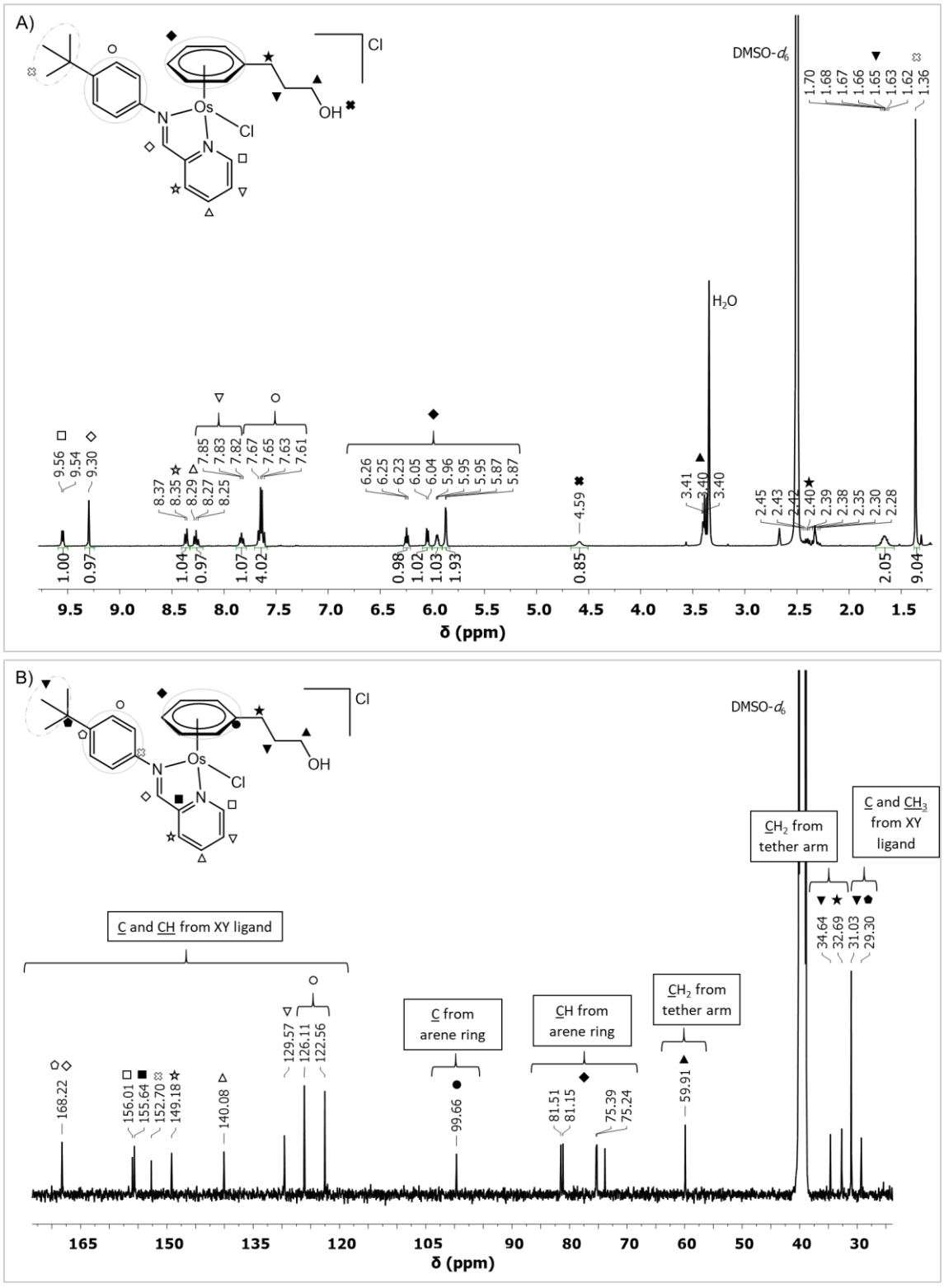

Figure S10. ^{1}H and $^{13}C\{^{1}H\}$ NMR spectra of complex **6**. (A) ^{1}H NMR (400 MHz, DMSO-d_6) and (B) $^{13}C\{^{1}H\}$ NMR spectra (101 MHz, DMSO-d_6) of [Os(η^6-$C_6H_5(CH_2)_3OH$)(tBuPh-impy)Cl]Cl.

Figure S11.

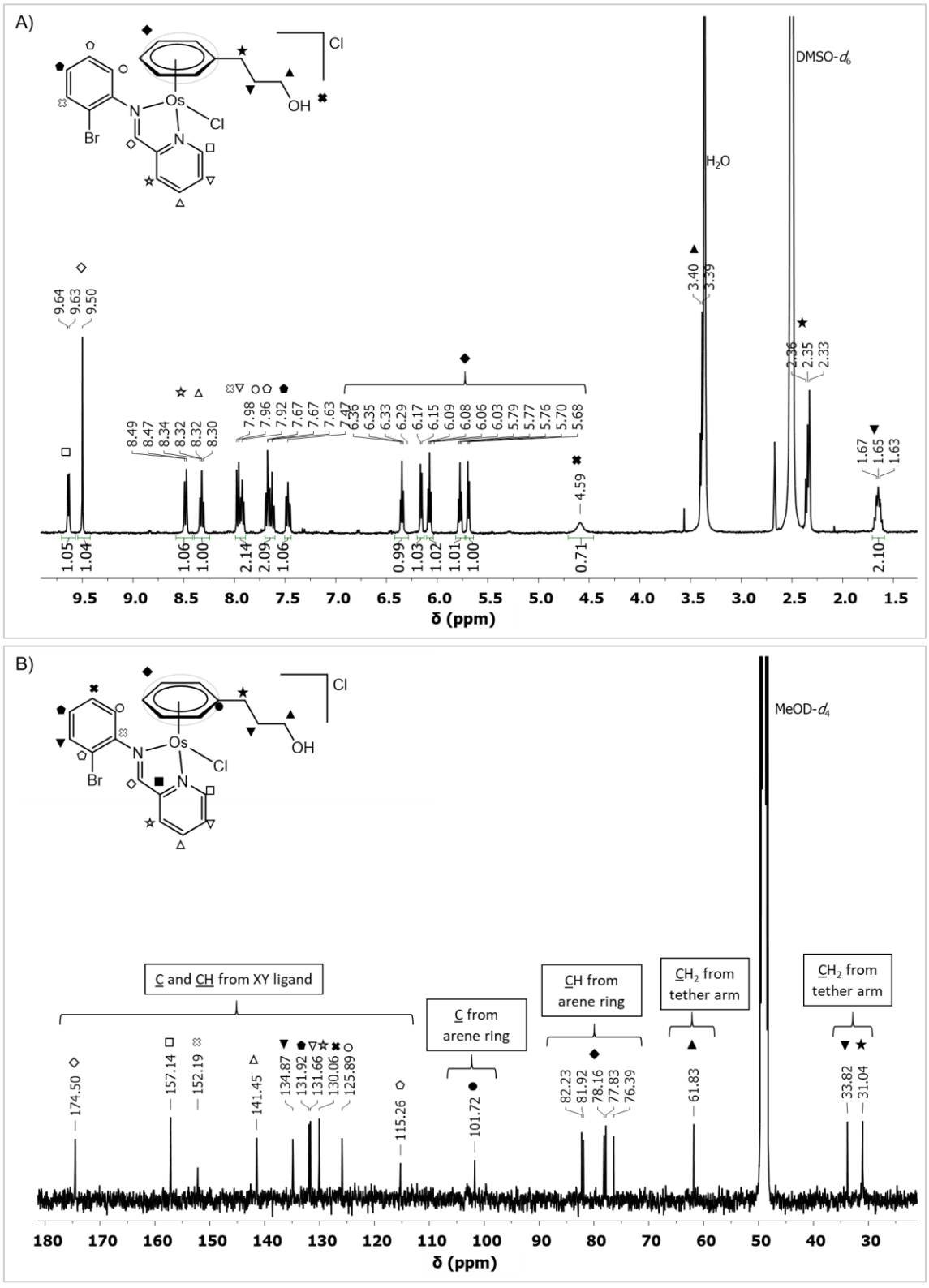

Figure S11. ^{1}H and $^{13}C\{^{1}H\}$ NMR spectra of complex **7**. It includes assignment of signals using 2D NMR spectra. (A) ^{1}H NMR (400 MHz, DMSO-d_6) and (B) $^{13}C\{^{1}H\}$ NMR spectra (101 MHz, CD_3OD) of $[Os(\eta^6\text{-}C_6H_5(CH_2)_3OH)(BrPh\text{-}impy)Cl]Cl$.

Figure S12.

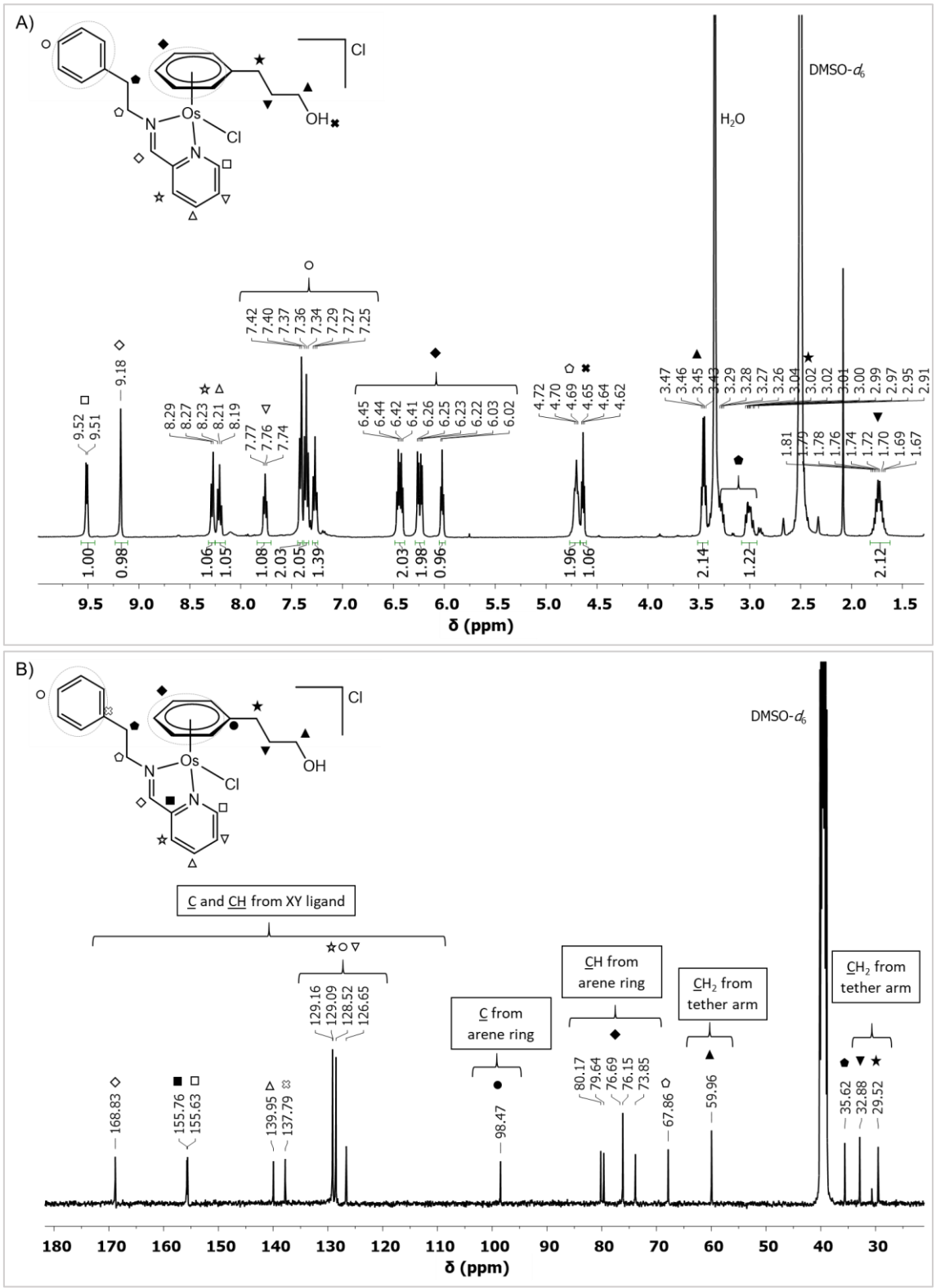

Figure S12. ^{1}H and $^{13}C\{^{1}H\}$ NMR spectra of complex **8**. It includes assignment of signals using 2D NMR spectra. (A) ^{1}H NMR (400 MHz, DMSO-d_6) and (B) $^{13}C\{^{1}H\}$ NMR spectra (101 MHz, DMSO-d_6) of [Os(η^6-$C_6H_5(CH_2)_3OH$)(PhEt-impy)Cl]Cl.

Figure S13.

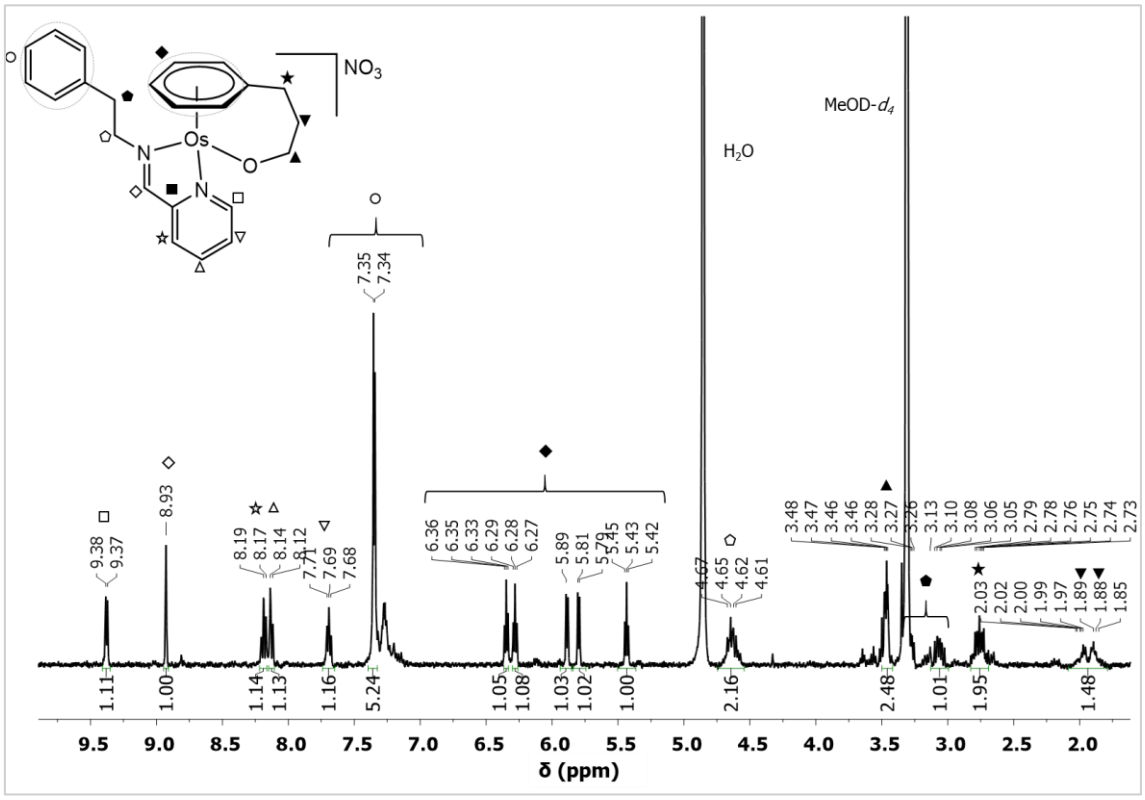

Figure S13. ^{1}H NMR spectrum of complex **8C**. It includes assignment of signals using 2D NMR spectra. ^{1}H NMR (400 MHz, CD_3OD) of $[Os(\eta^6{:}\kappa^1\text{-}C_6H_5(CH_2)_3O)(PhEt\text{-}impy)]NO_3$.

Figure S14.

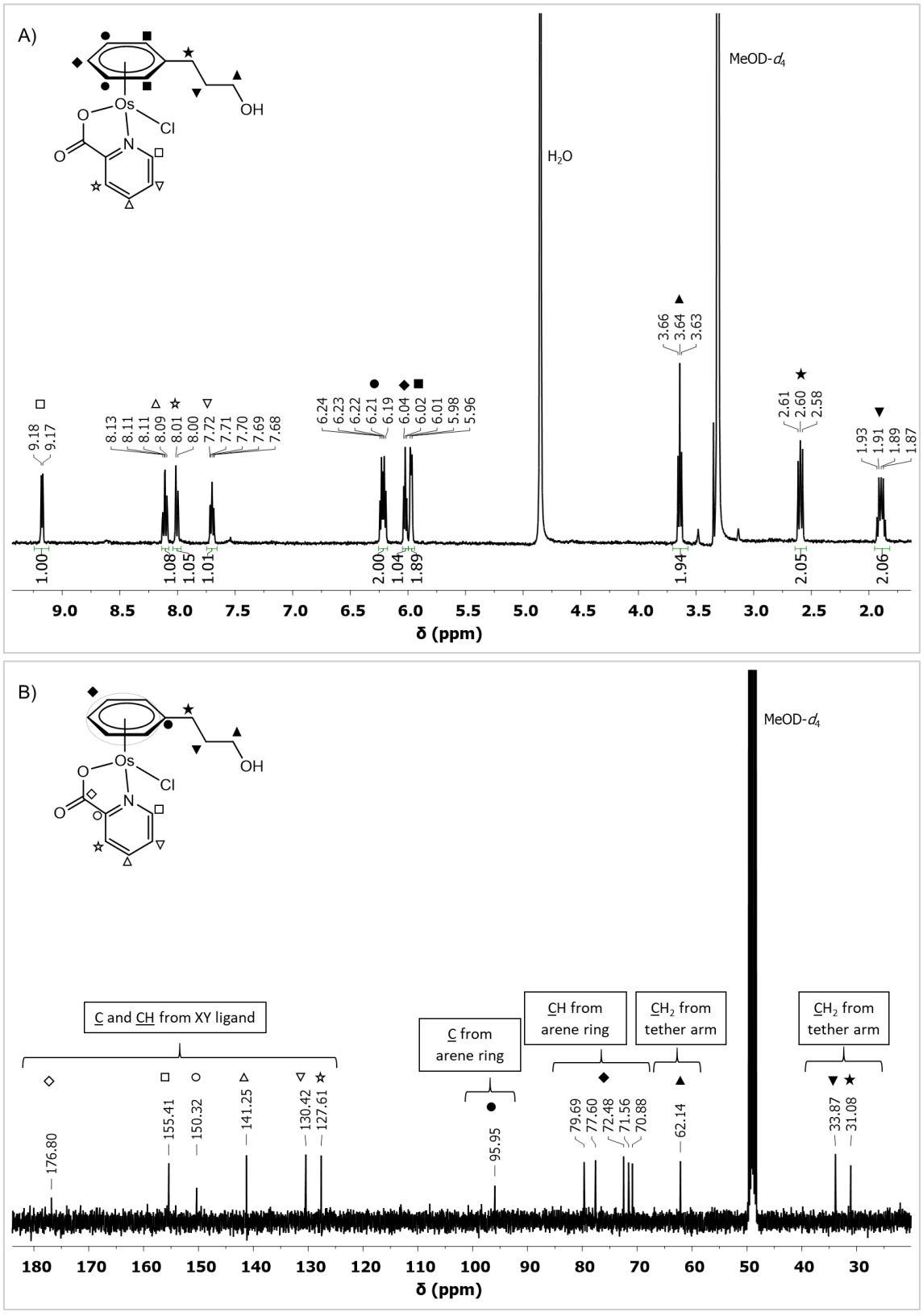

Figure S14. ^{1}H and $^{13}C\{^{1}H\}$ NMR spectra of complex **9**. (A) ^{1}H NMR (400 MHz, CD_3OD) and (B) $^{13}C\{^{1}H\}$ NMR spectra (101 MHz, CD_3OD) of [Os(η^6-$C_6H_5(CH_2)_3OH$)(pico)Cl].

Figure S15.

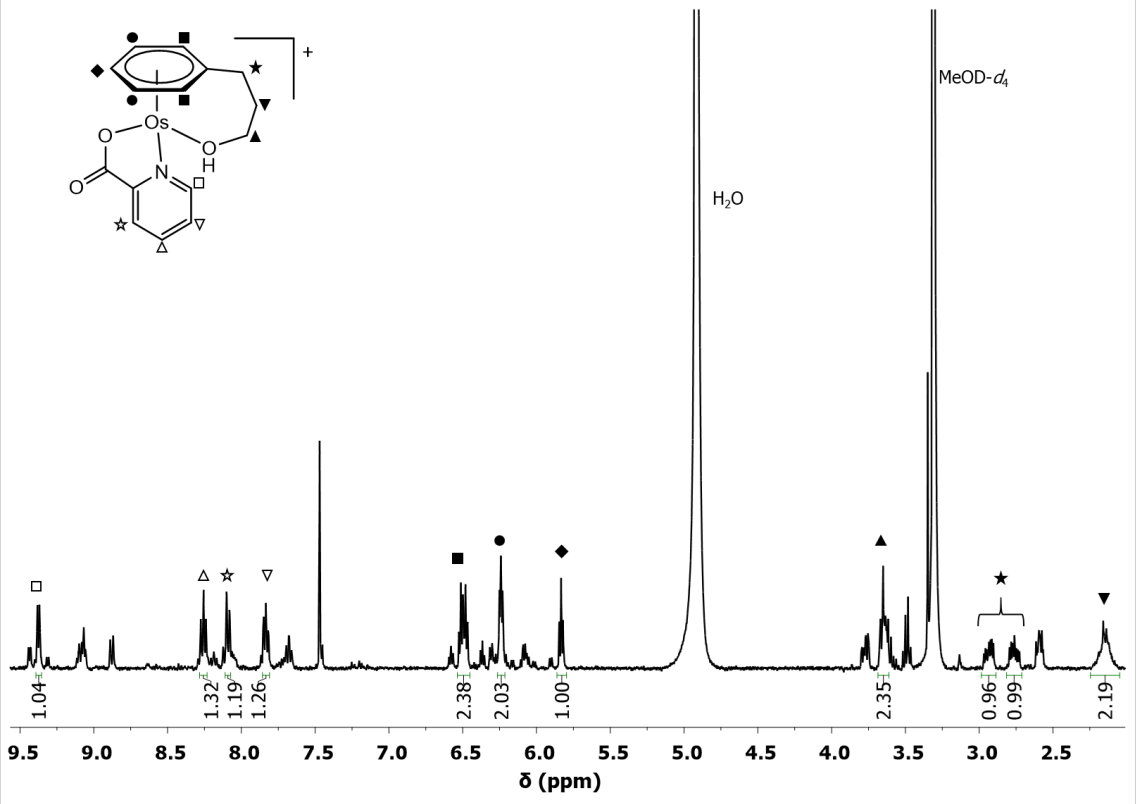

Figure S15. ^{1}H NMR spectra of a mixture containing **9C**. ^{1}H NMR (400 MHz, CD_3OD) of a mixture containing $[Os(\eta^6{:}\kappa^1\text{-}C_6H_5(CH_2)_3OH)(pico)]^+$.

Figure S16.

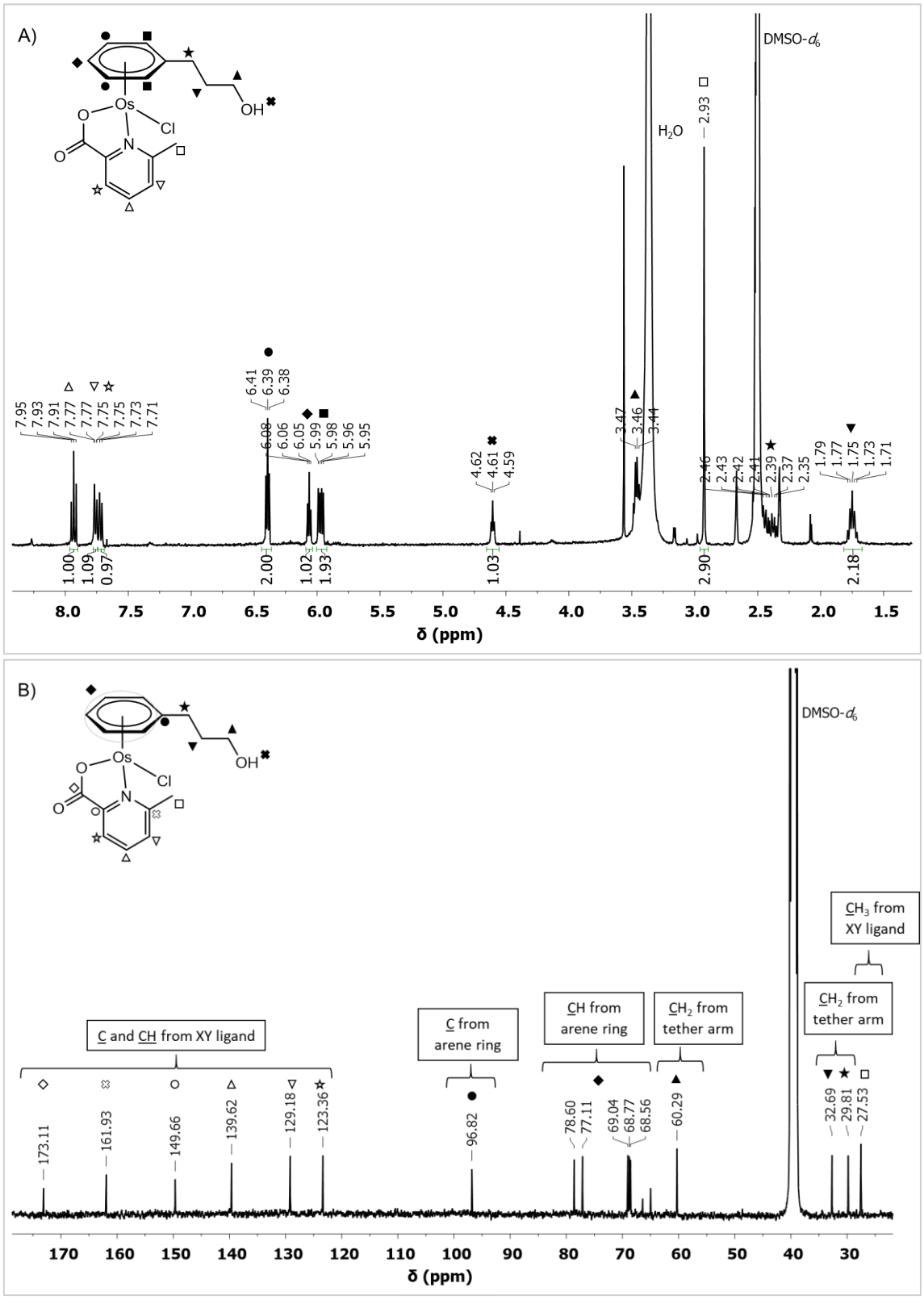

Figure S16. ^{1}H and $^{13}C\{^{1}H\}$ NMR spectra of complex **10**. It includes assignment of signals using 2D NMR spectra. (A) ^{1}H NMR (400 MHz, DMSO-d_6) and (B) $^{13}C\{^{1}H\}$ NMR spectra (101 MHz, DMSO-d_6) of [Os(η^6-$C_6H_5(CH_2)_3OH$)(6-Me-pico)Cl].

Figure S17.

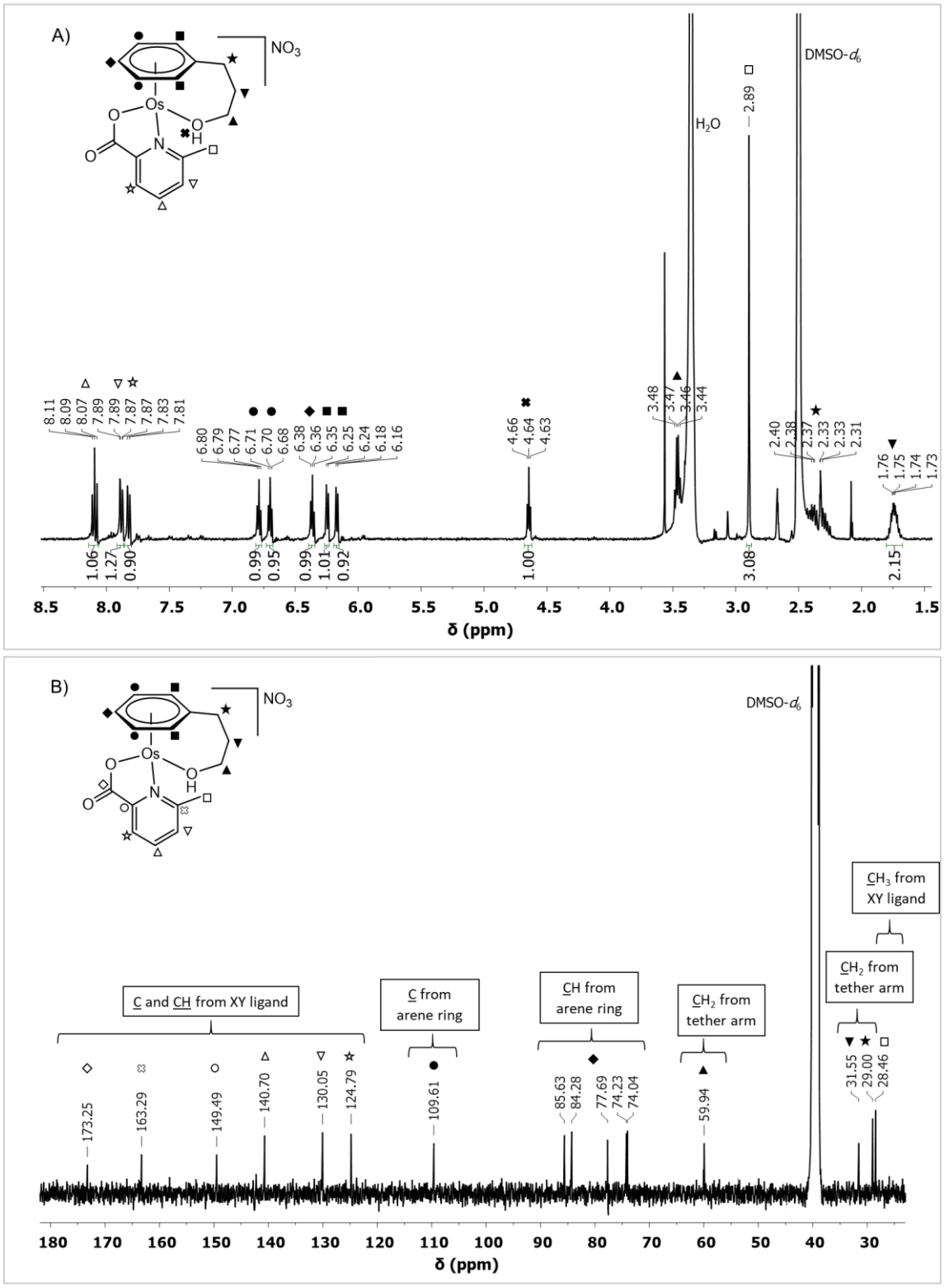

Figure S17. ^{1}H and $^{13}C\{^{1}H\}$ NMR spectra of complex **10C**. It includes assignment of signals using 2D NMR spectra. (A) ^{1}H NMR (400 MHz, DMSO-d_6) and (B) $^{13}C\{^{1}H\}$ NMR spectra (101 MHz, DMSO-d_6) of $[Os(\eta^6{:}\kappa^1\text{-}C_6H_5(CH_2)_3OH)(6\text{-Me-pico})]NO_3$.

Figure S18.

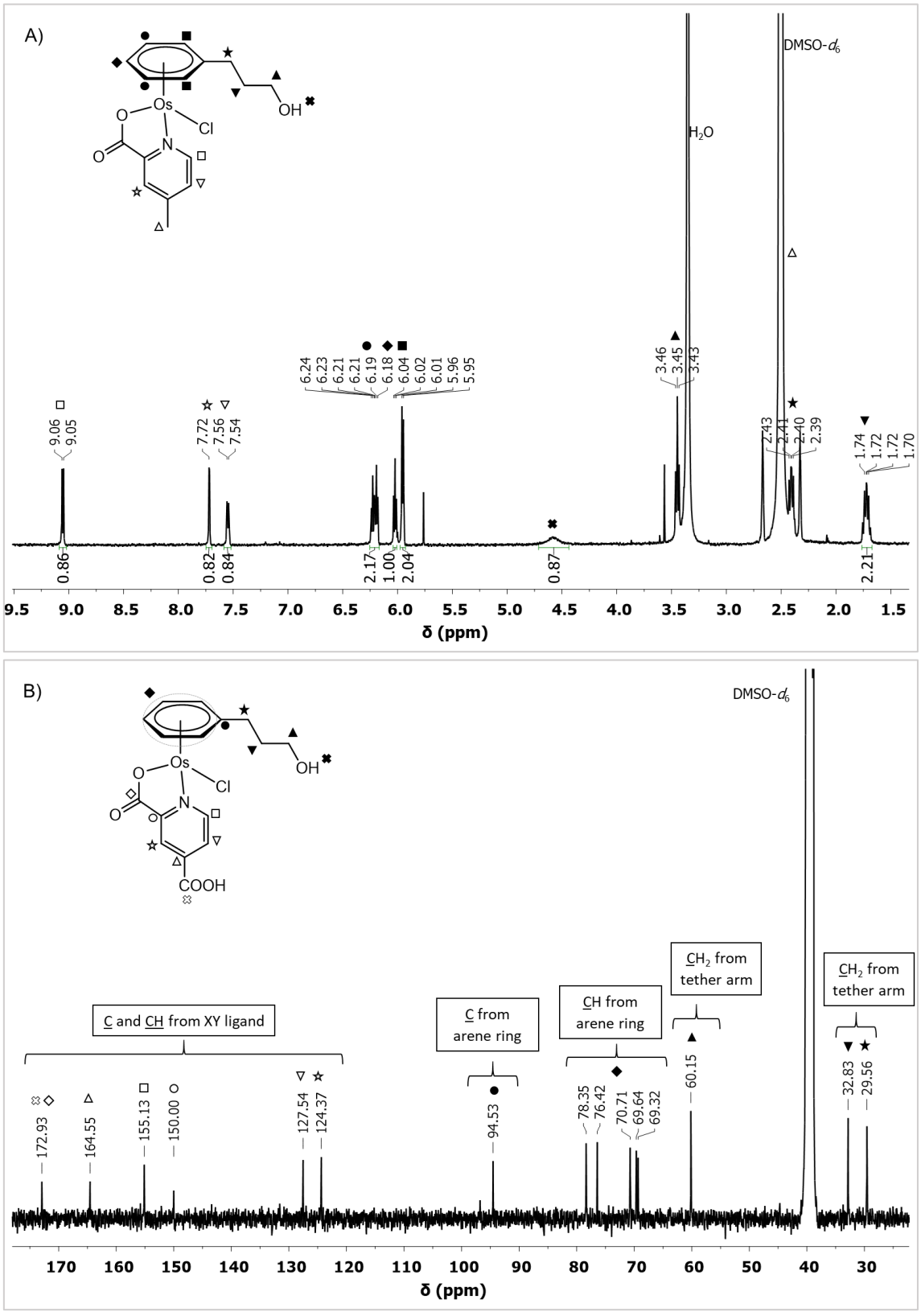

Figure S18. ^{1}H and $^{13}C\{^{1}H\}$ NMR spectra of complex **11**. (A) ^{1}H NMR (400 MHz, DMSO-d_6) and (B) $^{13}C\{^{1}H\}$ NMR spectra (101 MHz, DMSO-d_6) of [Os(η^6-$C_6H_5(CH_2)_3OH$)(4-Me-pico)Cl].

Figure S19.

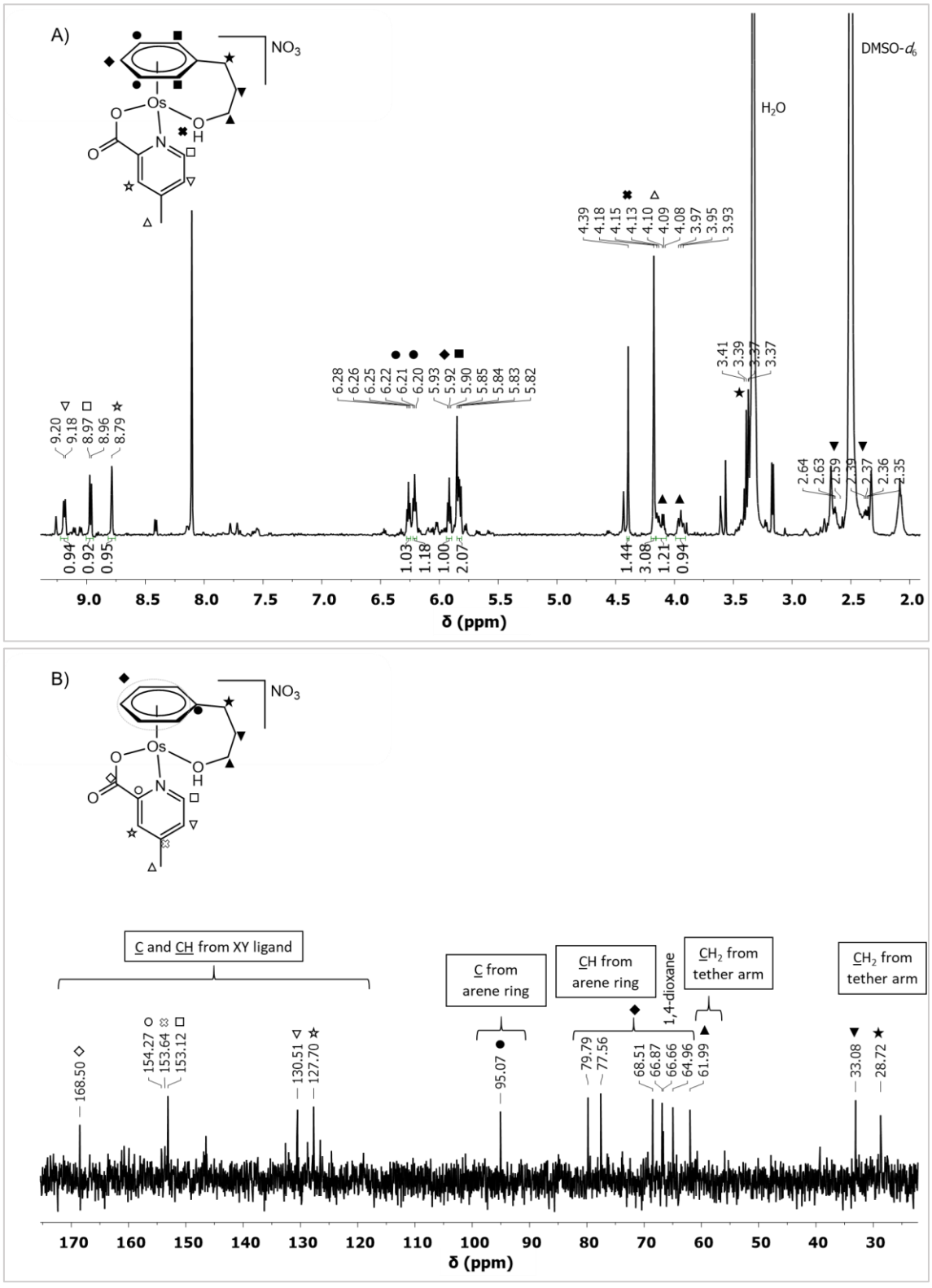

Figure S19. ^{1}H and $^{13}C\{^{1}H\}$ NMR spectra of complex **11C**. It includes assignment of signals using 2D NMR spectra. (A) ^{1}H NMR (400 MHz, DMSO-d_6) and (B) $^{13}C\{^{1}H\}$ NMR spectra (101 MHz, D_2O) of $[Os(\eta^6{:}\kappa^1\text{-}C_6H_5(CH_2)_3OH)(4\text{-Me-pico})]NO_3$

Figure S20.

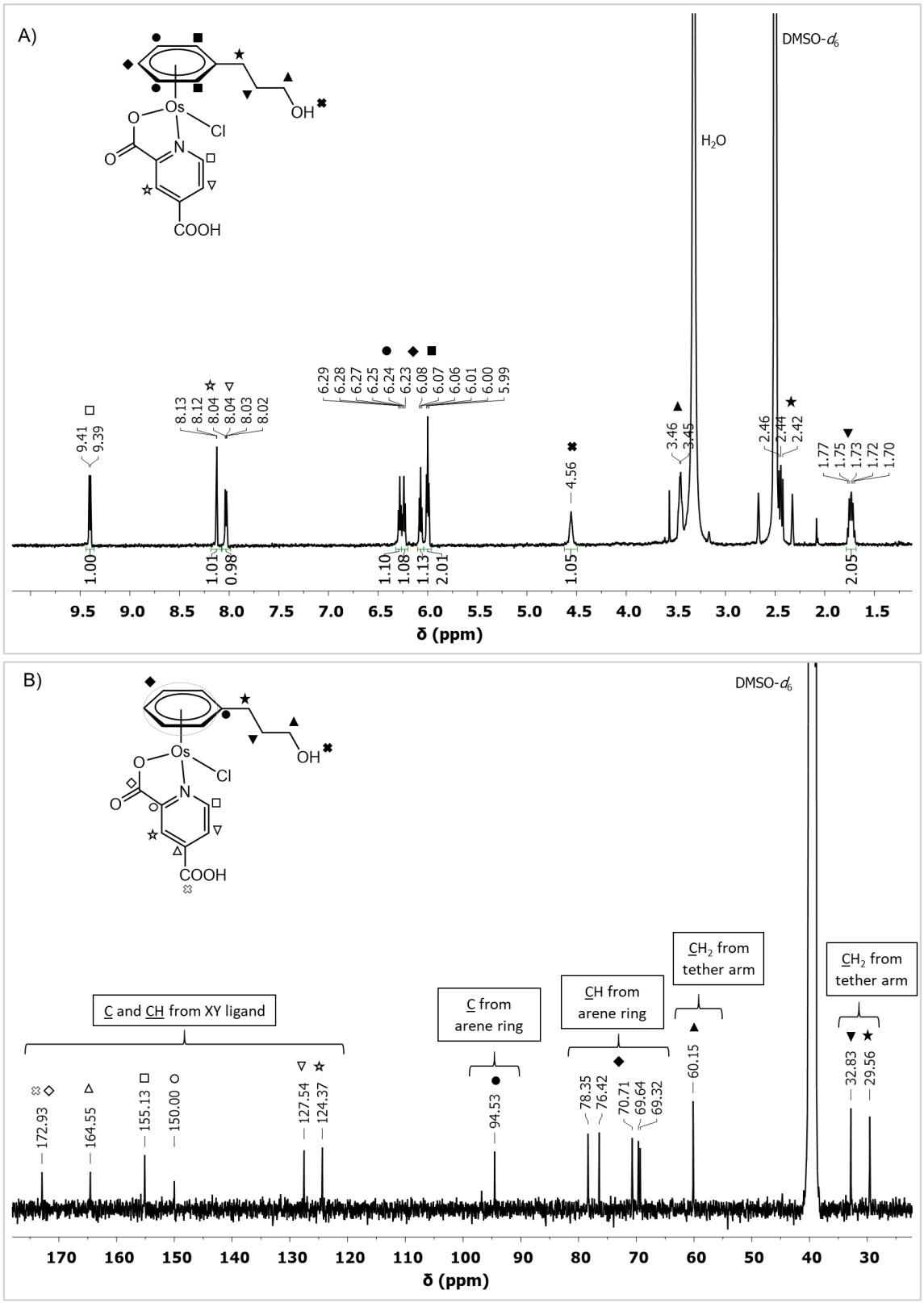

Figure S20. ^{1}H and $^{13}C\{^{1}H\}$ NMR spectra of complex **12**. (A) ^{1}H NMR (400 MHz, DMSO-d_6) and (B) $^{13}C\{^{1}H\}$ NMR spectra (101 MHz, DMSO-d_6) of [Os(η^6-$C_6H_5(CH_2)_3OH$)(4-COOH-pico)Cl].

Figure S21.

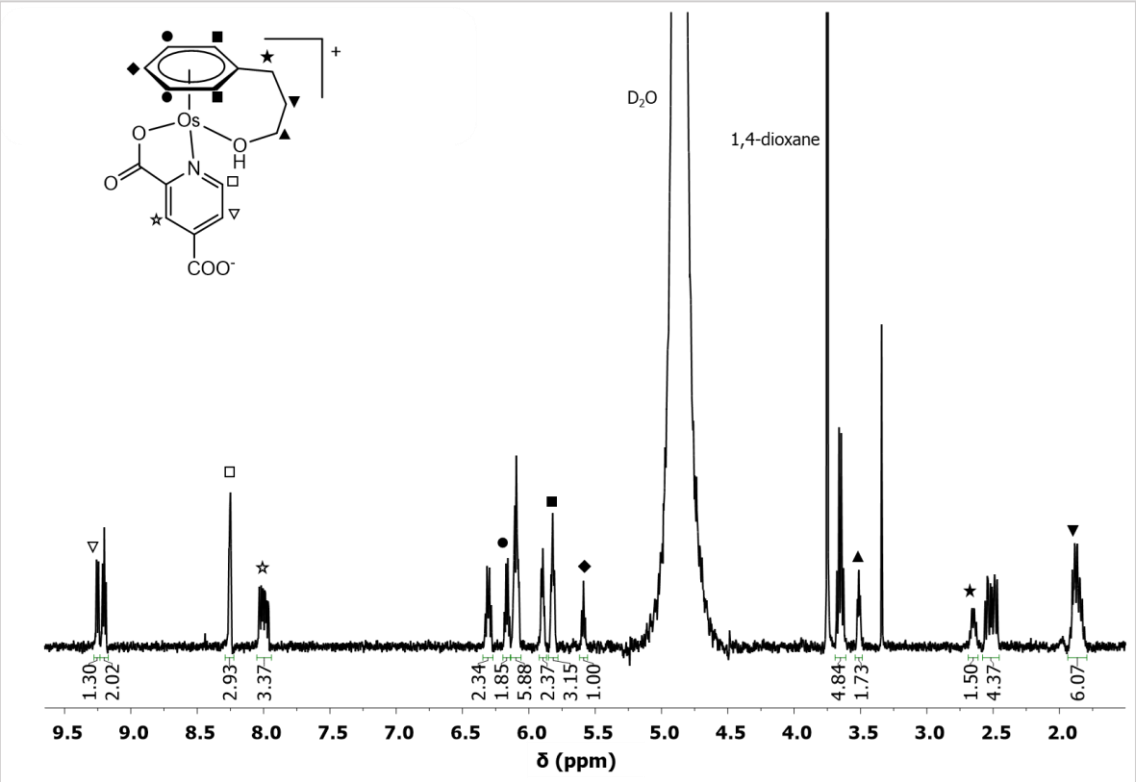

Figure S21. ^{1}H NMR spectrum of a mixture containing **12C**. ^{1}H NMR (400 MHz, D_2O) obtained at basic pH during a titration containing a mixture of: **12C**, $[Os(\eta^6{:}\kappa^1\text{-}C_6H_5(CH_2)_3OH)(4\text{-}COOH\text{-}pico)]^+$ (29%); **12**, $[Os(\eta^6\text{-}C_6H_5(CH_2)_3OH)(4\text{-}COOH\text{-}pico)Cl]$ (35%); and **12A** $[Os(\eta^6\text{-}C_6H_5(CH_2)_3OH)(4\text{-}COOH\text{-}pico)OH]$ (36%).

Figure S22.

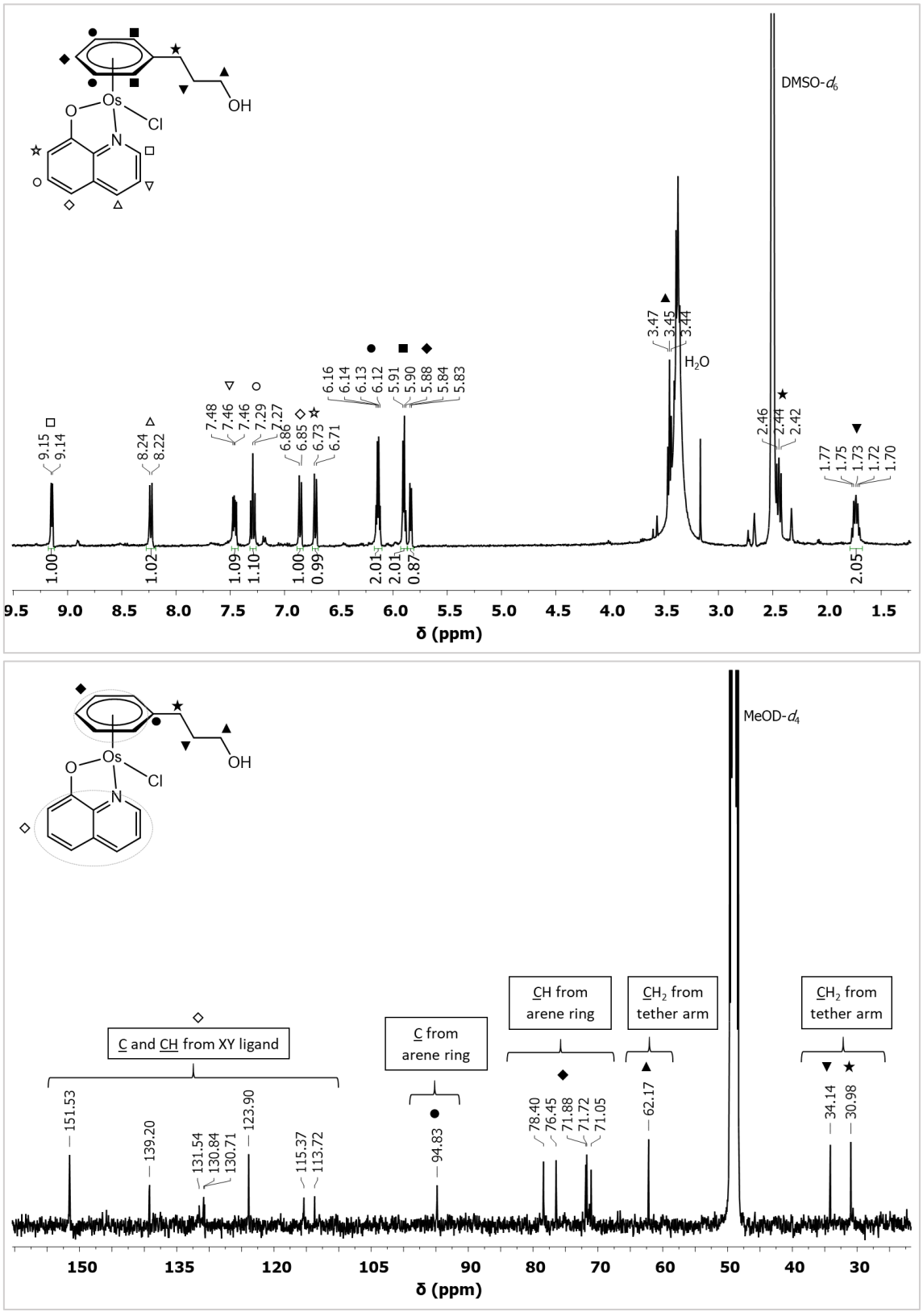

Figure S22. ^{1}H and $^{13}C\{^{1}H\}$ NMR spectra of complex **13**. (A) ^{1}H NMR (400 MHz, DMSO-d_6) and (B) $^{13}C\{^{1}H\}$ NMR spectra (101 MHz, CD_3OD) of [Os(η^6-$C_6H_5(CH_2)_3OH$)(quinol)Cl].

Figure S23.

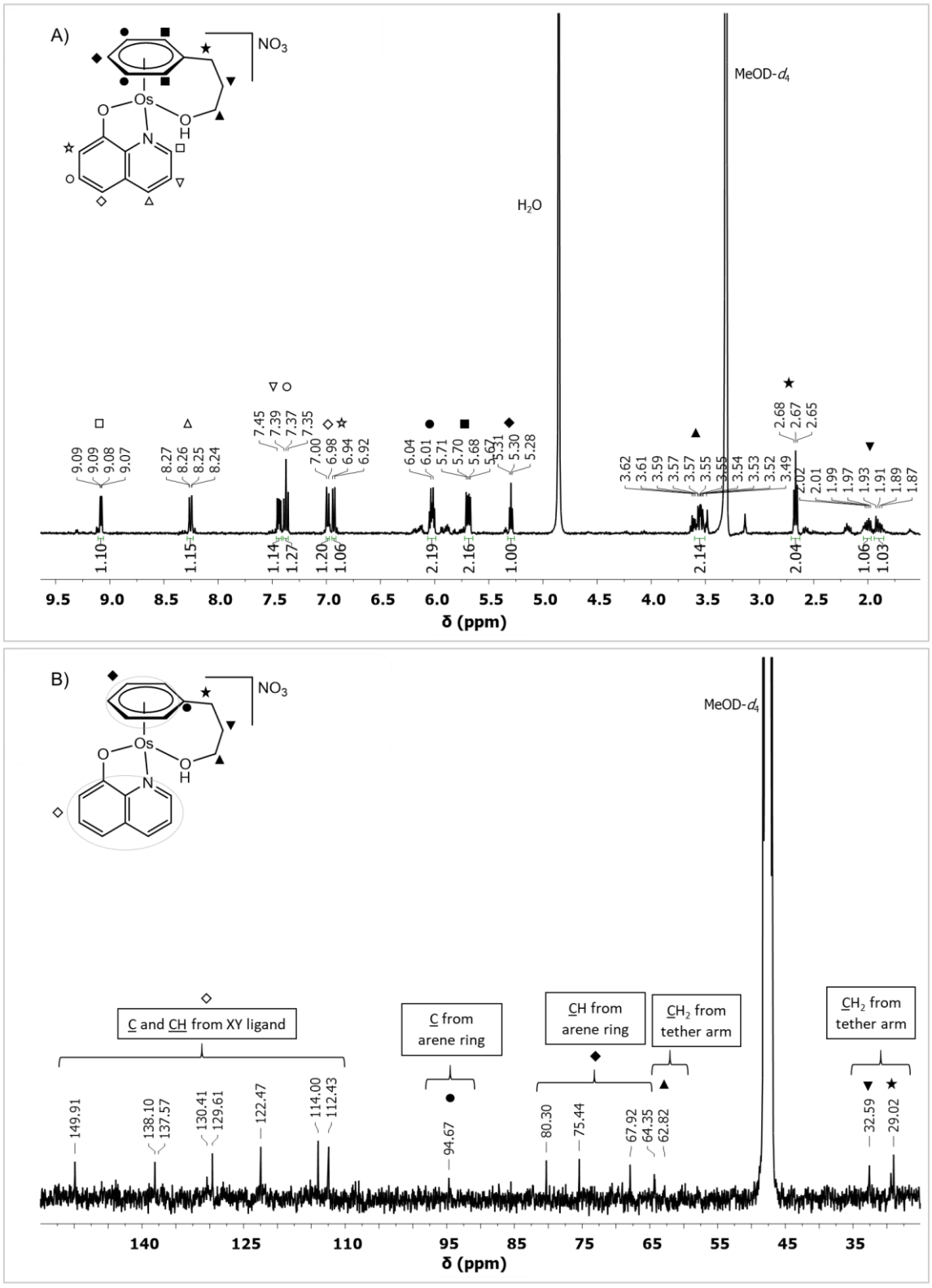

Figure S23. ^{1}H and $^{13}C\{^{1}H\}$ NMR spectra of complex **13C**. (A) ^{1}H NMR (400 MHz, CD_3OD) and (B) $^{13}C\{^{1}H\}$ NMR spectra (101 MHz, CD_3OD) of $[Os(\eta^6{:}\kappa^1\text{-}C_6H_5(CH_2)_3OH)(quinol)]NO_3$.

Figure S24.

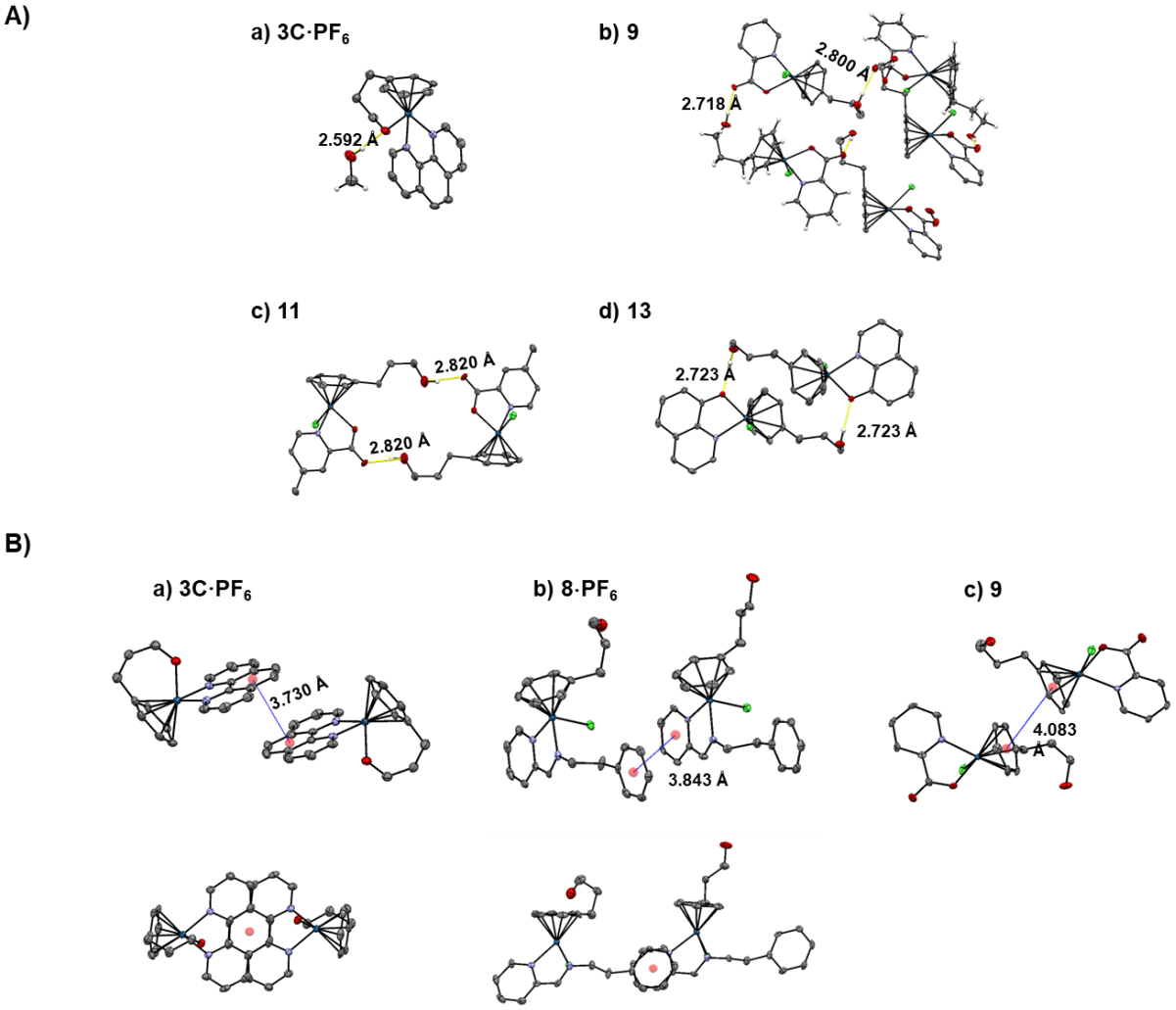

Figure S24. ORTEP diagrams showing (A) directional hydrogen bonding between adjacent molecules (50% probability ellipsoids) in (a) $[Os(\eta^6{:}\kappa^1\text{-}C_6H_5(CH_2)_3O)(phen)]^+$, **3C·PF$_6$**, (b) $[Os(\eta^6\text{-}C_6H_5(CH_2)_3OH)(pico)Cl]$, **9**, (c) $[Os(\eta^6\text{-}C_6H_5(CH_2)_3OH)(4\text{-Me-pico})Cl]$, **11**, and (d) $[Os(\eta^6\text{-}C_6H_5(CH_2)_3OH)(quinol)Cl]$, **13**. Numbers refer to D(donor)-to-A(acceptor) distances in Å (marked as yellow dotted lines); and (B) π-π intermolecular interactions in (a) $[Os(\eta^6{:}\kappa^1\text{-}C_6H_5(CH_2)_3O)(phen)]^{n+}$, **3C·PF$_6$**, (b) $[Os(\eta^6\text{-}C_6H_5(CH_2)_3OH)(PhEt\text{-impy})Cl]$, **8·PF$_6$**, and (c) $[Os(\eta^6\text{-}C_6H_5(CH_2)_3OH)(pico)Cl]$, **9**.

Figure S25.

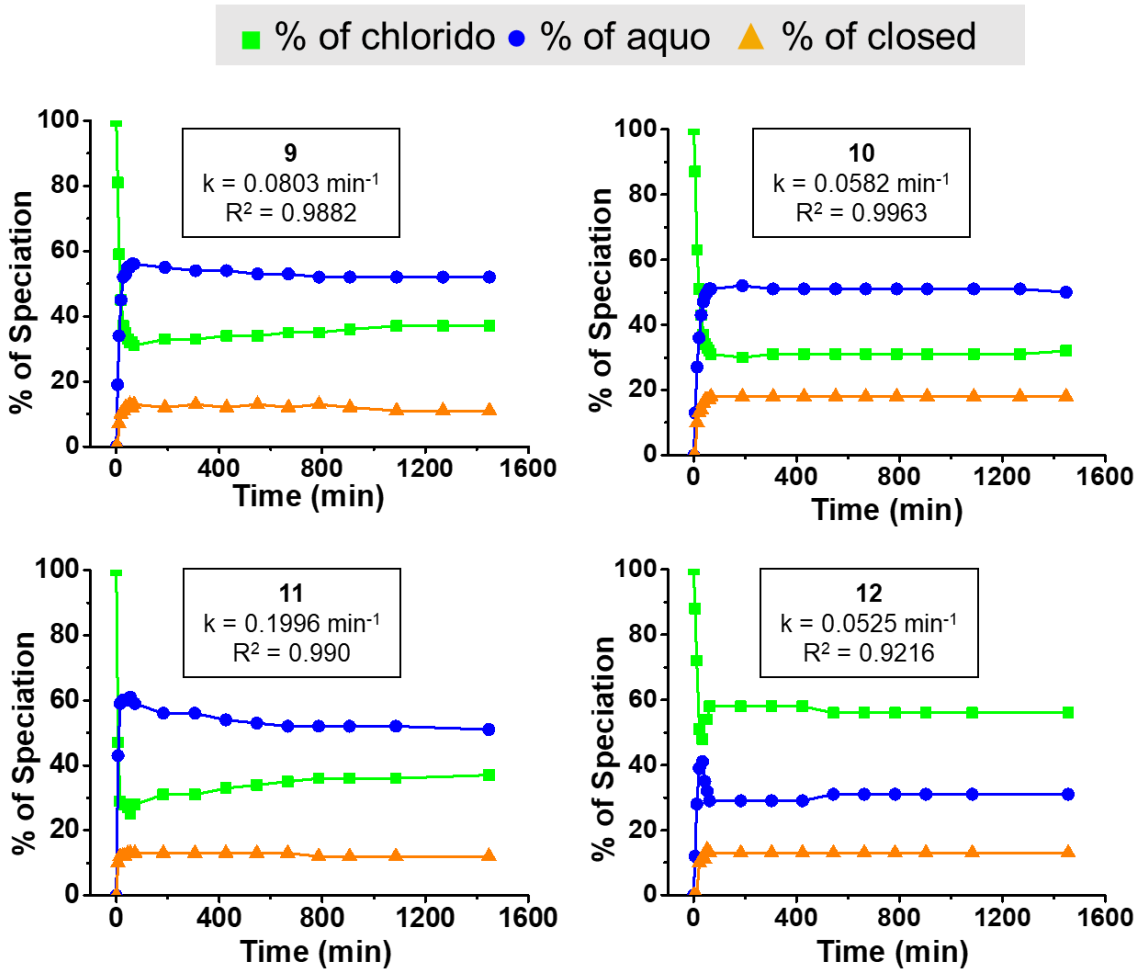

Figure S25. Time dependence on the consumption of the chlorido species (■), and the formation of aqua (●) and closed-tether (▲) species of complexes **9**, **10**, **11** and **12** (based on ^{1}H NMR peak integrals) during hydrolysis in acidic (pH* ca. 3) D_2O at ca. 300 K.

Figure S26.

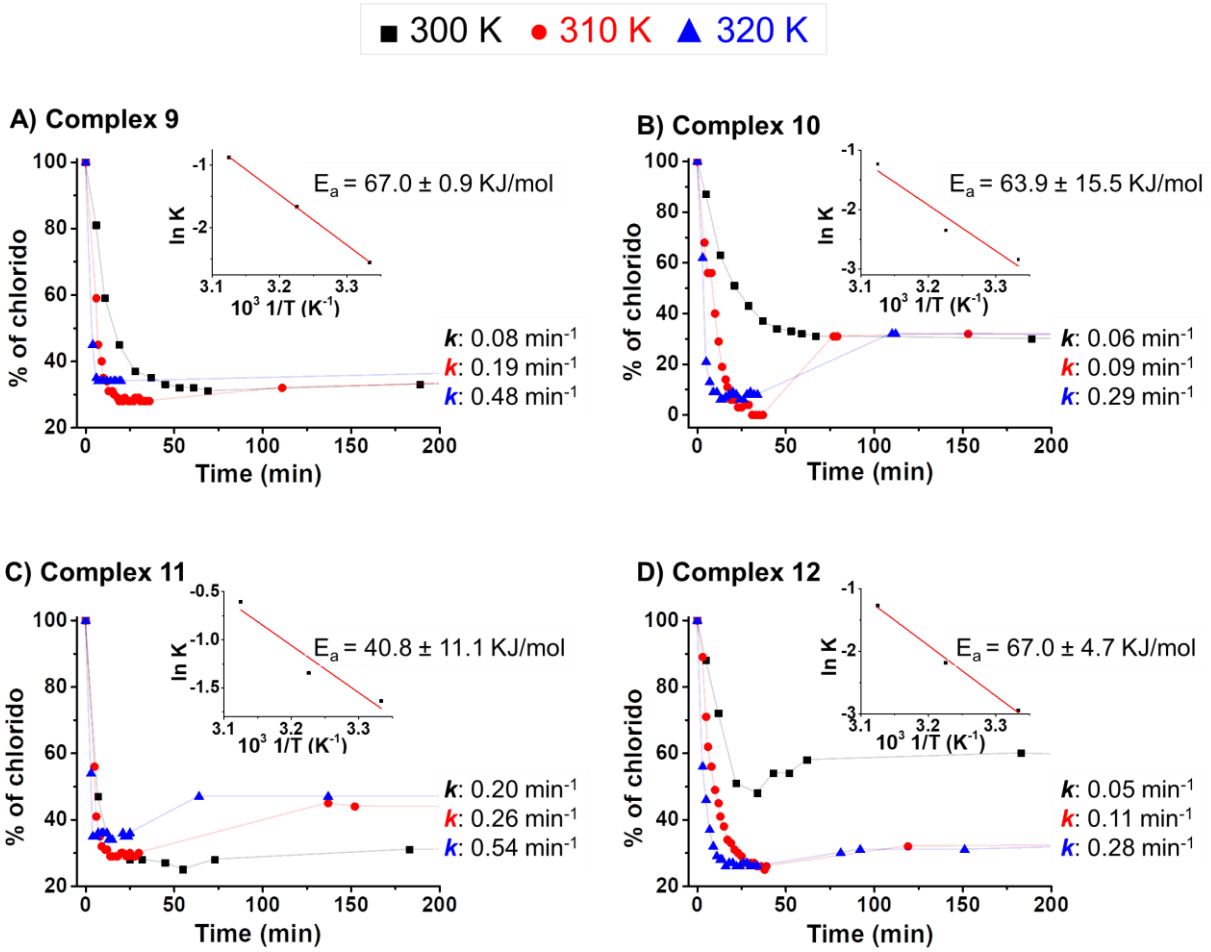

Figure S26. Hydrolysis of picolinate compounds A) **9**, [Os(η^6-$C_6H_5(CH_2)_3OH$)(pico)Cl], B) **10**, [Os(η^6-$C_6H_5(CH_2)_3OH$)(6-Me-pico)Cl], C) **11**, [Os(η^6-$C_6H_5(CH_2)_3OH$)(4-Me-pico)Cl], and D) **12**, [Os(η^6-$C_6H_5(CH_2)_3OH$)(4-COOH-pico)Cl] in D_2O. The time dependence for the consumption of the chlorido adduct is shown at 300 K (■), 310 K (●) and 320 K (▲) (based on ^{1}H NMR peak integrals). The insets show an Arrhenius plot, the slope of which gives the Arrhenius activation energy.

Figure S27.

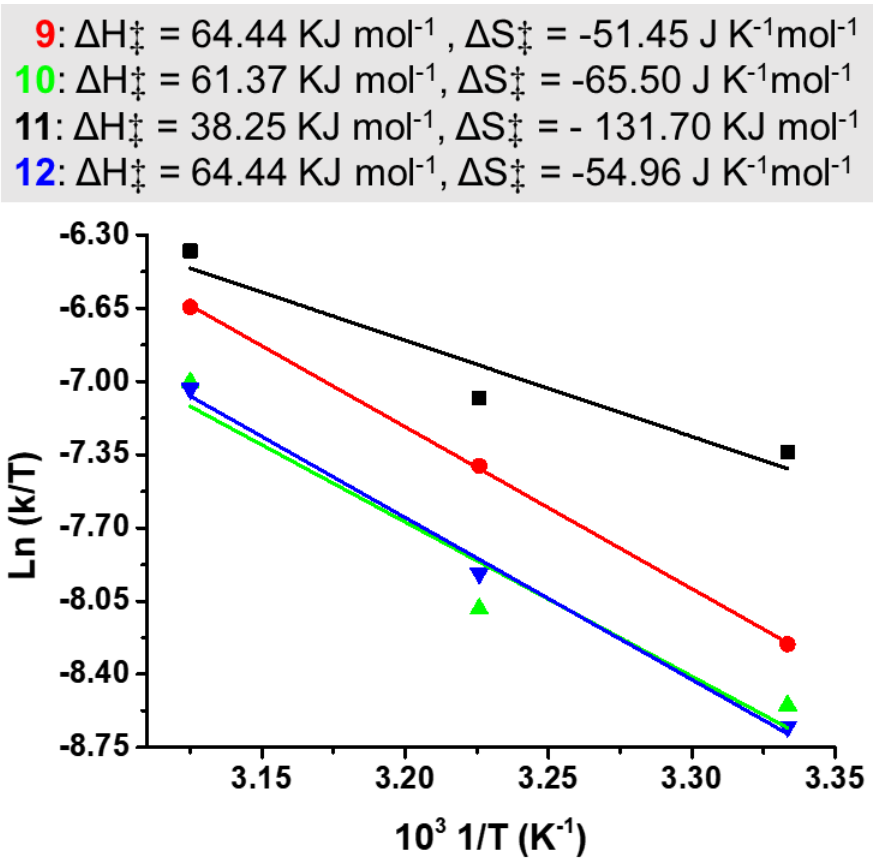

Figure S27. Eyring plot for the hydrolysis of picolinate derivative compounds **9** (●), **10** (▲), **11** (■) and **12** (▼). Enthalpy and entropy are calculated from the linear fit of Ln (*k*/T) vs 10^3/T.

Figure S28.

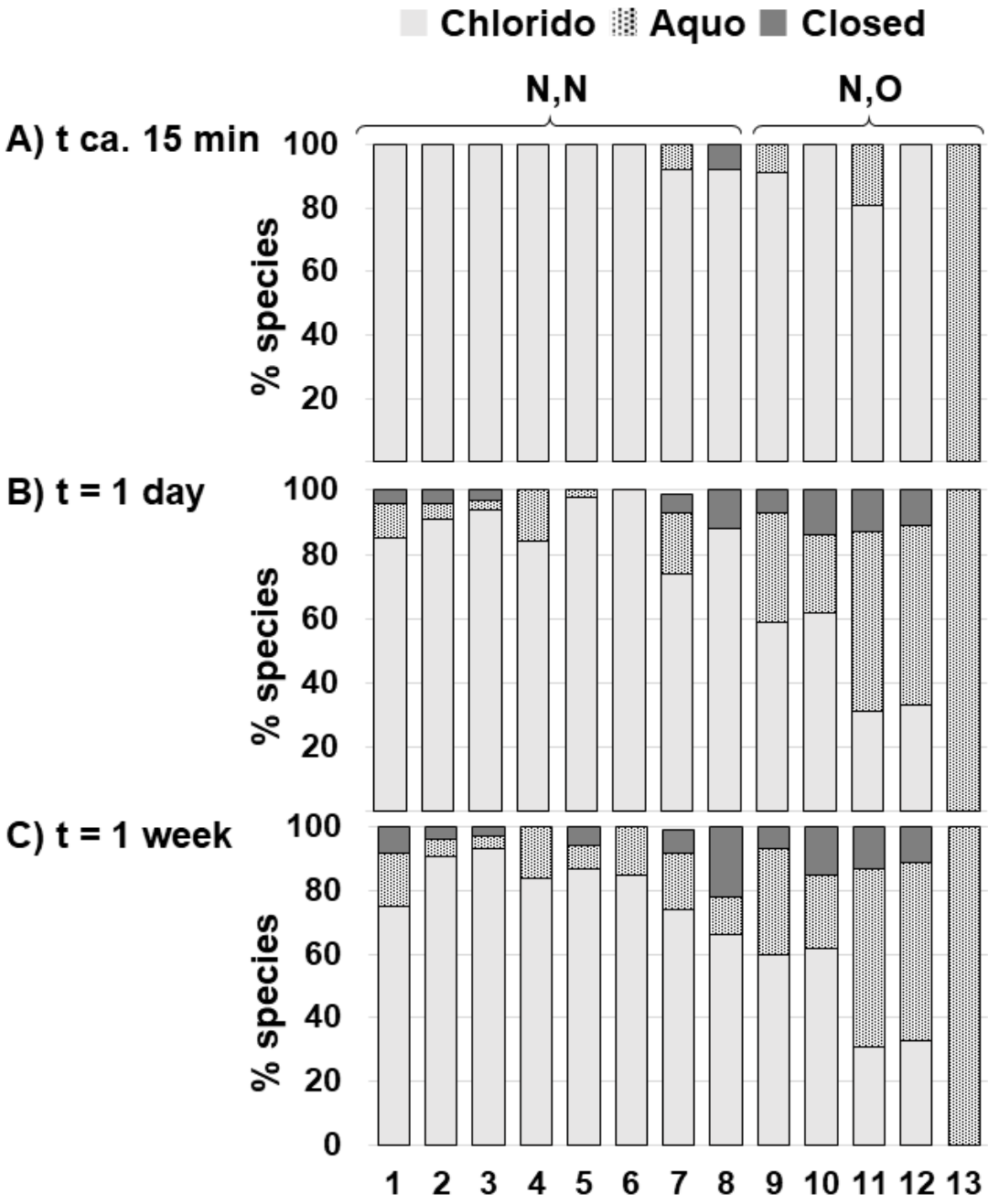

Figure S28. Percentage speciation of open-tether chlorido (**1**–**13**) / open-tether aqua (**1A**–**13A**) / closed-tether species (**1C**–**13C**) for the complexes studied in this work, as determined by ^{1}H NMR, at time (A) ca. 15 min, (B) 24 h (310 K incubation) and (C) one week (298 K incubation) in unbuffered D_2O.

Figure S29.

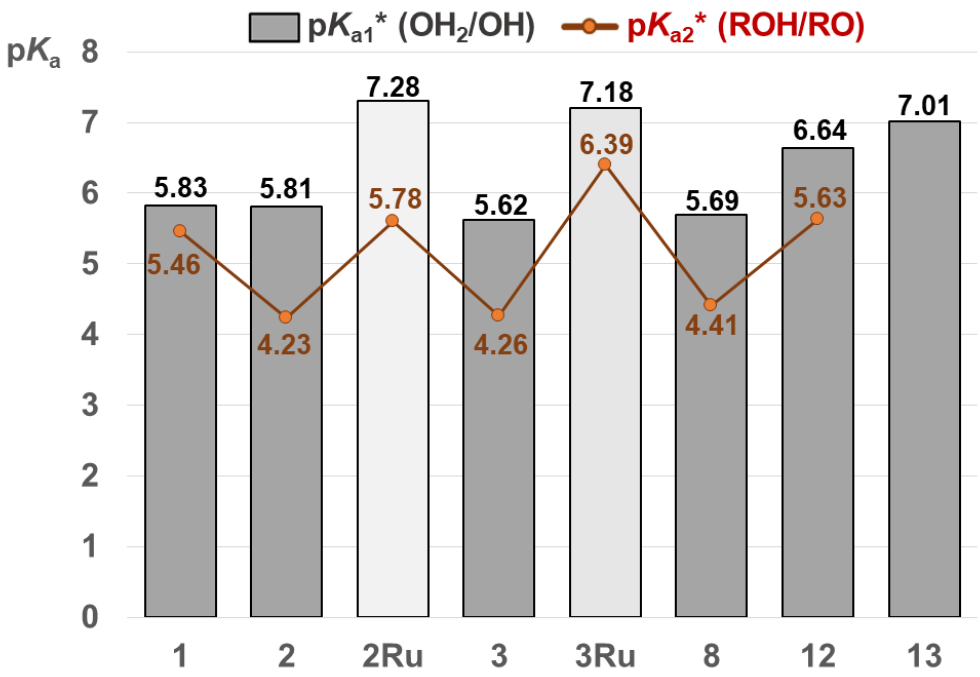

Figure S29. pK_{a1}* values for the aqua/hydroxido (OH_2/OH) adduct of formula [M(η^6-$C_6H_5(CH_2)_3OH$)(XY)(OH_2/OH)]$^{n+}$, for complexes **1A**, **2A**, **2ARu**, **3A**, **3ARu**, **8A**, **12A** and **13A**, and the pK_{a2}* values for the coordinated alcohol/alkoxy group (ROH/RO) in closed tether complexes of formula [M(η^6:κ^1-$C_6H_5(CH_2)_3OH$/O)(XY)]$^{n+}$, for complexes **1C**, **2C**, **2CRu**, **3C**, **3CRu**, **8C** and **12C** in aqueous solution.

Figure S30.

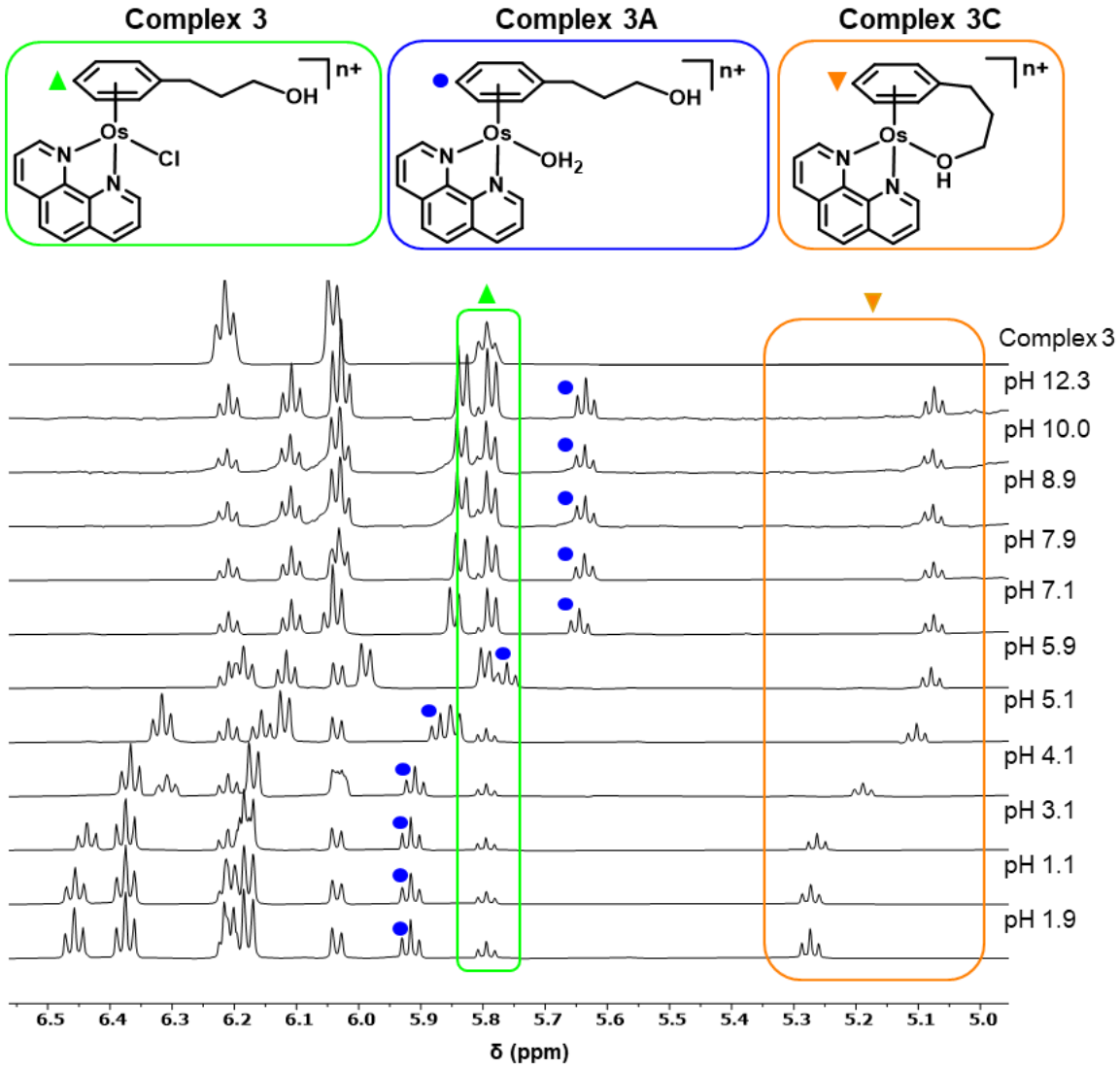

Figure S30. Spectra showing the pH* dependence of the ^{1}H NMR chemical shifts of a solution containing **3**, **3A** and **3C** in D_2O corresponding to the resonances in one of the protons in the η^6-bound arene (H_{para} to the alcohol-bearing chain). Assignments: chlorido complex (▲, green box) $[Os(\eta^6\text{-}C_6H_5(CH_2)_3OH)(phen)Cl]^+$; aqua complex (●, blue box) $[Os(\eta^6\text{-}C_6H_5(CH_2)_3OH)(phen)OH_2/OH]^{2+/+}$, and closed tether complex (▼, orange box) $[Os(\eta^6{:}\kappa^1\text{-}C_6H_5(CH_2)_3OH/O)(phen)]^{2+/+}$. The aqua adduct, **3A**, exhibits one deprotonation step to afford the hydroxo on the assumption that the observed chemical shifts are weighted averages according to the populations of the protonated and deprotonated species, as depicted in Chart 2 (main text). As the pH increases (spectra from bottom to top) the chemical shift of the H_{para} η^6-bond arene protons shifts to higher field as the alcohol tether complex **3C** losses the proton of the σ-bonded alcohol to afford the alkoxy tether.

Figure S31.

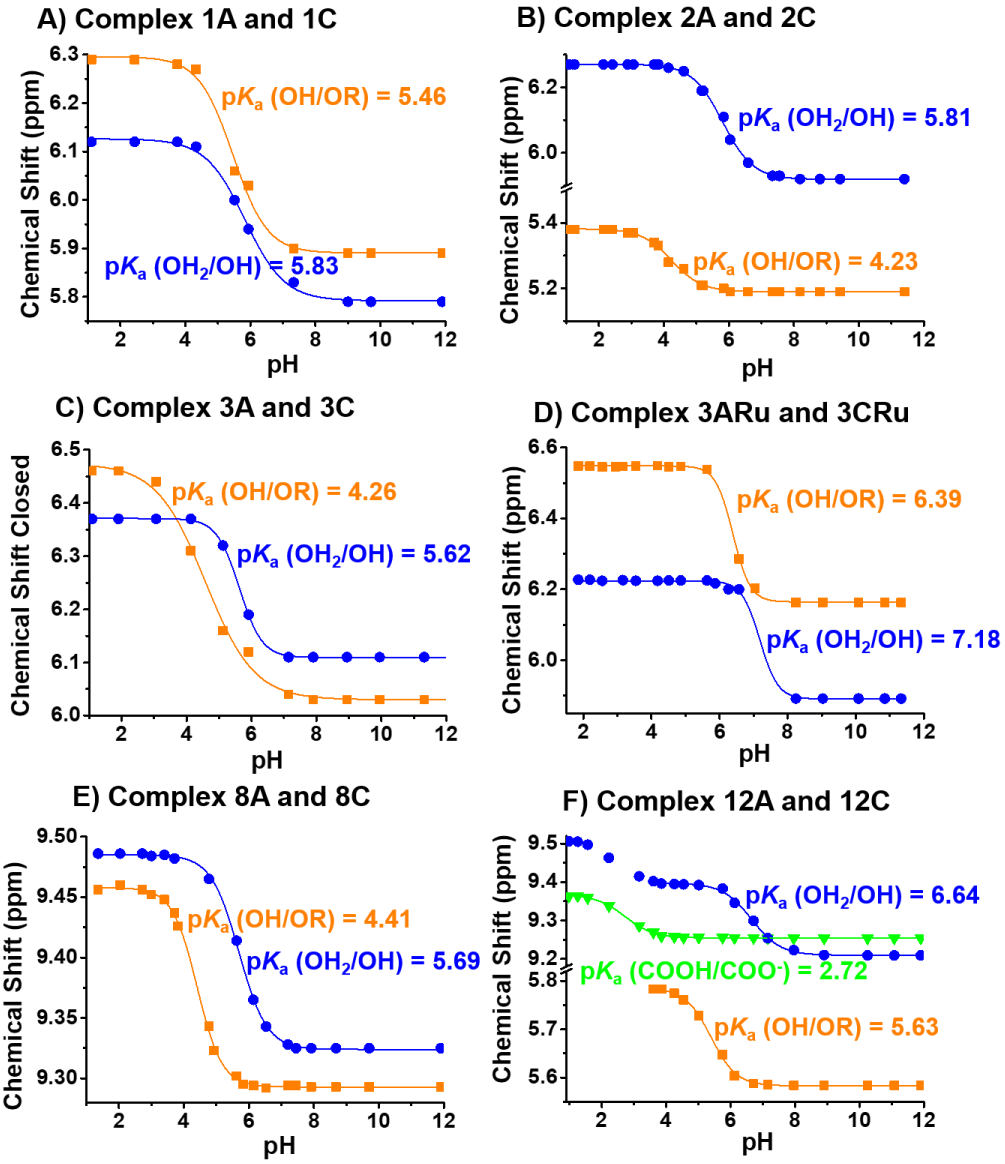

Figure S31. Determination of the pK_a* for the corresponding aqua adduct and closed tether of (A) **1**, (B) **2**, (C) **3**, (D) **3Ru**, (E) **8** and (F) **12** based on the ^{1}H NMR chemical shifts of the H_{para} of the η^6-coordinated arene ring for **1**–**3** and **3Ru**, or H_{ortho} of the pyridine contained in the chelating ligand in **8** and **12**. The proton chemical shifts were plotted against pH and the data were fitted to the Henderson−Hasselbalch equation, which afforded the pK_a* values of both the alcohol/alkoxy group in $[Os(\eta^6{:}\kappa^1\text{-}C_6H_5(CH_2)_3OH/O)(XY)]^{n+}$ (orange squares, ■) and the coordinated water in $[Os(\eta^6\text{-}C_6H_5(CH_2)_3OH)(XY)(OH_2/OH)]^{n+}$ (blue dots, ●). The chloride complex **12** (green triangles, ▼) has been plotted in (F) to show the deprotonation of the carboxylic acid in the picolinate ligand. Sigmoidal fits (same-coloured line) were calculated using OriginPro 9.0.0 program.

Figure S32.

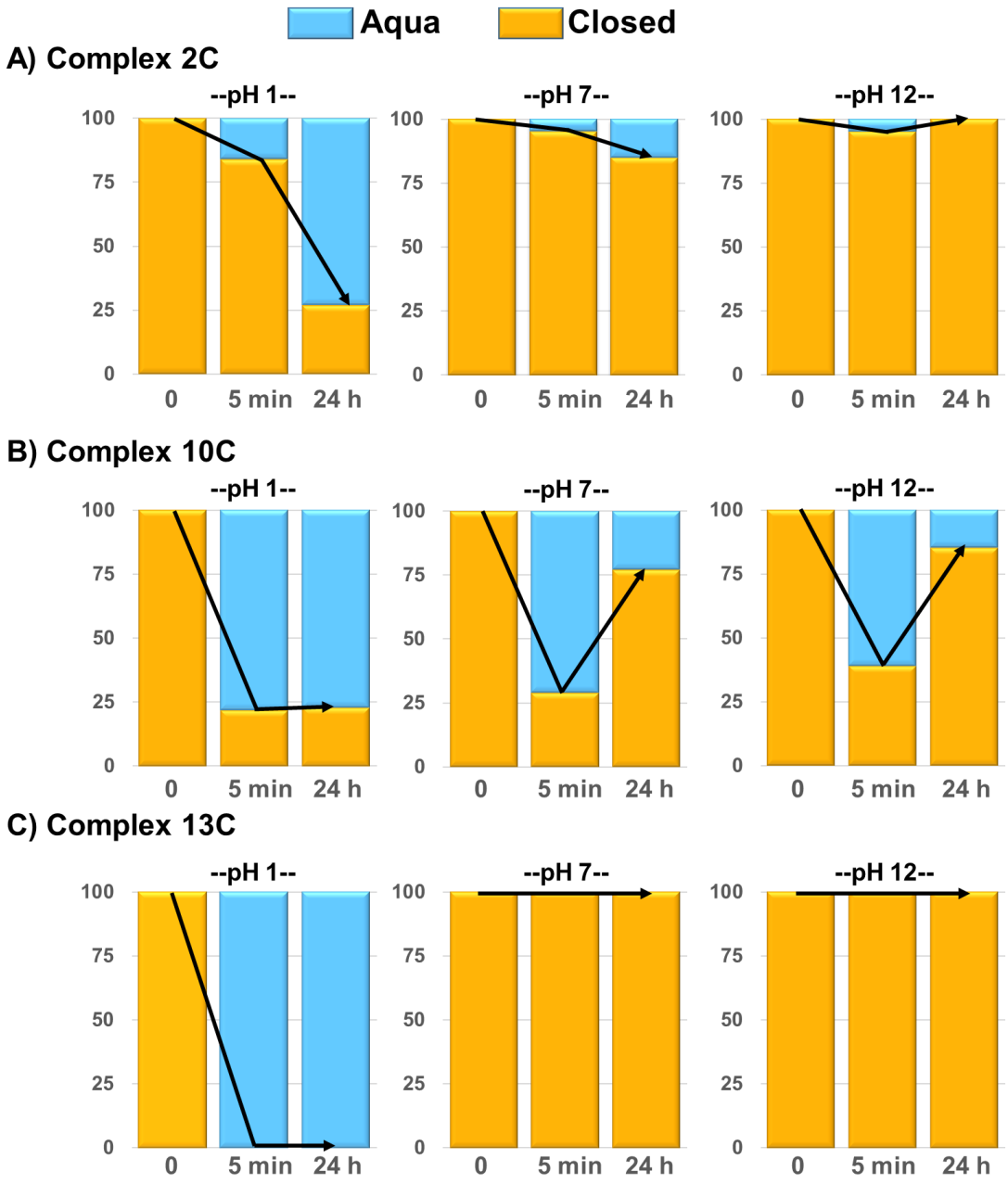

Figure S32. Speciation of closed tether complexes (A) **2C**, (B) **10C**, and (C) **13C**, at time ca. 5 min and after 24 h in unbuffered aqueous solutions at pH 1, 7 and 10. The arrow represents evolution of species towards equilibrium over time.

Figure S33.

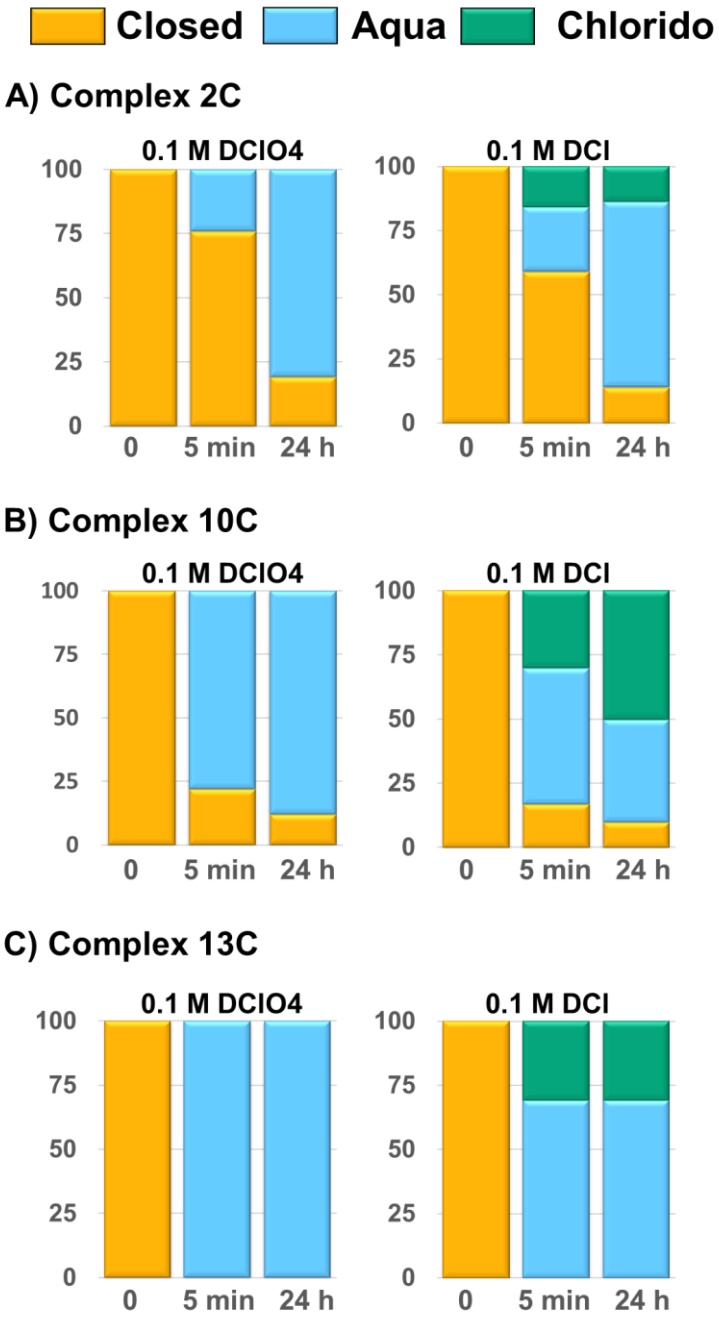

Figure S33. Speciation in aqueous solutions of closed tether compounds (A) **2C** (bipy), (B) **10C** (4-Me-pico) and (C) **13C** (quinol), calculated as the percentages of Os(II) species by means of ^{1}H NMR, at different chlorido concentrations in acidic environments at 5 min and 24 h of dissolution.

Figure S34.

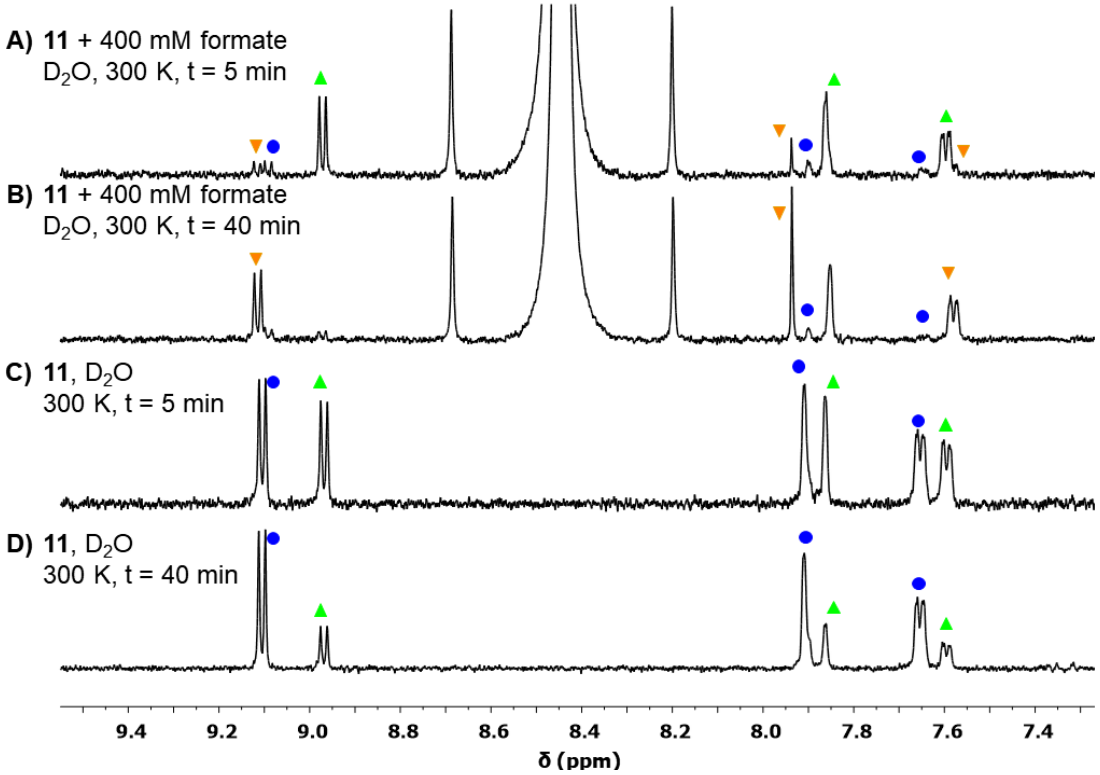

Figure S34. Formation of **11·formate** adduct overtime. (A) A solution of **11** and 400 mM of formate were dissolved in D_2O and evaluated by ^1H NMR. Three species were observed at equilibrium, assigned to chlorido (▲), aqua (●) and formate (▼) adduct. After 40 min in solution the formate adduct appears to be the predominant species. The singlet at ca. 7.9 ppm is attributed to Os-bound formate. (C) A solution of **11** in D_2O was evaluated by ^1H NMR as control. Two species were observed upon dissolution, the chlorido and the aqua species. (D) After 40 min in solution, complex **11** (▲) evolved to the aqua species (●).

Figure S35.

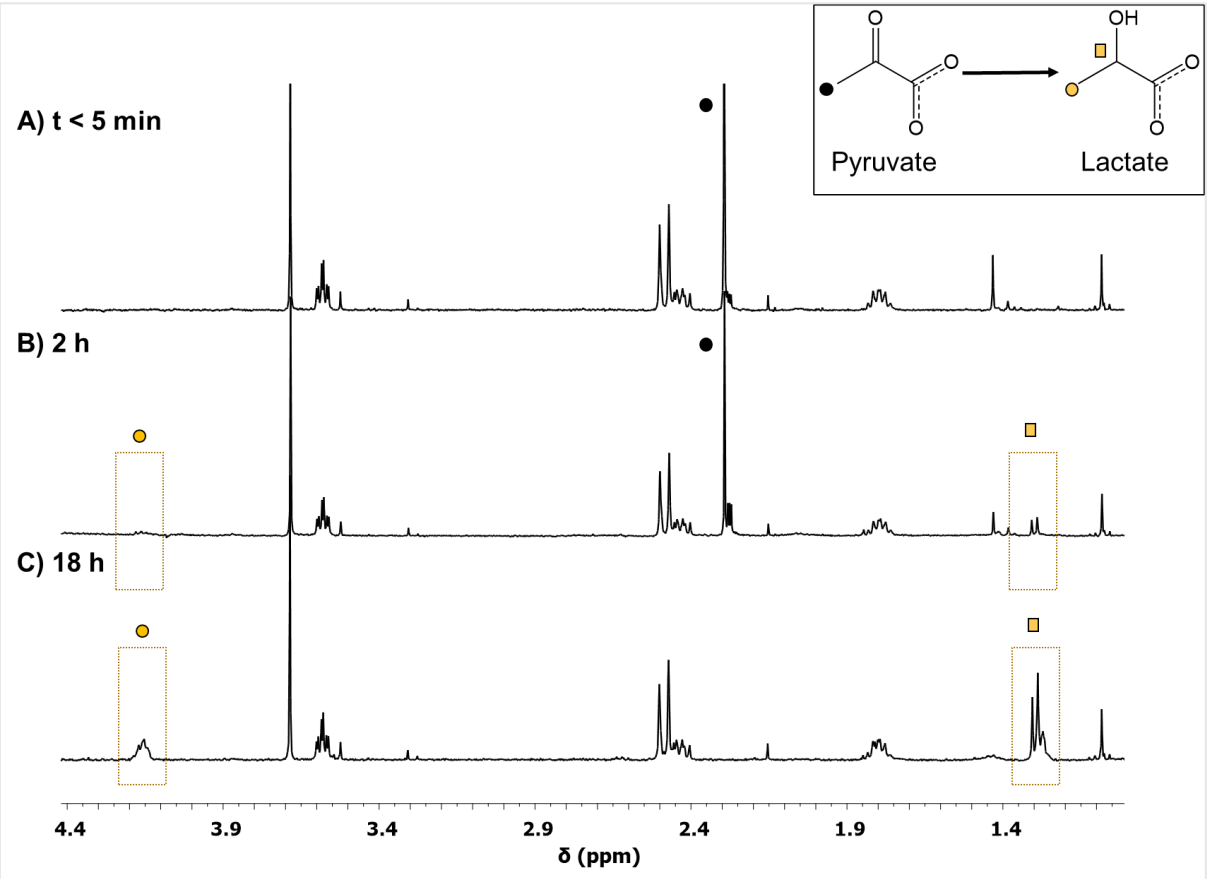

Figure S35. Conversion from pyruvate to lactate by complex **11** using 100 mM of sodium formate as the hydride source at pH 4 and 310 K. (A) ^{1}H NMR spectrum recorded after immediately after dissolution (t < 5 min). (B) ^{1}H NMR spectrum recorded after 2 h of reaction, both pyruvate and lactate are present in the solution. (C) After 18 h of reaction the ^{1}H NMR spectrum shows that all the pyruvate has been transformed into lactate.

Figure S36.

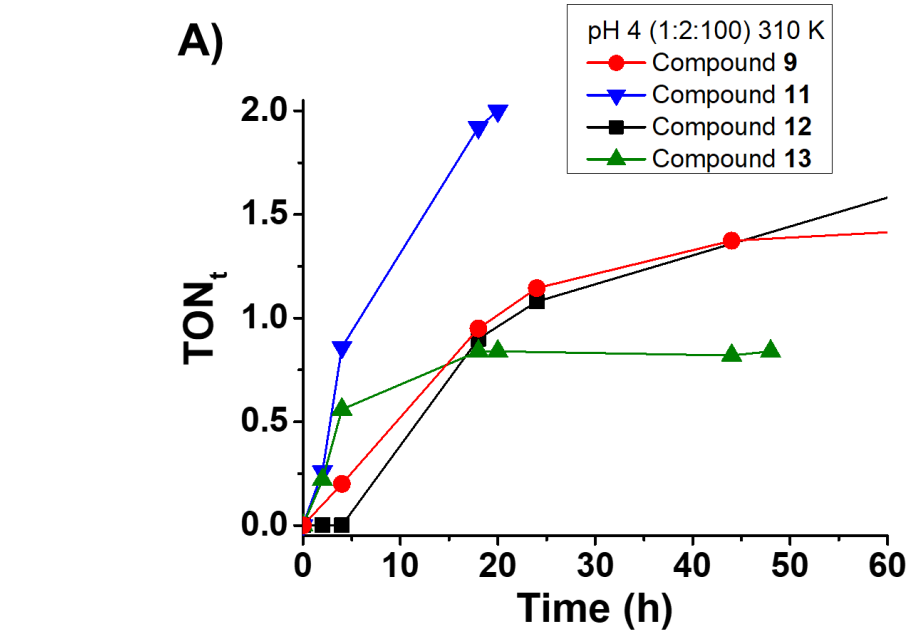

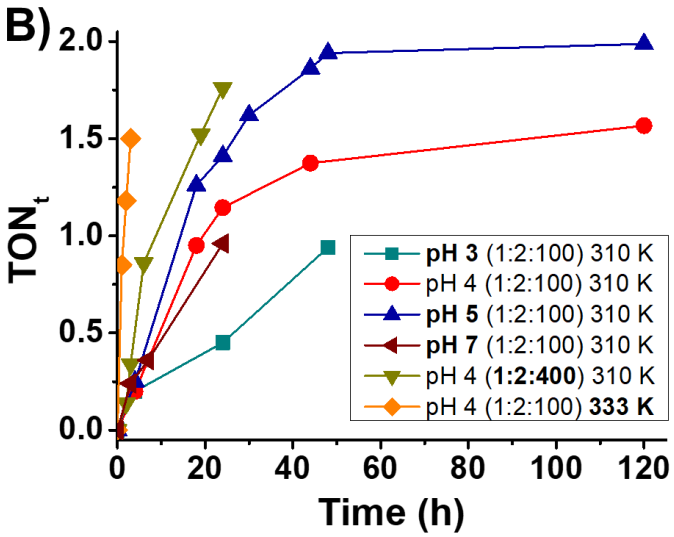

Compound	T (K)	HCOONa (mM)	pH	TOF_{max} (h^{-1})	R^2
9	310	100	3	0.018	0.969
	310	100	4	0.049	0.992
	310	100	5	0.071	0.999
	310	100	7	0.051	0.855
	310	400	4	0.148	0.946
	333	100	4	0.590	0.878

Figure S36. Catalysis data for the reduction of pyruvate to lactate by selected Os(II) arenes in D_2O. (A) Turn over number over time for the reduction of pyruvate by complexes **9**, **11**, **12** and **13** in D_2O (2 equivalents of pyruvate per equivalent of Os) at pH 4, 310 K and 100 mM of hydride source (sodium formate). (B) Reduction of pyruvate (2 mM) by complex **9** (1 mM) in D_2O at different conditions of pH, temperature and amount of hydride source (sodium formate). TON_t, turnover number at time 't' monitored by ^1H NMR spectroscopy. TOF_{max} is obtained as the slope in the linear fit equation for TON_t over time following the equation described in the main text.

Figure S37.

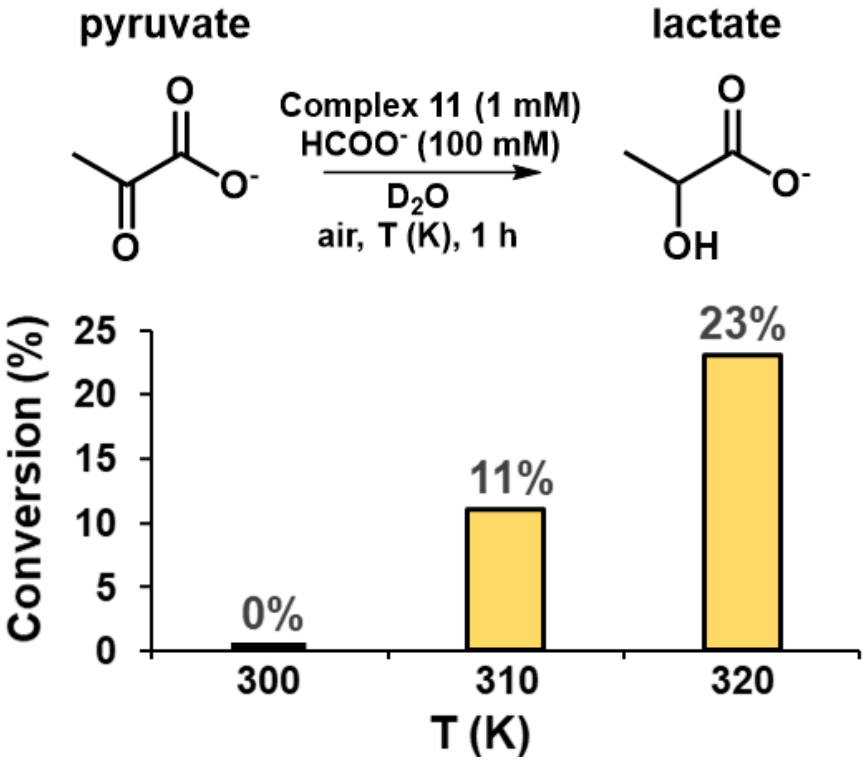

Figure S37. Evaluation of the transfer hydrogenation efficiency of complex **11** (1 mM) to convert pyruvate (2 mM) to lactate at different temperatures in a deuterium oxide solution with HCOONa as the H-source (100 mM) at pH 4 after 1 h of reaction, as determined by ^{1}H NMR.

Figure S38.

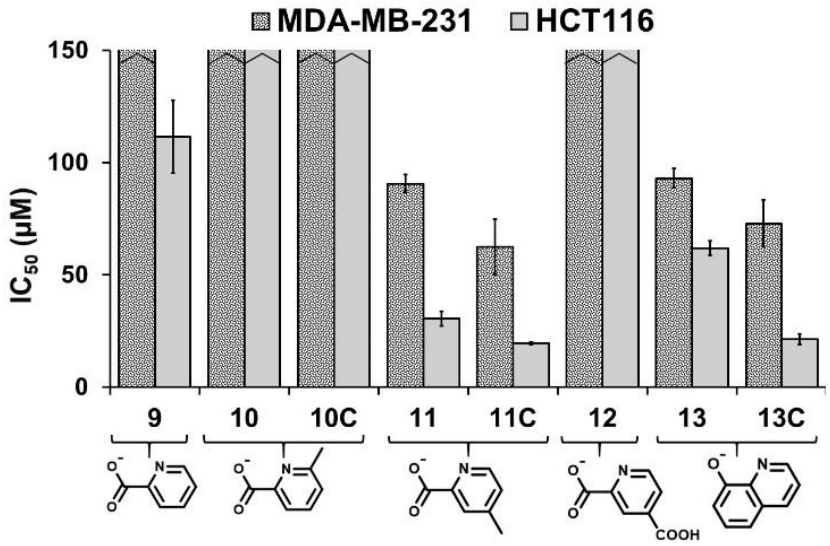

Figure S38. Antiproliferative activity of osmium(II) picolinate and quinolinate complexes. Cell viability was determined in MDA-MB-231 and HCT116 cells upon 24 h of exposure to complexes **9**, **10**, **10C**, **11**, **11C**, **12**, **13**, and **13C** (cells were allowed to recover for 72 h). Cisplatin was used as positive control (IC_{50} = 12.2 ± 1.9 μM for MDA-MB-231 and 5.3 ± 1.0 μM for HCT116).

Figure S39.

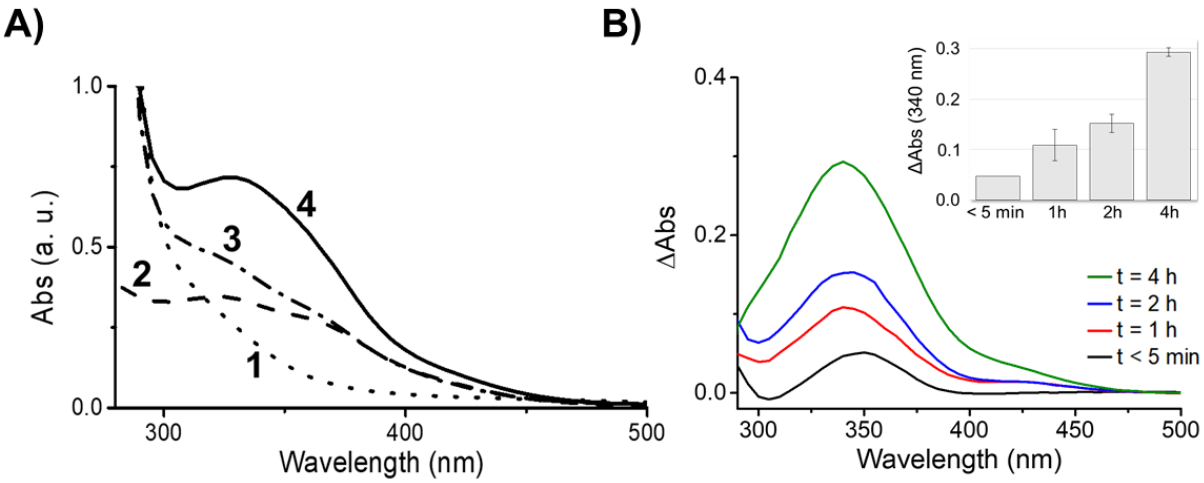

Figure S39. (A) UV–vis spectra showing the formation of NADH resulting from enzymatic (LDH) transformation when lactate is the substrate, using NAD^+ as a coenzyme. Lactate is produced catalytically by reduction of pyruvate by [Os(η^6-$C_6H_5(CH_2)_3OH$)(4-Me-pico)Cl] (**11**) in the presence of formate. (1) Dotted line: formate, pyruvate, NAD^+ in a phosphate buffer solution where LDH enzyme is added. (2) Dashed line: mixture containing **11**, pyruvate and formate, heated at 333 K for 4 h. (3) Dot-dashed line: mixture in (2) upon addition of ca. 2 mM NAD^+. (4) Solid line: mixture in (3) upon addition of L-LDH, affording NADH (from coenzyme NAD^+) demonstrating the presence of L-lactate in the sample contained in (2). Samples in (1), (3) and (4) were incubated for 15 min at 310 K before the UV–vis was recorded. Concentrations in (2), (3), and (4) are **11** = 0.25, pyruvate = 0.5, formate = 100 mM. (B) UV–vis spectra showing increasing NADH concentrations (band at 340 nm) as a direct determination of lactate catalytically produced by **11**. Complex **11** was heated at 333 K with pyruvate and sodium formate and aliquots were taken at different time points, to be incubated with NAD^+ and LDH for 15 min at 310 K. ΔAbs indicates the variation in the absorbance between the sample and the blank (sample prior addition of LDH). The inset shows the variation in the absorbance increases over time.

Supplementary Tables

Table S1. ^{1}H NMR data for the arene proton signals of complexes in DMSO-d_6 at 25 °C.

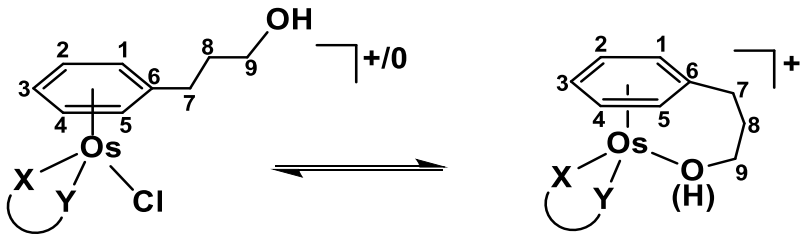

Open tether (1-13) ⇌ Closed tether (1C-13C)

Compound	δ (ppm)							
	H1 and H5 (doublet)[a]	H2 and H4 (triplet)[a]	H3 (triplet)	H7	H8	H9	OH[b]	Span H2 – H3
Unbound (free) arene $C_6H_5(CH_2)_3OH$		7.29-7.14		2.60	1.71	3.42	4.46	
1	5.72	5.90	5.76	2.41	1.70	3.45	4.56	0.14
2	6.20	6.44	6.02	2.46	1.72	3.45	4.58	0.42
2C	5.79	6.26	5.58	2.63	1.75	3.25	n.a.	0.68
3	6.35	6.57	6.03	2.53[c]	1.74	3.46	4.57	0.54
3C	5.96	6.43	5.50	2.66	1.77	3.17	n.a.	0.93
4	5.98 / 5.88	6.15 / 6.10	5.92	2.37	1.70	3.44	4.58	0.23
5	6.04 / 5.87	6.25 / 5.95	5.80	2.39	1.66	3.38	4.58	0.45
6	6.05 / 5.87	6.25	5.95	2.39	1.66	3.40	4.59	0.30
7	6.17 / 5.70	6.35 / 6.08	5.77	2.35	1.72	3.45	4.65	0.58
7C	5.96 / 5.93	6.38 / 5.62	5.36	2.71	1.98	3.48	n.a.	1.02
8	6.26 / 6.22	6.45 / 6.42	6.01	2.50[c]	1.73	3.46	4.61	0.44
8C	5.89 / 5.81	6.35 / 6.28	5.43	2.78	1.96	3.46	n.a.	0.92
9	5.98	6.25 / 6.21	6.05	2.43	1.73	3.46	4.56	0.20
10	6.00 / 5.97	6.39	6.06	2.40	1.75	3.47	4.61	0.33
10C	6.25 / 6.18	6.79 / 6.70	6.36	2.37	1.75	3.47	4.64	0.43
11	5.96	6.23 / 6.19	6.02	2.41	1.72	3.45	4.58	0.21
11C	5.85 / 5.83	6.26 / 6.21	5.92	3.39	2.59	3.95	4.39	0.34
12	6.00	6.28 / 6.24	6.07	2.44	1.73	3.45	4.56	0.21
13	5.90 / 5.84	6.15 / 6.13	5.90	2.45	1.73	3.45	4.54	0.25

[a] Due to the asymmetry of the chelating ligand, for most of chiral complexes, the resonances for the aromatic protons (C−H) of the arenes are not the same and two different signals are found for H1/H5 and H2/H4 protons. [b] The proton signal corresponding to the pendant OH group is missing in those closed tether complexes that bear N,N-chelating ligands since the proton is released upon coordination to the metal centre. [c] The ^{1}H NMR signal corresponding to CH_2 groups in the tether arm overlaps with the residual peak of the deuterated solvent (DMSO-d_6). 2D experiments in DMSO and in different solvents, such as CD_3OD, were recorded to help identify this signal.

Table S2. Selected bond lengths (Å) and angles (°) for compounds **5·PF$_6$**, **8·PF$_6$**, **9–11**, **13**, **3C·PF$_6$ and dichlorido complex [Os(η^6:κ^1-C$_6$H$_5$(CH$_2$)$_3$OH)Cl$_2$]**.

	5·PF$_6$	**8·PF$_6$**	**9**	**10**	**11**	**13**
Os–C1	2.206(10)	2.209(5)	2.179(14)	2.165(14)	2.184(6)	2.197(4)
Os–C2	2.172(9)	2.186(5)	2.167(11)	2.133(14)	2.165(6)	2.145(4)
Os–C3	2.183(11)	2.164(5)	2.170(13)	2.210(15)	2.178(6)	2.169(4)
Os–C4	2.202(10)	2.164(5)	2.143(15)	2.153(13)	2.141(6)	2.166(4)
Os–C5	2.208(10)	2.187(5)	2.179(14)	2.226(13)	2.176(5)	2.194(4)
Os–C6	2.238(11)	2.210(5)	2.217(14)	2.180(14)	2.194(6)	2.204(4)
Os–centroid	1.685	1.688	1.651	1.663	1.648	1.660
Os–Cl1	2.388(2)	2.407(19)	2.398(3)	2.395(3)	2.4107(14)	2.4064(10)
Os–N1	2.082(8)	2.093(6)	2.096(11)	2.141(13)	2.095(5)	2.104(3)
Os–N2/O2	2.092(7)	2.073(7)	2.100(10)	2.057(10)	2.087(4)	2.081(3)
N1-Os-Cl1	83.4(2)	83.80(17)	83.9(4)	83.8(3)	84.03(11)	83.81(9)
N1-Os-N2/O2	76.1(4)	76.5(3)	76.2(4)	77.1(5)	76.68(16)	77.67(12)
Cl1-Os-N2/O2	87.4(2)	84.59(19)	85.4(3)	87.7(3)	84.69(10)	82.77(8)
Os-C6-C7	128.4(8)	126.9(4)	131.2(10)	131.0(10)	127.6(4)	129.6(3)
C6-centroid-Os	91.17	91.25	91.63	90.48	90.47	91.02
C7-Offset[a]	0.074(+)	0.090 (+)	0.003 (+)	0.036 (-)	0.093 (+)	0.049 (+)
	3C·PF$_6$		**Dichlorido**			
Os–C1	2.192(4)		2.184(6)			
Os–C2	2.161(4)		2.159(6)			
Os–C3	2.205(4)		2.165(6)			
Os–C4	2.171(4)		2.142(6)			
Os–C5	2.173(4)		2.173(6)			
Os–C6	2.198(4)		2.159(6)			
Os–centroid	1.663		1.636			
Os–O1	2.054(3)		2.142(4)			
Os–N1/Cl1	2.097(3)		2.4166(16)			
Os–N2/Cl2	2.098(3)		2.4029(17)			
N1/Cl1-Os-O1	79.65(11)		80.96(12)			
N1/Cl1-Os-N2/Cl2	77.39(12)		86.27(6)			
O1-Os-N2/Cl2	80.99(11)		82.22(12)			
Os-C6-C7	124.9(3)		125.1(5)			
C6-centroid-Os	90.37		89.49			
C7-Offset[a]	0.138 (+)		0.193 (+)			
σ[b]	5.13		1.54			

[a] Offset of C7 with respect to the plane containing the Os-bound arene (carbons C1-C6); (+) towards osmium, (-) away from osmium. [b] Torsion angle of the planes containing O1, Os1, C6 and C7.

Table S3. Intermolecular interactions between the O(alcohol) hydrogen atoms for complex **3C·PF$_6$** and the oxygens from an adjacent methanol molecule and selected hydrogen-bonding intermolecular interactions with the O(alcohol) hydrogen atoms and the oxygen atoms on the O(XY-chelating ligand) for complexes **9**, **11** and **13**.

	D–H···A	**H···A (Å)**	**D···A (Å)**	**∠ D–H···A (°)**
3C·PF$_6$	O(1)–H···O(3W)	1.755	2.592(4)	175.21
9	O(1)–H···O(6)	1.968	2.80(1)	171.23
	O(4)–H···O(3)	1.882	2.72(1)	172.55
11	O(1)–H···O(3)	2.003	2.820(6)	164.05
13	O(1)–H···O(2)	1.883	2.723(4)	178.32

Table S4. Crystallographic data of **5·PF$_6$**, **8·PF$_6$**, **9**–**11**, **13**, **3C·PF$_6$** and dichlorido complex [Os(η^6:κ^1-$C_6H_5(CH_2)_3OH$)Cl_2].

	5·PF$_6$	**8·PF$_6$**	**9**	**10**	**11**	**13**	**3C·PF$_6$**	**Dichlorido**
Formula	$C_{21}H_{22}ClF_6N_2OOs$	$C_{23}H_{26}ClF_6N_2OOs$	$C_{15}H_{16}ClNO_3O$	$C_{16}H_{18}ClNO_{3.25}O$	$C_{16}H_{18}ClNO_3O$	$C_{18}H_{18}ClNO_2O$	$C_{23}H_{27}F_6N_2O_3Os$	$C_{18}H_{24}Cl_4O_2Os$
Molecular	689.02	717.08	483.94	501.96	497.96	505.98	714.63	794.57
Crystal	Prismatic	Prismatic	Prismatic	Needle	Needle	Prismatic	Prismatic	Prismatic
Crystal size	0.150 x 0.048 x	0.132 x 0.057 x	0.116 x 0.046	0.465 x 0.123 x	0.312 x 0.039	0.174 x 0.033	0.262 x 0.134 x	0.17 x 0.12 x
λ (Å)	0.71073	0.71073	0.71073	0.71073	0.71073	0.71073	0.71073	0.71073
T (K)	150	150	150	150	150	150	150	150
Crystal	Orthorhombic	Monoclinic	Monoclinic	Trigonal	Monoclinic	Orthorhombic	Monoclinic	Monoclinic
Space	$P\,2_1\,2_1\,2_1$	$P\,1\,2_1\,1$	$P\,1\,2_1\,1$	$P\,3_1\,2\,1$	$P\,1\,2_1/c\,1$	$Pbca$	$P\,1\,2_1/n\,1$	$C\,1\,2/c\,1$
a (Å)	8.9047(3)	7.2647(3)	10.0552(3)	12.3794(4)	5.9791(2)	15.5999(4)	14.5072(3)	13.5256(10)
b (Å)	13.1177(3)	19.3763(9)	11.2003(3)	12.3794(4)	18.0925(8)	7.8848(3)	11.0750(2)	9.3193(5)
c (Å)	19.5010(6)	17.3860(6)	13.0423(4)	17.8331(6)	14.6578(5)	25.8551(8)	15.5411(3)	16.0284(12)
α (°)	90	90	90	90	90	90	90	90
β (°)	90	100.4733(19)	96.9160(10)	90	97.5759(19)	90	104.4256(7)	90.590(4)
γ (°)	90	90	90	120	90	90	90	90
Volume	2277.90(12)	2406.53(17)	1458.15(7)	2366.77(17)	1571.79(10)	3180.23(18)	2418.22(8)	2020.3(2)
Z	4	4	4	6	4	8	4	4
R[a]	0.0348	0.0321	0.0313	0.0417	0.0443	0.0344	0.0318	0.0404
R_w[b]	0.0780	0.0445	0.0673	0.1032	0.0582	0.0424	0.0550	0.0503
GOF[c]	1.071	1.034	1.032	1.071	1.006	1.016	1.019	1.030

[a] Residual factor for all reflections satisfying the resolution limits established (R_factor_all) not only the residual factor for the significantly intense reflections. [b] Weighted residual factors for all reflections included in the refinement (wR_factor_ref) not only the significantly intense reflections. [c] The least-squares goodness-of-fit parameter S for all reflections included in the refinement after the final cycle of refinement.

Table S5. Cytotoxicity determination, by means of the IC_{50} values, of osmium complexes studied in this work toward human MDA-MB-231 breast and HCT116 colon cancer cells. Cisplatin was used as positive control.[a]

		IC_{50}[b] (μM) ± SD	
Compound	**Ligand**	**MDA-MB-231**	**HCT116**
1	N,N	>200	>200
2	N,N	>200	>200
2C		>200	>200
3	N,N	269.5 ± 14.9	>200
3C		>200	>200
4	N,N	>200	>200
5	N,N	>200	>200
6	N,N	>200	123.0 ± 8.20
7	N,N	>200	>200
8	N,N	135.0 ± 6.0	126.6 ± 5.1
9	N,O	>200	111.5 ± 16.3
10	N,O	>200	>200
10C		>200	>200
11	N,O	90.6 ± 4.0	30.5 ± 3.3
11C		62.5 ± 12.2	19.5 ± 0.6
12	N,O	>200	>200
13	N,O	93.0 ± 4.3	61.9 ± 3.2
13C		72.8 ± 10.5	21.4 ± 2.4
cisplatin		12.2 ± 1.9	5.3 ± 1.0

[a] The drug treatment period was 24 h (+72 h cell recovery). [b] Experiments were performed in cuadriplicate, and data are displayed as an average of at least three independent experiments. All values were compared to the non-treated controls and to one another for statistical significance calculations; $p<0.001$.

Table S6. Cellular accumulation of osmium upon 24 h exposure to 50 μM of complexes **2C**, **3C**, **10C**, **11C**, **12**, and **13C** (as ng Os/10^6 Cells), in MDA-MB-231 and HCT116 cancer cells.

Internalization (ng Os/10^6 cells)		
Complex	MDA-MB-231	HCT116
2C	5.24 ± 0.61	5.44 ± 0.27
3C	6.86 ± 1.34	7.44 ± 0.58
10C	3.56 ± 0.15	4.58 ± 0.27
11C	34.43 ± 2.32	48.78 ± 2.81
12	2.79 ± 0.43	1.59 ± 0.26
13C	29.44 ± 6.83	46.36 ± 7.88

Table S7. Reported compounds selected for comparison purposes. Selected bound lengths (Å) and angles (°) for the published compounds.

	Ru(II) COMPLEXES [a]				**Os(II) COMPLEX**
	OPEN: $[Ru(\eta^6\text{-}C_6H_5(CH_2)_3OH)(bipy)Cl]^+$ CLOSED: $[Ru(\eta^6{:}\kappa^1\text{-}C_6H_5(CH_2)_3\mathbf{O})(\mathbf{phen})]^+$ CLOSED: $[Ru(\eta^6{:}\kappa^1\text{-}C_6H_5(CH_2)_3\mathbf{O})(\mathbf{bipy})]^+$				$[Os(\eta^6{:}\kappa^1\text{-}C_6H_5(CH_2)_3\mathbf{O})(\mathbf{phen})]^+$
	Bipy_open	**Bipy_closed**	**Bpop_closed**	**Phen_closed**	**3C·PF$_6$**
Ru-C1 (Å)	2.188(5)	2.191(8)	2.13(5)	2.189(4)	2.192(4)
Ru-C2 (Å)	2.158(5)	2.185(9)	2.11(4)	2.168(4)	2.161(4)
Ru-C3 (Å)	2.158(5)	2.203(8)	2.18(3)	2.163(5)	2.205(4)
Ru-C4 (Å)	2.196(5)	2.178(7)	2.20(2)	2.165(4)	2.171(4)
Ru-C5 (Å)	2.192(5)	2.179(7)	2.13(3)	2.196(4)	2.173(4)
Ru-C6 (Å)	2.211(5)	2.205(7)	2.24(3)	2.204(4)	2.198(4)
Ru-centroid (Å)	1.677	1.686	1.666	1.671	1.663
Ru-Cl1/O1 (Å)	2.397(1)	2.050(5)	2.11(2)	2.145(3)	2.054(3)
Ru-N1 (Å)	2.077(4)	2.064(6)	2.10(2)	2.096(3)	2.097(3)
Ru-N2 (Å)	2.080(4)	2.107(6)	2.14(2)	2.096(3)	2.098(3)
N1-Ru-Cl1/O1 (º)	85.2(1)	82.5(2)	85.2(8)	81.0(1)	79.65(11)
N1-Ru-N2 (º)	76.9(1)	77.6(3)	82.0(8)	77.9(1)	77.39(12)
Cl1/O1-Ru-N2 (º)	84.5(1)	80.9(2)	81.6(8)	83.2(1)	80.99(11)
Ru-C6-C7 (º)	130.4(4)	122.4(5)	127(2)	126.2(3)	124.9(3)
C6-centroid-Ru (º)	90.52	90.12	90.80	89.03	90.37
Offset C7 [b]	0.031 (+)	0.189 (+)	0.129 (+)	0.119 (+)	0.138 (+)
σ [c]		27.52	15.20	9.77	5.13

[a] As described by Miyaki et al.[19] [b] Offset of C7 with respect to the plane formed by Os-bound arene (carbons C1-C6) (+) towards to osmium (-) away from osmium. [c] Torsion angle of the planes containing O1, Os1, C6 and C7.

Bibliography

1. A. Krężel and W. Bal, *J. Inor. Biochem.*, 2004, **98**, 161-166.
2. Bruker. APEX2, SAINT and SADABS, Bruker AXS: Madison: 2008.
3. Bruker. SHELXTL Version 6.10, Structure Determination Package, Bruker AXS: Madison, WI: 2000.
4. G. M. Sheldrick, *Acta Crystallogr. Sect. A: Found. Crystallogr.* , 2008, **64**, 112-122.
5. G. M. Sheldrick, *Acta Crystallogr. Sect. C: Struct. Chem.* , 2015, **71**, 3-8.
6. J. P. C. Coverdale, I. Romero-Canelón, C. Sanchez-Cano, G. J. Clarkson, A. Habtemariam, M. Wills and P. J. Sadler, *Nat. Chem.*, 2018, **10**, 347-354.
7. P. Skehan, R. Storeng, D. Scudiero, A. Monks, J. McMahon, D. Vistica, J. T. Warren, H. Bokesch, S. Kenney and M. R. Boyd, *J. Natl. Cancer Inst.*, 1990, **82**, 1107-1112.
8. V. Vichai and K. Kirtikara, *Nat. Protoc.*, 2006, **1**, 1112-1116.
9. M. H. M. Klose, M. Hejl, P. Heffeter, M. A. Jakupec, S. M. Meier-Menches, W. Berger and B. K. Keppler, *Analyst*, 2017, **142**, 2327-2332.
10. S. H. van Rijt, A. F. A. Peacock, R. D. L. Johnstone, S. Parsons and P. J. Sadler, *Inorg. Chem.*, 2009, **48**, 1753-1762.
11. A. Habtemariam, S. Betanzos-Lara and P. J. Sadler, in *Inorganic Synthesis*, ed. T. B. Rauchfuss, John Wiley & Sons,, 2010, ch. 160-163.
12. R. Bejot, S. Tisserand, D. R. Li, J. R. Falck and C. Mioskowski, *Tetrahedron Lett.*, 2007, **48**, 3855-3858.
13. J. Heo, H. Lee and S. Nayab, *J. Coord. Chem.*, 2017, **70**, 3837-3858.
14. A. F. A. Peacock, A. Habtemariam, R. Fernandez, V. Walland, F. P. A. Fabbiani, S. Parsons, R. E. Aird, D. I. Jodrell and P. J. Sadler, *J. Am. Chem. Soc.*, 2006, **128**, 1739-1748.
15. J. Tönnemann, J. Risse, Z. Grote, R. Scopelliti and K. Severin, *Eur. J. Inorg. Chem.*, 2013, **2013**, 4558-4562.
16. Y. Fu, M. J. Romero, A. Habtemariam, M. E. Snowden, L. Song, G. J. Clarkson, B. Qamar, A. M. Pizarro, P. R. Unwin and P. J. Sadler, *Chem. Sci.*, 2012, **3**, 2485-2494.
17. A. F. A. Peacock, A. Habtemariam, S. A. Moggach, A. Prescimone, S. Parsons and P. J. Sadler, *Inorg. Chem.*, 2007, **46**, 4049-4059.
18. M. J. Chow, C. Licona, D. Yuan Qiang Wong, G. Pastorin, C. Gaiddon and W. H. Ang, *J. Med. Chem.*, 2014, **57**, 6043-6059.
19. Y. Miyaki, T. Onishi and H. Kurosawa, *Inorg. Chim. Acta*, 2000, **300**, 369-377.
20. T. Ohnishi, Y. Miyaki, H. Asano and H. Kurosawa, *Chem. Lett.*, 1999, **28**, 809-810.
21. Y. Fu, R. Soni, M. J. Romero, A. M. Pizarro, L. Salassa, G. J. Clarkson, J. M. Hearn, M. Wills, A. Habtemariam and P. J. Sadler, *Chem. Eur. J.*, 2013, **19**, 15199-15209.
22. Y. Fu, A. Habtemariam, A. M. B. H. Basri, D. Braddick, G. J. Clarkson and P. J. Sadler, *Dalton Trans.*, 2011, **40**, 10553–10562.
23. Y. Fu, A. Habtemariam, A. M. Pizarro, S. H. van Rijt, D. J. Healey, P. A. Cooper, S. D. Shnyder, G. J. Clarkson and P. J. Sadler, *J. Med. Chem.*, 2010, **53**, 8192-8196.
24. J. M. Gichumbi, B. Omondi and H. B. Friedrich, *Eur. J. Inorg. Chem.*, 2017, **2017**, 915-924.
25. A. F. A. Peacock, S. Parsons and P. J. Sadler, *J. Am. Chem. Soc.*, 2007, **129**, 3348-3357.

26. F. Martínez-Peña, S. Infante-Tadeo, A. Habtemariam and A. M. Pizarro, *Inorg. Chem.*, 2018, **57**, 5657-5668.

27. J. Čubrilo, I. Hartenbach, T. Schleid and R. F. Winter, *Z. anorg. allg. Chem.*, 2006, **632**, 400-408.

28. H. Chen, J. A. Parkinson, S. Parsons, R. A. Coxall, R. O. Gould and P. J. Sadler, *J. Am. Chem. Soc.*, 2002, **124**, 3064-3082.

29. A. Matsumoto, T. Odani, M. Chikada, K. Sada and M. Miyata, *J. Am. Chem. Soc.*, 1999, **121**, 11122-11129.

30. T. Steiner, *Angew. Chem. Int. Ed.*, 2002, **41**, 48-76.

31. G. A. Jeffrey, *An Introduction to Hydrogen Bonding*, Oxford University Press, 1997.

32. L. Schaeffer, in *The Practice of Medicinal Chemistry*, 2008, DOI: 10.1016/b978-0-12-417205-0.00014-6, pp. 359-378.

33. H. Chen, J. A. Parkinson, O. Novakova, J. Bella, F. Wang, A. Dawson, R. Gould, S. Parsons, V. Brabec and P. J. Sadler, *Proc. Natl. Acad. Sci. U. S. A.*, 2003, **100**, 14623-14628.